NASA/TM-2007-XXXXXX

C-9 and Other Microgravity Simulations

Summary Report

Report prepared by
Space and Life Sciences Directorate
Human Adaptation and Countermeasures Office
Johnson Space Center, Houston

Lyndon B. Johnson Space Center
Houston, Texas

September 2007

THE NASA STI PROGRAM OFFICE . . . IN PROFILE

Since its founding, NASA has been dedicated to the advancement of aeronautics and space science. The NASA Scientific and Technical Information (STI) Program Office plays a key part in helping NASA maintain this important role.

The NASA STI Program Office is operated by Langley Research Center, the lead center for NASA's scientific and technical information. The NASA STI Program Office provides access to the NASA STI Database, the largest collection of aeronautical and space science STI in the world. The Program Office is also NASA's institutional mechanism for disseminating the results of its research and development activities. These results are published by NASA in the NASA STI Report Series, which includes the following report types:

- TECHNICAL PUBLICATION. Reports of completed research or a major significant phase of research that present the results of NASA programs and include extensive data or theoretical analysis. Includes compilations of significant scientific and technical data and information deemed to be of continuing reference value. NASA's counterpart of peer-reviewed formal professional papers but has less stringent limitations on manuscript length and extent of graphic presentations.

- TECHNICAL MEMORANDUM. Scientific and technical findings that are preliminary or of specialized interest, e.g., quick release reports, working papers, and bibliographies that contain minimal annotation. Does not contain extensive analysis.

- CONTRACTOR REPORT. Scientific and technical findings by NASA-sponsored contractors and grantees.

- CONFERENCE PUBLICATION. Collected papers from scientific and technical conferences, symposia, seminars, or other meetings sponsored or cosponsored by NASA.

- SPECIAL PUBLICATION. Scientific, technical, or historical information from NASA programs, projects, and mission, often concerned with subjects having substantial public interest.

- TECHNICAL TRANSLATION. English-language translations of foreign scientific and technical material pertinent to NASA's mission.

Specialized services that complement the STI Program Office's diverse offerings include creating custom thesauri, building customized databases, organizing and publishing research results . . . even providing videos.

For more information about the NASA STI Program Office, see the following:

- Access the NASA STI Program Home Page at http://www.sti.nasa.gov

- E-mail your question via the Internet to help@sti.nasa.gov

- Fax your question to the NASA Access Help Desk at (301) 621-0134

- Telephone the NASA Access Help Desk at (301) 621-0390

- Write to:
  NASA Access Help Desk
  NASA Center for AeroSpace Information
  7115 Standard
  Hanover, MD 21076-1320

NASA/TM-2007-XXXXXX

C-9 and Other Microgravity Simulations

Summary Report

Report prepared by
Space and Life Sciences Directorate
Human Adaptation and Countermeasures Office
Johnson Space Center, Houston

Lyndon B. Johnson Space Center
Houston, Texas

September 2007

C-9 and Other Microgravity Simulations
Summary Report – September 30, 2007

National Aeronautics and Space Administration
Lyndon B. Johnson Space Center

Prepared by: _____ _____

Noel C. Skinner, MS — Date
C-9 Coordinator
Wyle

_____ _____

Wanda L.Thompson, RN, BC, NMCC — Date
Alternate C-9 Coordinator
JES Tech, LLC

Approved by: _____ _____

Jeannie L. Nillen, MT (ASCP) — Date
Manager
Human Adaptation and Countermeasures Group
Wyle

Approved by: _____ _____

Todd T. Schlegel, MD — Date
Technical Monitor
Human Adaptation and Countermeasures Office
Reduced Gravity Program
NASA Johnson Space Center

Available from:

NASA Center for AeroSpace Information
7115 Standard Drive
Hanover, MD 21076-1320

National Technical Information Service
5285 Port Royal Road
Springfield, VA 22161

This report is also available in electronic form at http://ston.jsc.nasa.gov/collections/TRS

PREFACE

This document represents a summary of medical and scientific evaluations conducted aboard the C-9 or other NASA-sponsored aircraft from June 30, 2006, to June 30, 2007. Included is a general overview of investigations manifested and coordinated by the Human Adaptation and Countermeasures Office. A collection of brief reports that describe tests conducted aboard the NASA-sponsored aircraft follows the overview. Principal investigators and test engineers contributed significantly to the content of the report, describing their particular experiment or hardware evaluation. Although this document follows general guidelines, each report format may vary to accommodate differences in experiment design and procedures. This document concludes with an appendix that provides background information about the Reduced Gravity Program.

CONTENTS

Overview of Flight Activities Sponsored by the Human Adaptation and Countermeasures Office

This section summarizes C-9 flight activities for the year June 30, 2006, to June 30, 2007. Seven weeks were reserved for flights sponsored by the Human Adaptation and Countermeasures Office (HACO). In addition, we were able to obtain seating during 8 weeks for HACO customers with other organizations sponsoring the flight weeks. A total of 36 flights with about 40 parabolas per flight were completed. The average duration of each flight was 2 hours. The C-9 coordinator assisted principal investigators and test engineers of 30 different experiments and hardware evaluations in meeting the requirements for flying aboard the C-9 or other NASA-sponsored aircraft and in obtaining the required seating and floor space. HACO customers purchased a total of 296 seats. The number of seats supported and number of different tests flown by flight week are provided below:

Flight Week	Seats	# Tests Flown	Sponsor
July 20, 2006	5	1	HACO
July 25 – 28	8	2	Undergraduate Program
Aug. 8 – 9	12	3	Undergraduate Program
Aug. 15 – 16	4	1	Undergraduate Program
Aug. 22 – 25	47	4	HACO
Oct 17 – 20	44	2	HACO
Feb. 8 – 9, 2007	4	1	NASA Explorer School
Feb. 27 – Mar. 2	60	2	HACO
Mar. 13 – 14	4	1	Undergraduate Program
Mar. 20 – 23	23	4	HACO
Mar. 29 – 30	4	1	Undergraduate Program
April 27	4	1	Undergraduate Program
May 3 – 4	4	1	Undergraduate Program
May 23 – 24	24	3	HACO
June 19 – 22	49	3	HACO

Support was provided to the undergraduate program during 3 weeks in July and August 2006 and during March, April, and May 2007. Support was also provided to middle-school teachers participating in the NASA Explorer School program during February 2007. A large ground crew from the respective academic institution supported the inflight experiments.

Other HACO-sponsored flight opportunities are scheduled for several weeks during July and September 2007. Additional flights will be added throughout the remainder of calendar year 2007 to accommodate customers as needs arise.

Medical and Scientific Evaluations during Parabolic Flights

TITLE
Space Medicine DC-9 Familiarization Flight

FLIGHT DATE
July 20, 2006

PRINCIPAL INVESTIGATOR
David Stanley, Wyle

CO-INVESTIGATORS
Kevin Rosenquist, Wyle
Robert Haddon, M.D., University of Texas Medical Branch
Keith Holubec, Wyle
Heather VanVelson, Wyle

GOAL

To familiarize Space Medicine Branch personnel with the effects of a zero-g environment by having them perform activities utilizing the medical equipment and procedures in parabolic flight, to better facilitate crew training and biomedical engineering support for ISS procedures.

OBJECTIVES

All co-investigators accomplished some or all of the following objectives:

Preflight

1. Attended preflight briefing and participated in ground-based practice session
2. Attended Test Readiness Review (TRR)
3. Attended Medical Briefing
4. Conducted final inventory of all hardware and supplies, and transported equipment to Ellington Field for scheduled reporting time
5. Properly loaded and secured hardware in the aircraft

In-Flight

1. Experienced and evaluated the effects of microgravity on intravenous insertion and drug administration, and on medical fluids
2. Experienced and evaluated the effects of microgravity on cardiopulmonary resuscitation (CPR), patient restraint, and rescuer restraint
3. Experienced and evaluated the effects of microgravity on using two different types of instruments that are used in intubation (establishing an airway)

Postflight

1. Unloaded hardware from aircraft
2. Prepared a C-9 final report

INTRODUCTION

As new personnel join the Space Medicine Branch, it is critical that the co-investigators understand the effects of microgravity while using medical procedures, hardware, and supplies. The familiarization flight provided personnel with a better understanding of the effects of microgravity for use of (1) medical procedures, (2) patient and rescuer restraint, and (3) medical training for spaceflight. Using the procedures to perform the tasks on the familiarization flight allows the operator to understand the limitations imposed by microgravity, helps in the composition of procedures for spaceflight, and helps operators assist astronauts in execution of onboard procedures.

The flight process also provided experience in preparation and execution of flight lesson plans, and preparation of a final report. In addition, first-time fliers gained insight into their performance level in microgravity for future flights.

METHODS AND MATERIALS

An initial training session was held to familiarize the new fliers with the documentation and skills necessary to fly on the C-9. The documentation required for requesting and reporting a C-9 flight was covered in detail and the co-investigators were given a template for writing their final reports. A skill session on the medical procedures that would be attempted during flight was also held. Fliers were introduced to the tasks required at each station and were given additional time to build confidence in their skills by practicing these tasks.

The procedures and equipment were divided into three stations: an intubation station, an intravenous (IV) administration station, and conducting cardiopulmonary resuscitation (CPR).

The intubation station was composed of a plastic model of the human head, neck, and chest that is designed specifically for practicing the establishment of an airway. Two methods of intubation were practiced: (1) Intubating Laryngeal Mask Airway (ILMA) device (Figure 1) and (2) laryngoscope (Figure 2) and endotracheal tube. The established medical checklist procedures for the insertion of these devices were followed.

Figure 1. Laryngoscope

Figure 2. Laryngeal Mask Airway

The IV administration station consisted of an artificial human arm with the correct anatomic landmarks for practicing intravenous catheter insertion. The arm and IV equipment (Figure 3) were fixed to a small metal table. The procedures for establishing peripheral intravenous access were followed and procedures for injecting medication into the intravenous line were practiced. A Tubex drug injection system was used for this purpose. The established medical checklist procedure for this technique was followed.

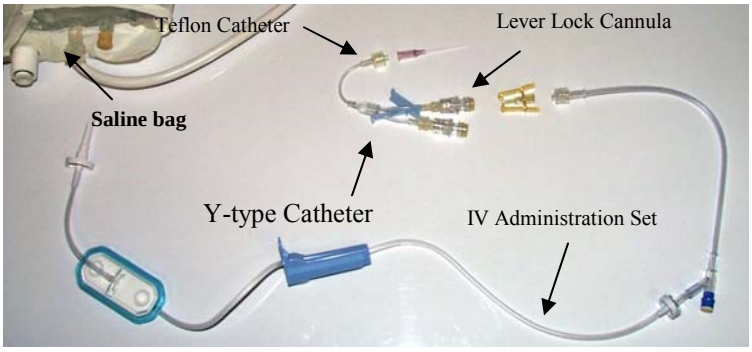

Figure 3. IV Equipment

Finally, the CPR station was established to practice the performance of CPR on a simulated ill crew member. The Crew Medical Restraint System (CMRS) was deployed and used to immobilize the simulated ill crew member. Three approaches to the performance of CPR were practiced for the designated crew medical officer (CMO): (1) CMO beside the patient, (2) CMO straddled on the patient, and (3) handstand position.

During the flight, the co-investigators were stationed as outlined in Table 1.

Table 1. C-9 familiarization flight procedure assignments.

Parabolas		**0-10**	**11 – 20**	**21 - 30**	**31 -40**
Activities	CPR	Holubec	Holubec	Rosenquist	----------
	CPR	VanVelson	VanVelson	---------	----------
	IV	Haddon	Haddon	VanVelson	Rosenquist
	Intubation	Rosenquist	Rosenquist	Holubec	VanVelson

RESULTS

Intubation Station

The medical checklist procedures were followed for the insertion of the ILMA. The lack of gravitational influence made it necessary to secure all small loose objects so that they would not drift away. The laryngoscope/endotracheal tube method of intubation was performed according to established procedures. Both of these intubation methods were repeated twice. All of the objectives for this station were met.

IV Station

The insertion of an intravenous catheter was achieved using the standard procedures. Intravenous fluid tubing was connected to the catheter. Afterward, Tubex drug injection was practiced. The management of sharp waste was particularly important due to the tendency of objects to float in simulated microgravity. All the objectives for this station were met.

Figure 4. Bob Haddon

Figure 5. Kevin Rosenquist

CPR Station

The CMRS was deployed and secured to the aircraft floor before flight. Established procedures for use of the restraint system were used to secure the simulated ill crew member (mannequin) to the CMRS. The designated CMO was able to perform CPR in all three of the positions desired: side-by-side, straddled, and inverted. The inverted position was clearly the most effective position, as the other two positions required significant counter pressure from restraints. All of the objectives for this station were met.

Figure 6. Heather VanVelson

Figure 7. Keith Holubec

DISCUSSION

Performing the medical operations procedures on the C-9 flight gave the co-investigators a greater understanding of the conditions involved in space operations. This knowledge will prove very useful for the co-investigator, especially during contingency situations with the flight crew and/or training sessions.

Experiencing weightlessness presented many difficulties that the co-investigators did not originally expect. They found the lack of control while floating to be the most difficult aspect of weightlessness. The lack of control was most apparent while they were performing time-critical medical activities. The co-investigators spent a larger amount of time securing themselves and maintaining proper positioning than they had originally anticipated. They felt that this time would most likely be reduced with extended exposure to microgravity. With this information, the co-investigators will be able to make more accurate and effective recommendations to a crew member during nominal and emergency situations.

This familiarization flight is extremely beneficial for supporting the crew and also for supporting console operations. The co-investigators gained a greater understanding and appreciation of the difficulties the crew faces because of their working environment This experience will give them a better ability to walk the crew through any procedure, not just the ones performed during the flight.

CONCLUSION

Overall, the objectives of the C-9 Familiarization Flight were met. All co-investigators agreed that the C-9 Familiarization Flight and associated training provided them with an excellent knowledge level from which to conduct their own flights. This was a very valuable training session and is highly recommended for all biomedical engineers, flight surgeons, and instructors. It is especially beneficial for anyone who expects astronauts to perform complex tasks that require the use of many items of loose equipment.

PHOTOGRAPHS

JSC2006E29056 to JSC2006E29091

VIDEO

- Zero G flight week 7/17 – 7/21/2006, 2006, Master: 721640

Videos available from Imagery and Publications Office (GS4), NASA/JSC.

CONTACT INFORMATION

David Stanley
Wyle
1290 Hercules Suite 120
Houston, Tx 77058
dstanley@wylehou.com

TITLE

Undergraduate Program Flights – SpaceBubbles Team

FLIGHT DATES

July 25 – 26, 2006

PRINCIPAL INVESTIGATORS

Laura Gadzala, University of Michigan
Andrew Klesh, University of Michigan
Chris Schoeps, University of Michigan
Nicholas Schoeps, University of Michigan

FOREWORD

The University of Michigan SpaceBubbles team conducted experiments to reduce embolisms caused by injection during future long-term space missions. We have created an experiment that utilizes a centrifuge to purge air bubbles from syringes. This experiment was tested on board a NASA C-9 reduced-gravity flight in July, 2006. The purpose of this report is to describe our experiment, its successes, and room for improvement.

SUMMARY

Twenty-four syringes were tested over two flights; ten broke or did not plunge in zero-gravity conditions. Of the remaining 14, eight were successfully evacuated and six had substantial quantities of air left, yielding a success rate of 57.14%.

INTRODUCTION

In the near future, humans will be traveling on extended space missions. On these missions, there is the potential for astronauts to become ill and require fast-acting treatment. Here on Earth, that treatment can be administered by injecting medicine directly into the body using hypodermic needles. In space, to the best of our knowledge, injections are given with syringes that have been pre-loaded with medicine on Earth. When using hypodermic needles and syringes, the threat of an air embolism looms large. On Earth, because of gravity, a doctor can simply point the syringe up, tap it, and depress the plunger to remove air. In a reduced-gravity environment, this is not possible because the air will not travel to one end of the syringe when it is turned upside down. This presents a major problem if an injection is to be administered in space because air injected into the astronaut's body may cause an embolism. We have conducted an experiment in which the air is removed from syringes, providing a safe way of injecting medicine into humans in space.

Our experiment involves removing air bubbles from a syringe while in microgravity. Our experiment utilized a centrifuge to force the fluid to one end of the syringe, thus allowing any air to be removed from the syringe. The system needed to be tested in a microgravity environment to determine its effectiveness in eliminating syringe air bubbles in space. This technology would be utilized in actual space missions; therefore our study in microgravity is very relevant.

Our hypothesis is that spinning syringes loaded with water and a small amount of air in a centrifuge followed by an automatic plunging process will allow us to remove air from a syringe.

A syringe loaded with water and a small amount of air was spun in the set-up shown in Figure 1 below. After plunging the air, we sealed the syringes and placed them in a container for later analysis. Once on the ground, we analyzed how much air was left in each syringe.

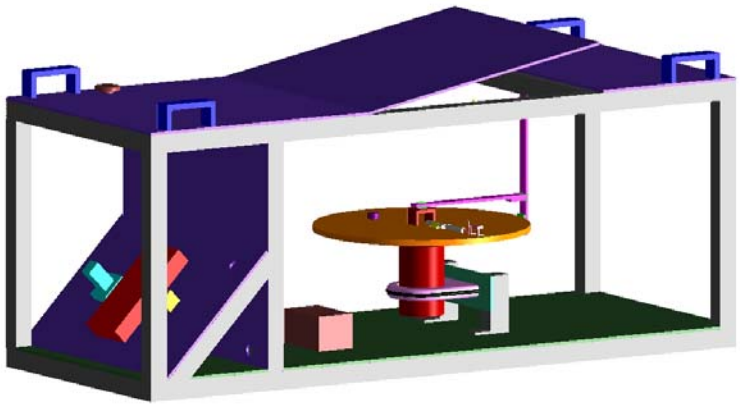

Figure 1. Design of Space Bubbles test equipment.

METHODS AND MATERIALS

Procedure

Before takeoff, the experiment was loaded with 12 syringes. Each syringe was pre-loaded with 1.5 cc of sterile water, and 0.5 cc of air. The sterile syringes were labeled and placed in convenient clips that held them to the experiment. Used syringes were in a different area, held with similar clips. The water container used to fill the syringes was not brought on board the aircraft, nor were the hypodermic needles of the syringes.

The C-9 flight creates 20 seconds of near-zero-gravity conditions per parabola. When the aircraft enters 0gravity, a button is pushed on the control panel, beginning a pre-programmed sequence. During this sequence, the centrifuge spins the syringes at a speed of 100 rpm. As the disk is spinning, a servo motor is actuated, plunging the syringe. This subsequently causes the air to be evacuated into a capsule at the end of the syringe. The syringes are equipped with a stopcock mechanism that we used to seal them before they were removed. Removed syringes were placed in a clip. In this manner, a syringe was tested in one out of every two parabolas. The aircraft made 32 parabolas per flight. Flight crews took the first two parabolas to become acquainted with the zero-g environment. The last two parabolas are representations of martian and lunar gravity, and are not considered for this experiment.

RESULTS

Of the 24 original syringes, only 14 yielded data points. The remaining ten were damaged during the procedure, and were omitted from our analysis. Of the 14 syringes that were successfully plunged in 0gravity, 8 of them were cleared of any noticeable air bubbles. Any syringe with a noticeable amount of air was considered to have failed. This is similar to what happens in a clinical setting, in which a nurse will visually inspect a syringe before administering medication. The data gave a 57.14% success rate for the experiment.

During the flight, team members observed that the centrifuge did not always seem to be spinning as fast as expected.

Table 1. Syringe purge results.

Syringe #	Complete	Failed
1	1	
2		1
3		1
4		1
5		X
6		1
7		X
8		X
9		1
10		X
11		1
12	1	
13		X
14	1	
15		X
16		X
17	1	
18	1	
19		X
20	1	
21	1	
22	1	
23		X
24		X
Total	**8**	**6**

An x signifies a syringe that failed mechanically, through separated stopcock or non-plunge.

CONCLUSION

The University of Michigan SpaceBubbles team created an experiment to eliminate air bubbles from syringes in 0gravity to prevent air embolisms. Our experiment yielded mixed results: 14 successfully tested syringes out of 24, with a 57.14% success rate. The relatively poor results could be attributed to the slow centrifuge rotation observed by the team members during flight. Also, since the centrifuge was manually triggered for each run, the start times varied in zero-gravity conditions, which could lead to a syringe being purged relatively earlier or later than another syringe. Suggestions for an improved success rate include a higher rotation speed for the centrifuge and vibration of the syringes before and/or during testing to ensure that air bubbles flow freely in the syringe. Ten of our 24 total syringes were broken and could not be used. For future tests, the use of a cyanoacrylate adhesive instead of epoxy to bond the syringe and stopcock should be considered. This would prevent the large rate of breakage that we encountered. We believe the centrifuge method holds promise, and can deliver an improved success rate in future tests modified as discussed above.

REFERENCES

1) Greg Hukill, Arianne Liepa, Travis Palmer, Christy Schroeder. "University of Michigan Characterization of Magnesium Combustion." University of Michigan. 2004 Reduced Gravity Student Flight Opportunity Program: Test Equipment Data Package. Project Number 2004-520.

2) Michael Chilvers. "Cerebral Air Embolism Following a Small Volume of Air Inadvertently Injected Via a Peripheral Arterial Cannula: Case Report." The Internet Journal of Advanced Nursing Practice. 2004. Internet Scientific Publications, LLC. 21 September 2004. www.ispub.com/ostia/index.php?xmlFilePath=journals/ijanp/vol2n2/air.xml.

3) Microgravity University: Reduced Gravity Student Flight Opportunity Program. L. Mauricio Rodriguez. 2004. National Aeronautics and Space Administration. 20 October 2004. www.microgravityuniversity.jsc.nasa.gov/students/index.cfm

4) Laura Gadzala, Andrew Klesh, Rene Kreis, Jeff Lance, Nick Schoeps. "University of Michigan Prevention of Air Embolism Caused by Injection through Hypodermic Needles." University of Michigan 2005 Reduced Gravity Student Flight Opportunity Program: Test Equipment Data Package Project Number 2005-1753.

5) Laura Gadzala, Andrew Klesh, Rene Kreis, Jeff Lance, Nick Schoeps. "University of Michigan Prevention of Air Embolism Caused by Injection through Hypodermic Needles." University of Michigan 2006 Reduced Gravity Student Flight Opportunity Program: Test Equipment Data Package Project Number 2006-1753.

PHOTOGRAPHS

JSC2006E31007
JSC2006E31013 to JSC2006E31018
JSC2006E31022 to JSC2006E31025
JSC2006E31035
JSC2006E31037 to JSC2006E31041
JSC2006E31125 to JSC2006E3128
JSC2006E31104 to JSC2006E31105
JSC2006E31111
JSC2006E31114

VIDEO

- Zero G flight week 7/24 – 7/28/2006, 2006, Master: 721633 and 721634

Videos available from Imagery and Publications Office (GS4), NASA/JSC.

TITLE

Undergraduate Program Flights – Gravitational Stress Alters Immune Function in Acheta domesticus by Activating a Cold Shock Response.

FLIGHT DATES

August 8 – 9, 2006

PRINCIPAL INVESTIGATOR

Madeline Leong, Duke University Medical Center
David S. Wheeler, University of Pittsburgh School of Medicine

INTRODUCTION

An understanding of the deleterious effects of abnormal gravity on the human immune system is necessary for the success of long-term space missions. Insects such as *Drosophila melanogaster* have been used to study gravitational effects since the early 1990s. However, no study has yet addressed the underlying mechanism of immune response to gravitational extremes.

METHODS AND MATERIALS

In this study, house crickets (*Acheta domesticus*) were used to identify the stress response pathway activated by gravitational extremes. Crickets were exposed to either gravitational stress (1 hour of microgravity–2g cycles at ambient temperature aboard NASA's C-9 aircraft) or common stress (heat shock, cold shock, motor stress, or ischemia.) Using a battery of immune and metabolic functional assays, we found that gravitational stress significantly decreased immune function and metabolism. These changes were most consistent with those observed in crickets exposed to cold shock or ischemia.

Since ischemia activates the cold shock pathway in animals, we hypothesized that gravitational stress also activates this pathway. To confirm this, we showed upregulation of chaperonin-containing *t*-complex alpha (CCTα), a cold shock protein, at 0 h and 24 h after gravitational stress.

RESULTS AND CONCLUSION

Our results indicate that crickets respond to gravitational stress by activating some or all of the cold shock response pathways. Inhibition of this pathway in crickets (or the homologous pathway in humans) may ameliorate many of the harmful effects that abnormal gravity has on the immune system.

PHOTOGRAPHS

JSC2006E33460 to JSC2006E33462
JSC2006E33490
JSC2006E33494 to JSC2006E33495
JSC2006E33500
JSC2006E33512
JSC2006E33523
JSC2006E33885
JSC2006E33891

VIDEO

- Zero G flight week Aug. 7-11, 2006, Master: DV0649

Videos available from Imagery and Publications Office (GS4), NASA/JSC.

TITLE

Undergraduate Program Flights – Emergency Severe Wound Containment/Treatment Device Evaluation

FLIGHT DATES

August 8 – 9, 2006

PRINCIPAL INVESTIGATORS

Mitchell R. Roth, BoonShoft Museum
Jasmine Cammick, BoonShoft Museum
Amber Cospy, BoonShoft Museum
Greg Gamble, BoonShoft Museum
Robert Gamble, BoonShoft Museum
John Ciprian, BoonShoft Museum
Robert W. Von Derau, BoonShoft Museum
C. Scott Wright, BoonShoft Museum

INTRODUCTION

The probability of suffocation from oxygen loss due to space suit damage has precluded the need for severe hemorrhage trauma procedures in previous missions. As efforts move toward assembly of orbital constructions necessary for larger missions to or stations on the moon, Mars, and beyond, personnel will work with larger equipment in larger areas, possibly without specialized atmospheric apparel. Terrestrial experience commonly shows that larger hardware and work areas eliminate the ability to avoid all potential bodily injury. The probability of trauma situations occurring increases as the scale of projects or missions increases. The release of body fluids in

weightlessness due to severe injury has great potential to compromise mission objectives[1] as well as pose a threat to mission personnel.

Although it has been observed that fluids tend to form "domes" that can adhere to the wound site,[2] dispersion into the environment due to forces generated by victim transport is likely. In addition, the microgravity environment greatly reduces the time window of treatment for any personnel experiencing hemorrhage trauma. As cited by Kirkpatrick et al., a typical loss rate yields 2-hour survivability terrestrially. This window reduces to about 30 minutes in microgravity.[3]

Challenges to physical interaction between mission personnel and between personnel and equipment can also be considerable under reduced-gravity conditions, as was experienced by those addressing cardiopulmonary resuscitation in reduced gravity.[4] This fact was also confirmed in discussions with NASA personnel regarding microgravity deployment procedures while the trauma treatment device was demonstrated. The basic deployment characteristics of this type of trauma treatment need to be established. Both initial wound treatment and fluid containment under microgravity conditions show a need for quickly available and effective means. To minimize mission expenditures, the means of treatment must be effective despite limited medical training or reduced-gravity experience of personnel, or proximity to available medical treatment. Time is critical to survival and reduction of mission hazards and risks.

Kirkpatrick indicates a "Tactical Tourniquet" as an appropriate treatment device for severe injury.[5] Ideally, this device would incorporate the preferred pneumatic-type tourniquet, with examination access to facilitate initial diagnosis, while maintaining containment, supporting the premise that an emergency-use multi-function device is desirable and was the focus of the original hardware evaluation. It is evident, however, that the desire for compact storage and ease of use overshadows the necessity for incorporated tourniquet and examination access, as both aspects occur less frequently with respect to mission-threatening injury.

GOAL

The goal of this investigation is to evaluate a wound treatment system.

METHODS AND MATERIALS

During research and development of a device simulator with the conceptual victim-hardware interface, a more compact and versatile solution appeared. A collection of single-person deployable devices was discovered at relatively low cost, containing two bandages, extra gauze packing for each, a tourniquet, burn treatment, and even nitrile gloves, delivering all functions except examination access.

This collection uses novel vacuum packaging techniques and textile-based materials and is roughly the same size and weight as a single conceptual device. It also provides wound compression for hemostasis through a wrap-around elastic band passed through an attached hook and pulled tight around the wound. It is subsequently wrapped around the appendage or abdomen and secured at the end by a hook-loop-type fastening strip. Moreover, it delivers treatment for

multiple wounds and/or wound types and is even capable of victim self-deployment, neither of which the conceptual device could deliver.

Although proven simple with quick deployment potential terrestrially, baseline implementation time and containment potential need to be established before consideration of the device as the mission standard.

The experiment evaluated containment potential using induced gas (air) flow traveling through a sealed line to an induced flow sensor, then to an isolated "wound site" on the mannequin inner thigh and then to a second flow sensor. The "wound site" was a pocket sealed by an insert with a pattern of openings toward the outer surface sized to represent roughly 80% of absorbing pad surface area of the device. The absorption pad provided by the test device was covered with a thin, adhesive, non-porous polymer film so that it provided a complete seal over any openings to force the induced gas to travel through the exhaust line and exhaust sensor. A laptop computer automatically recorded flow measurements to and from the "wound site."

RESULTS AND CONCLUSION

The logged containment evaluation data were invalidated by failure of the internal exhaust housing, but it was determined that deployment requires less than one minute, as all fliers felt that the interruption due to preparations for increased gravity greatly increased the average 2-parabola or less deployment time. It was also determined that no additional modifications (fastenings) are required due to development of a "looped finger" deployment that allows the material to be easily controlled. It was also determined that the raised bar foot anchoring provided by the anchor base was extremely effective and versatile. In fact, it provided stability and mobility superior to standard methods provided by the Reduced Gravity Office.

REFERENCES

1. Kirkpatrick Campbell et al. "Extraterrestrial Hemorrhage Control: Terrestrial Developments in Technique, Technology, and Philosophy with Applicability to Traumatic Hemorrhage Control in Long-Duration Spaceflight." January 2005 J Am Coll Surg Vol. 200, No.1, 64-65.
2. Kirkpatrick Campbell et al. "Blunt Trauma and Operative Care in Microgravity: Review of Microgravity Physiology and Surgical Investigations with Implications for Critical Care and Operative Treatment in Space." May 1997 J Am Coll Surg 601.
3. Kirkpatrick Campbell et al. "Extraterrestrial Hemorrhage Control: Terrestrial Developments in Technique, Technology, and Philosophy with Applicability to Traumatic Hemorrhage Control in Long-Duration Spaceflight." January 2005 J Am Coll Surg Vol. 200, No.1, 67.
4. Jay G D, Lee P et al. "Comparison of Three Positions and a Mechanical Device." Aviat Space Environ Med Vol. 74, No. 11, November 2003, 1183–1189.
5. Kirkpatrick Campbell et al. "Extraterrestrial Hemorrhage Control: Terrestrial Developments in Technique, Technology, and Philosophy with Applicability to Traumatic Hemorrhage Control in Long-Duration Spaceflight. January 2005 J Am Coll Surg Vol. 200, No.1, 67.

PHOTOGRAPHS

JSC2006E33913 to JSC2006E33920
JSC2006E33442 to JSC2006E33448
JSC2006E33449 to JSC2006E33450
JSC2006E33456 to JSC2006E33457
JSC2006E33531 to JSC2006E33534

VIDEO

- Zero G flight week Aug. 7-11, 2006, Master: DV0649

Videos available from Imagery and Publications Office (GS4), NASA/JSC.

CONTACT INFORMATION

Mitchell R. Roth, BoonShoft Museum
mroth@boonshoftmuseum.org

TITLE

Undergraduate Program Flights – The Effects of Gravity on Enzymatic Reaction Rates

FLIGHT DATES

August 8 – 9, 2006

PRINCIPAL INVESTIGATORS

Timothy Ritter, University of North Carolina at Pembroke
Charlotte Branch, University of North Carolina at Pembroke
Megan Grimsley, University of North Carolina at Pembroke
Brandon Locklear, University of North Carolina at Pembroke
Janet Sanford, University of North Carolina at Pembroke

CO-INVESTIGATORS

Siva Mandjiny, University of North Carolina at Pembroke

GOAL

The goal of this investigation was to determine if the reaction rate between a substrate and an enzyme depends on gravitational force.

OBJECTIVES

The question we were investigating with this project was the following: "Does molecular recognition depend on gravitational force?" Our original hypothesis was that the buoyancy-driven convective flow within the fluid would have an effect on enzymatic reaction rates. To test this hypothesis, the University of North Carolina (UNC) at Pembroke/University of North Carolina at Charlotte team conducted an enzyme/substrate reaction in both the 0g and 2g portions of the parabolic curves flown by NASA's C-9 aircraft. This experiment was performed to test how both increased and decreased gravitational fields affect the enzymatic activity of biological fluids. A second experiment was also conducted as a part of our outreach program. The results from this second experiment clearly show how the 0g and 2g fields affect the motion of an object falling through a translucent viscous fluid.

METHODS AND MATERIALS

To investigate enzyme reaction rates, we studied the reaction between a glucose solution (0.4 g dissolved in 10 mL distilled water) and a reagent composed of glucose oxidase (GOD) and peroxidase (POD). To show whether the reaction happens or not, a colorizing agent, O-dianisidine, is contained in the GOD/POD reagent. The colorizing agent acts as an indicator when it reacts with glucose and turns a shade of pink. The reaction was stopped by injecting a denaturing chemical, hydrochloric acid (HCl), to stop the reaction. The level of reaction between the glucose and GOD/POD for each sample is determined by measuring the absorption levels of the solution.

During the flight, both experiments were housed within a double-walled glove box (Figure 1), and access to the equipment was provided by heavy-duty industrial rubber gloves. The Measuring Enzyme Activity (MEA) apparatus is shown in Figure 2.

Figure 1. (Upper) Glove box with mounting bar inside. Note: top is not on glove box and cameras are not mounted. (Lower) Mounting bar removed from glove box to show 2 kinematics tubes and 12 MEAs.

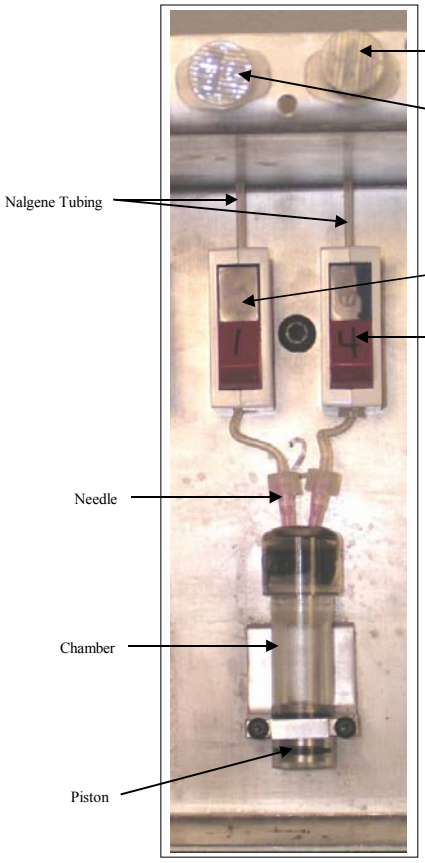

Figure 2. Single MEA apparatus showing all the major components. There are a total of 12 MEAs mounted in glove box.

The primary components were two 10-mL syringes, two pinch valves, and the piston-in-cylinder chamber. At the beginning of the experiment, one of the syringes contained 1.0 mL of β-D glucose, the other syringe contained 4.0 mL of 1 molar HCl, and the chamber contained 2.0 mL of the GOD/POD reagent. As the aircraft entered the 0g portion of the flight, pinch valve #1 was opened, the contents of the corresponding syringe were injected into the GOD/POD reagent, and the pinch valve was closed. Just before the aircraft came out of the 0g portion of a parabola, pinch valve #2 was opened, its contents were injected into the chamber, and then this pinch valve was closed. The same process was followed during the 2g portion of several parabolas.

The kinematics apparatus is shown in Figure 3. The primary components are a clear cylinder, a viscous fluid, and a steel ball. During the 0g or 2g portion of the parabolas, the ball was lifted to the top of the tube, using a strong magnet, and released. A video camera captured all of the repetitions of this experiment during both flight days.

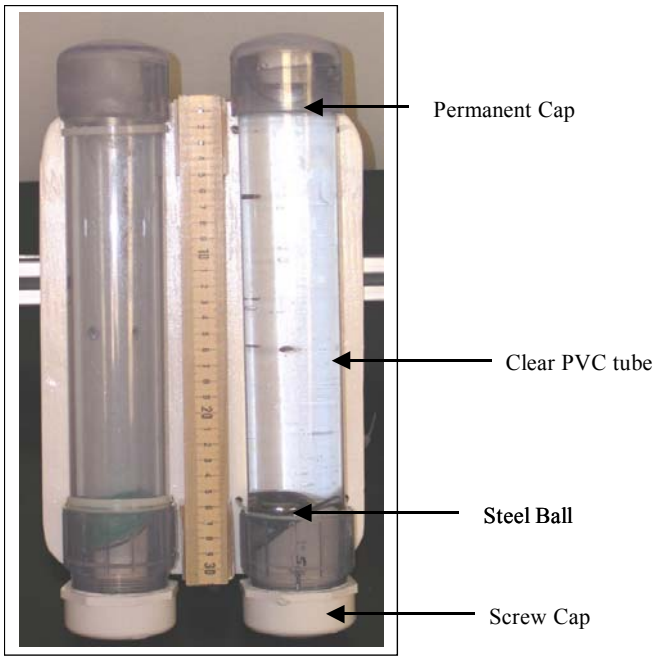

Figure 3: Kinematics Tubes shown on mounting board with meter stick in between.

RESULTS

To make the absorbance measurements in a timely manner, the team brought a spectrophotometer to Houston. Measurements were made on the 12 samples obtained from each flight, a total of 24 samples, immediately after the equipment was offloaded from the C-9 aircraft. During each flight, eight samples were created in 0g and four in 2g. Of the sixteen 0g samples obtained, five (two from the first flight group and three from the second) were determined to be unusable. The main reason for this was that mixing occurred outside of the 0g portion of the flight due to equipment difficulties. Of the eight 2g samples obtained, all four of the samples from the first flight group were usable while the four samples from the second flight

group were unusable. In this case the second flight group allowed the reactions to continue for a period of about 50 seconds, which was clearly outside the 2g window. The remaining valid measurements are shown in Figure 4.

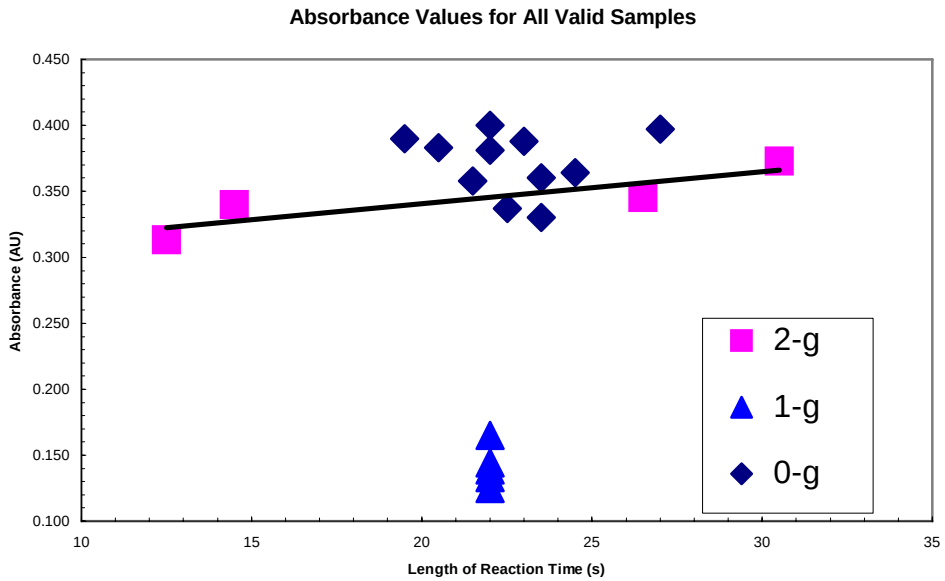

Figure 4. Plot of absorbance as a function of reaction time for the glucose-GOD/POD reaction. Both 0-g and 2-g measurements are shown. The linear fit is only to the 2-g data points.

To create the ground truth samples, the team waited until we returned to the laboratory setting at UNC Pembroke. Here the video of all 24 reactions was carefully observed. Each sample was determined to be either a 0g or a 2g sample and the exact timing of each reaction was recorded. From these data, five 1g samples were created using the average reaction time, 22 seconds, of the 0g samples. These reactions were conducted using the actual flight hardware to duplicate the conditions of the flight samples. The absorbance levels of these five samples were measured and the data are displayed, along with the 0g and 2g measurements, in Figure 4.

For the outreach experiment, we have already taken some of the video footage from the glove box video cameras and incorporated it into our outreach presentations. These video clips clearly show the metal balls suspended in the fluid during the 0g portion of the parabola and accelerating at a greater rate during the 2g portions. The two clips have been presented during several outreach presentations and have really been a surprise to the audience. We hope to analyze the actual rate of fall to determine both the velocity and acceleration of the object and also include these data in the presentations.

DISCUSSION

In Figure 4 the 0g data do not directly overlap the 2g data. This greater spread in the 2g data occurred because the hypergravity portion of each parabola is not as clearly defined as the 0g

portion. This is to be expected since the C-9 program is geared toward microgravity research, not 2g experiments. However, if a linear fit is applied to the 2g data, the line runs through the 0g data points. While the line is in the lower portion of the 0g grouping, it is clearly within the spread of the data and within the error limits on the 0g data. The average absorbance for the 0g samples shown in Figure 4 is 0.37 and the average of the four 2g measurements is 0.34. Therefore, from these results we must conclude that there was no significant difference in the reaction rates between the 0g and 2g samples.

The absorbance measurements of the five 1g samples that were produced after flight are shown in comparison with the 2g and 0g measurements in Figure 4. The average absorbance value of these samples was 0.14, clearly much lower than either the 0g or 2g data. As of the time this report is being written, we are trying to determine why this large difference occurred. We do not attribute this effect to a difference in the reaction rate due to the 1g gravitational field. Currently, we believe the reason for the significant difference is a temperature variation of the GOD/POD reagent between the flight samples and the ground truth samples. The GOD/POD is kept refrigerated when not in use. In the lab setting there is about a one-half-hour lapse in time between removal of the GOD/POD from refrigeration and performance of the experiment. During this time the reagent is in a room-temperature environment. In the case of the flight samples, however, there was a lapse of several hours between refrigeration and mixing due to the required loading process of the equipment for flight. Also, the temperature on the C-9 aircraft before flight is well above room temperature. It is our thought that the warming of the reagent had an effect on the reaction rates in the flight samples. As stated above, we are currently testing the validity of this explanation.

CONCLUSION

In this experiment we looked at the reaction rates of a glucose solution with a GOD/POD reagent in 0-g, 1-g, and 2g environments. The data for the 0g and 2g samples indicate that there is no gravitational influence on the reaction rate between these two materials. The 1g ground-truth samples created for this report were found to yield drastically different absorbance levels despite the fact that they were produced under conditions similar to those of the flight samples. We have proposed an explanation for this difference, and we hope that continued studies will shed new light on the energetics of this enzyme/substrate reaction.

REFERENCES

Berg, J.M., Tymoczko, J.L., Stryer, L., *Biochemistry*, 5th ed., W.H. Freeman and Co., New York, 2002.

Campbell, N.A., Reece, J.B., Mitchell, L.G., Taylor, M.R., *Biology: Concepts and Connections,* 4th ed., Benjamin Cummings, CA, 2003.

Faye, W.O., Lemke, T.L., Williams, D.A., *Principles of Medicinal Chemistry*, 4th ed., Williams and Wilkins, Philadelphia, 2002.

PHOTOGRAPHS

JSC2006E33459
JSC2006E33463 to JSC2006E33468
JSC2006E33491 to JSC2006E33492
JSC2006E334998 to JSC2006E33599
JSC2006E33501 to JSC2006E33502
JSC2006E33510 to JSC2006E33511
JSC2006E33513
JSC2006E33515
JSC2006E33520
JSC2006E33522
JSC2006E33524
JSC2006E33886
JSC2006E33892
JSC2006E33903 to JSC2006E33910

VIDEO

- Zero G flight week Aug. 7-11, 2006, Master: DV0649

Videos available from Imagery and Publications Office (GS4), NASA/JSC.

CONTACT INFORMATION

Dr. Timothy M. Ritter
Dept. of Chemistry and Physics
University of North Carolina at Pembroke
Pembroke, NC 28372
tim.ritter@uncp.edu.

TITLE

Undergraduate Program Flights – Volume and Mass Measurement of Liquids in Microgravity for Urine Analysis

FLIGHT DATES

August 15 – 16, 2006

PRINCIPAL INVESTIGATORS

Thierri Callier, Dartmouth University
A.J. Chammas, Dartmouth University
Edward Chien, Dartmouth University
James Preston, Dartmouth University

GOAL

The weightless environment of long-term spaceflight leads to bone loss as calcium leaves bone and is excreted into the urine. Measurements of urinary calcium excretion can be used as a marker for bone loss, helping to determine the effectiveness of bone loss countermeasures. Measuring urinary calcium output requires measurement of urinary calcium concentration and volume. The goal of our project is to contribute to solving the problem of bone loss by developing methods for measuring urine volume in space (Buckey).

OBJECTIVES

The aim of our project is to create two simple, robust, low-budget methods for determining the volume of a urine sample and to evaluate the performance of each device. Both of our methods rely on measurement of the mass of the urine sample, which is divided by the density of water to obtain our volume measurement. The first approach that we have devised determines sample mass by measuring the centripetal acceleration of a sample rotating at a known angular velocity and radius. The second approach determines sample mass by measuring the initial acceleration of a sample attached to a spring.

METHODS AND MATERIALS

Theory

In both of our approaches, we measure mass of the sample and then arrive at a volume estimate by assuming a constant density for urine. The density of urine differs from that of water by up to 2%, introducing 2% of error into our final volume estimates.

Centripetal Approach

In this approach, our device depends on measurement of the centripetal force on a rotating sample to obtain a mass measurement. The principle behind this is the fundamental relationship between the mass of a rotating object, the angular velocity of that object, the radius of its orbit, and the magnitude of the centripetal force on the object. This relationship is described by the following equation and diagram:

$T = M\omega 2r$

T = magnitude of centripetal tension force
M = mass of object
ω = angular velocity of rotation
r = radius of object's orbit

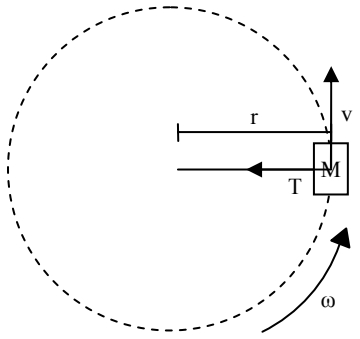

In our device, the object is the bag of urine/water. However, our model will be a little more complicated, because we have a linear scale to measure the tension force along the string. The model is described in the following diagram.

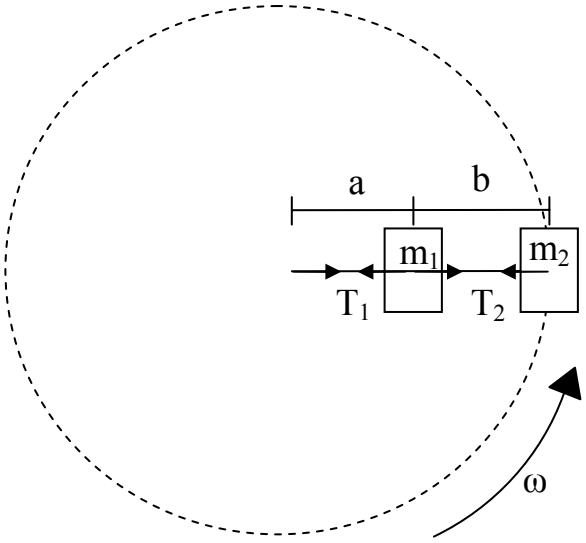

Knowns:

m1 = mass of object 1 (scale)
m2 = mass of object 2 (urine sample)
ω = angular velocity of the system
a = distance from axis of rotation to center of mass of object 1
b = distance from center of mass of object 1 to center of mass of object 2
T1 = magnitude of the tension force on the connection between the axis of rotation and m1
T2 = magnitude of the tension force on the connection between m1 and m2
T1 = mω2r
    m = mass of the system = m1 + m2
    ω = angular velocity of the system = ω
    r = distance from axis of rotation to center of mass of the system
    = (m1a + m2b) / (m1 + m2)
Thus, T1 = ω2(m1a + m2b)
T2 = mω2r
    m = m2
    ω = ω
    r = a + b
Thus, T2 = m2ω2(a + b)

Due to the nature of our scale, it measures only the tension force, T2. It is this measurement that allows us to obtain our mass measurement.

Scale reading = T2
m2 = mass of urine sample = T2 / (ω2(a + b))

Spring Approach

In this approach, our device depends on a measurement of the initial acceleration of a sample when it is attached to a spring with a known spring constant. The mass of the sample can be found by using Newton's second law (force = mass × acceleration) and the well-known equation for the magnitude of the force exerted by a spring (force = spring constant × spring extension from equilibrium).

Knowns:
a = initial acceleration of sample
k = spring constant of spring
x = spring extension from equilibrium position at release

Force on object = force exerted by spring = kx = ma
Thus, m = kx/a

Device and Materials

Centripetal Approach

- Chatillon DFS-0025 force gauge
- Wooden rod (1″ thick, about 9″ long; used as axis of rotation)
- 2 screw eyes
- Washer and bolt to keep screw eye from escaping the axis of rotation
- Wooden board (1/2 inch thick and as wide and long as the force gauge)
- Fishing line
- 4 samples of "urine" (water) of varying mass
- Net

The device is pictured below (Figure 1) with one of the sample masses.

Figure 1. Device for centripetal approach, with a sample mass (left).

The device is operated by two people. One person spins the device in a vertical plane parallel to that of the user's torso and the other person holds the metronome and helps to maintain a constant angular velocity. The spinner was held to the floor by a strap across the calves and knelt

while operating the device in flight. The person spinning the device brings it to the desired angular velocity, using the metronome as a guide, and spins for as much time as possible before the call for the end of the parabola. The force gauge was set up to time-average the force measurements once they breached a set threshold force.

Spring Approach

- Wooden board for bottom support, 1.5 x 3 feet, 1 inch thick
- 2 aluminum self-machined clamp supports, 6 inches tall
- Spring: k = 106 = 66.168 N/m, 11 inches long
- Accelerometer attached to Go! Link adapter connected to laptop
- Wooden box, 4x5x6 inches
- See Figure 2 for specifications on guide rail and rail block

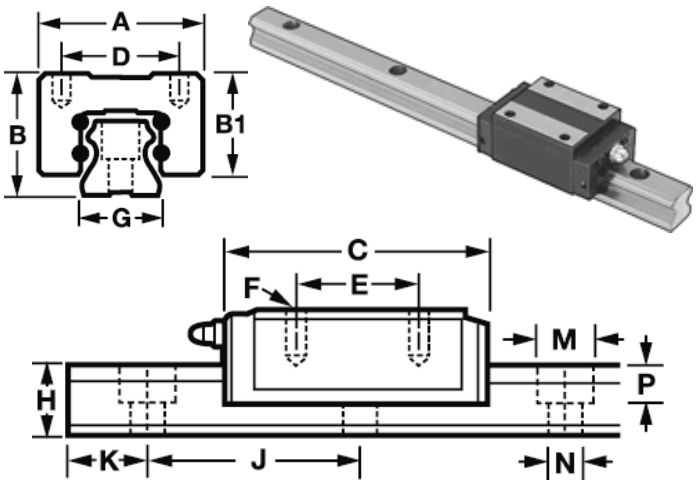

	Guide Block Dimensions (mm)							Rail Dimensions (mm)									
Dynamic Load Cap., lbs.	(A)	(B)	(B1)	(C)	(D)	(E)	Mtg. Holes, Dia. x Dp. (F)	(G)	(H)	(J)	(K)	(M)	(N)	(P)	Available Lengths	Guide Blocks Each	Rails Per mm
Threaded Blind-Hole Guide Blocks and Rails																	
1,872	34	28	23.3	57	26	26	M4 x 5	15	15	60	20	7.5	4.5	5.3	220, 460, 820, 1600	6709K12	6709K33

Figure 2. Device for spring approach. **NB**: rail is 820 mm long

The device is operated in the following way. First, the sample (within a bag) is loaded into the box. The box is closed after the bag's position in the vessel is secured. The accelerometer must be connected to Go-Link and the laptop with the software running properly. The testing is initiated via the laptop, and the operator pulls on the vessel until the spring is stretched 40 cm, then releases it gently and awaits the acceleration reading. Only the initial acceleration peak is considered in determining sample mass. The mass of the bag and vessel is considered in mass determination as well.

RESULTS AND DISCUSSION

Centripetal Approach

Out of 30 parabolas, we were able to get readings from 18 parabolas. We adjusted both the threshold force and the angular velocity throughout the flight. The mass of the samples is displayed in Table 1, next to the data from our trials. The total sample mass includes the weight of everything attached to the force gauge (which it would then measure), such as the plastic bags and netting. The maximum force, given by the gauge, is the maximum force measured while the tension is above the threshold and the gauge is time-averaging values. Several maxima were, in fact, lower than the average force; some of the forces were also lower than the threshold values. Neither of these should be possible according to our understanding of how the gauge is designed to operate; they may be anomalies or a result of the zero-gravity environment's effect on the gauge.

Table 1. Forces obtained using the centripetal approach, and mass of samples.

Trial	Angular Velocity (rpm)	Force (N)	Maximum Force (N)	Threshold Force (N)
A1	60	14.50	10.95	6.00
A2	60	13.55	16.50	6.00
A3	80	11.26	10.69	6.00
A4	80	5.27	14.35	6.00
A5	80	2.56	2.79	6.00
B1	80	1.10	1.65	1.00
B2	80	0.32	0.00	1.00
B3	100	0.92	50.00	1.00
B4	100	24.00		1.00
B5	100	0.07	0.00	1.00
B6	100	0.06	0.00	1.00
B7	100	39.44	50.18	15.00
B8	100	9.95	16.87	15.00
C1	100	39.96	85.86	25.00
C2	100	47.07	70.42	25.00
C3	100	25.14	30.15	25.00
C4	100	50.53	76.81	25.00
C5	100	57.88	74.80	25.00

Sample	Sample Mass (kg)	Water Mass (kg)
A	1.030	0.924
B	0.563	0.464
C	0.765	0.659

Displayed below (Table 2) are the average values of each parabola compared with the theoretical values. For both A and B, because angular velocity was adjusted midway, only the data obtained with the same angular velocity were averaged. The expected force was found using $F = m\omega 2r$, where we convert the units of rotations per minute to radians per second using ω = (angular velocity in rpm) / $60*2\pi$.

Table 2. Average values of each parabola compared with the theoretical values.

Parabola	Radius of Center of Mass (m)	Sample Mass (kg)	Angular Velocity (rpm)	Expected Centripetal Force (N)	Average Measured Force (N)	Error (N)	Error (%)
A	0.63	1.030	60	25.617502	14.025	-11.5925	-45.2523
B	0.63	0.563	100	38.896045	12.40667	-26.4894	-68.103
C	0.63	0.765	100	52.851642	44.116	-8.73564	-16.5286

Unfortunately, none of these are very accurate, but there are some good data. Shown below are the averages of the three samples, all of the trials using the third sample, and the averages of all data from the trials that fell within 15% of the expected value. These last two (no datum from the first trial was within 15%), whether coincidentally or not, are quite accurate compared to the rest of the data. This could lead to optimism about the data, but B′ consists of only one value and C′ of only three.

Table 3. Averages of the three samples, all of the trials using the third sample, and the averages of all data from the trials that fell within 15% of the expected value.

Sample	Expected Centripetal Force (N)	Average Measured Force (N)	Error (N)	Error (%)
A	25.6175	14.025	-11.5925	-45.2523
B	38.89605	12.40667	-26.4894	-68.103
C	52.85164	44.116	-8.73564	-16.5286
C1	52.85164	39.96	-12.8916	-24.3921
C2	52.85164	47.07	-5.78164	-10.9394
C3	52.85164	25.14	-27.7116	-52.4329
C4	52.85164	50.53	-2.32164	-4.39275
C5	52.85164	57.88	5.028358	9.514099
B'	8.887977	38.89605	0.543955	1.398483
C'	52.85164	51.82667	-1.02498	-1.93934

Therefore, we can say that this method may be more accurate than our trials would first suggest, but there are not enough data to prove it.

Spring Approach

Table 1. Test runs in normal gravity and microgravity.

Liquid 1g	**Empty**	**100 g**	**200 g**	**300 g**	**500 g**
1		21.87	19.91	18.73	18.4
2		22.1	21.4	19.95	17.31
3		21.47	20.87	19.36	17.7
4		23.21	20.99	21.1	18.7
5		22.5	21.33	19.78	16.8
Avg	24.729	22.23	20.9	19.784	17.782
Liquid 0 g	**Empty**	**100 g**	**200 g**	**300 g**	**500 g**
1	28.67	24.34	22.31	17.65	17.2
2	24.64	22.17	19.5	20.3	18.3
3	24.15	22.76	23	20.2	19.2
4	23.85			22.04	
Avg	25.3275	23.09	21.60333	20.0475	18.23333
Mass	**955**	**1055**	**1105**	**1205**	**1405**
1g avg	24.729	22.23	20.9	19.784	17.782
0g avg	25.3275	23.09	21.603	20.0475	18.233

The first table includes sample readings taken the day of the flight in normal gravity. The second contains the results of our runs in microgravity.

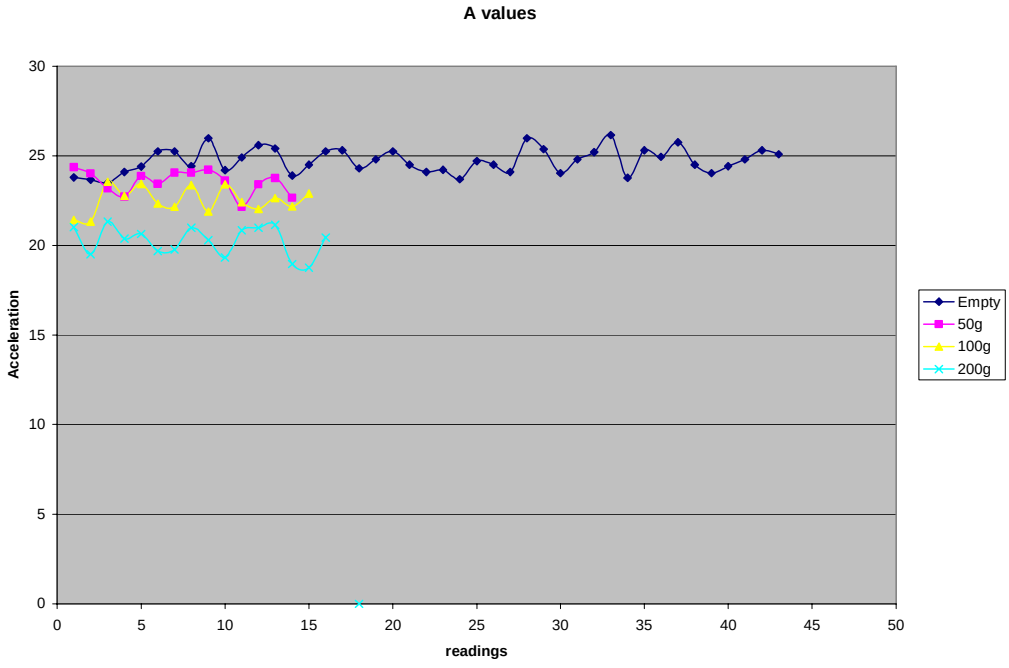

Figure 1. Acceleration readings with various masses in normal gravity.

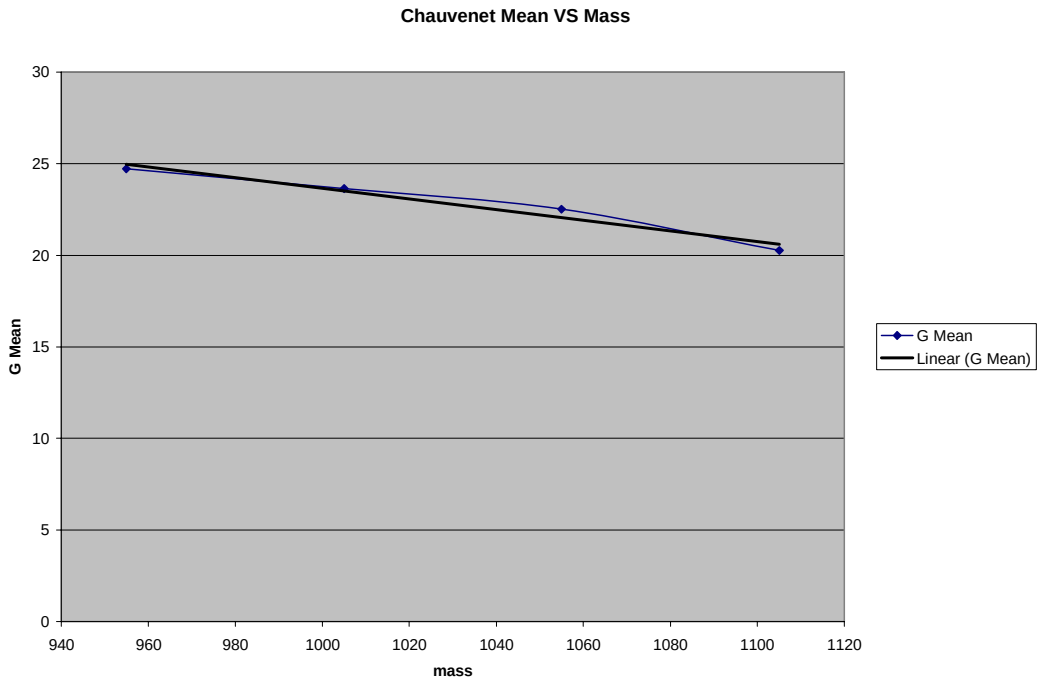

Figure 2. Average acceleration values for each mass. The acceleration values used were determined with Chauvenet's method.

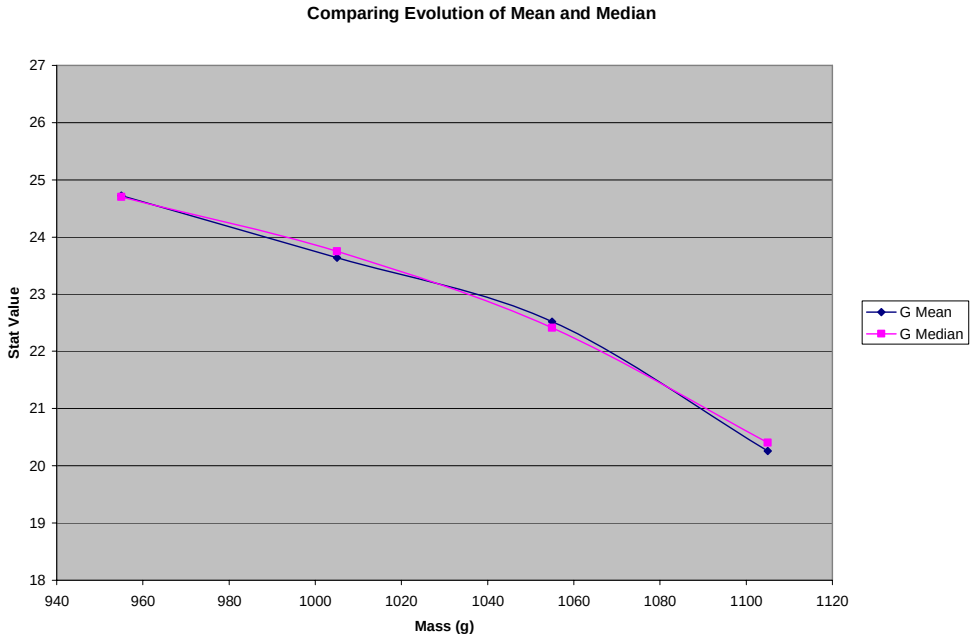

Figure 3. The evolution of mean and median with mass.

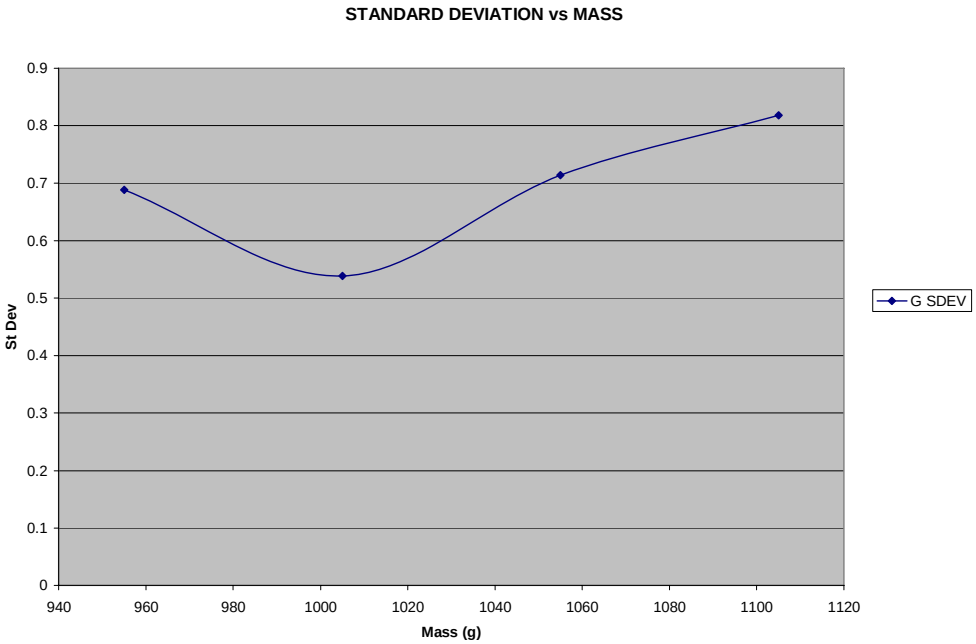

Figure 4. Evolution of the standard deviation of our results versus mass.

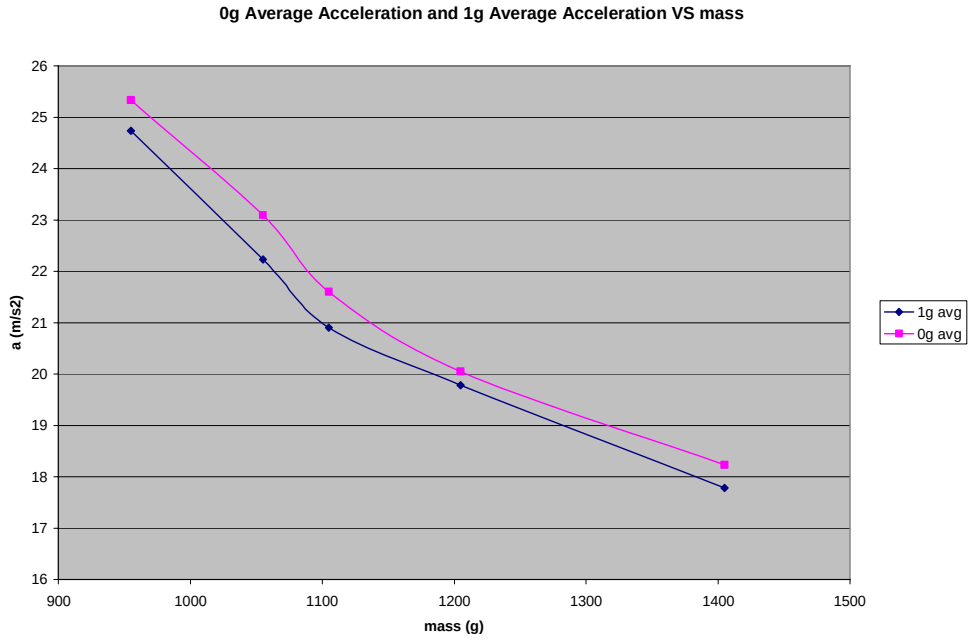

Figure 5. Results in normal gravity (1 g) and microgravity.

In Table 1 and Figure 1, we see that the measured acceleration decreased as the tested mass increased. The individual data points in Figure 1 give an idea of the precision of the device.

Figure 2 shows the average acceleration values we get for each mass. The acceleration values used were determined with Chauvenet's method.

Figure 3 shows the evolution of both mean and median with mass. They have similar trends, which further verifies the accuracy of our results.

Figure 4 shows us the evolution of the standard deviation of our results versus mass, and gives us an idea of the evolution of the device's precision as we measure more mass. It shows an upward trend. We attribute the dip at 1000g to a small number of test runs.

We compare our results in normal gravity and microgravity in Figure 5. The average readings were slightly higher in 0g. This is to be expected as the force of friction is decreased in microgravity.

CONCLUSION

Centripetal Approach

In conclusion, we found that our device is not very accurate, but an average of many data points has the potential to give a reasonable estimate of sample mass. A refinement of test procedure and more trials might have resulted in more accurate averages. Indeed, in practice astronauts could perform many trials and adjust their use of the device, as they would have more than thirty 15-second intervals of 0gravity. With regard to implications for future research, I think we can definitively say that the accuracy of the device could improve greatly and development must not stop at this point. However, further development would require an abandonment of the goal of a simple, low-budget method unless the problem is approached from a different angle.

One idea that should be adopted in further development is a stable axis of rotation, which would allow a more stable measure of the centripetal force to be obtained. A stable connection between the axis of rotation and the sample mass could also help to stabilize force readings. If those two ideas were implemented, then the device would probably be heavier, would take up more space, and would be more expensive. To offset these losses, the device would need to be miniaturized. As mentioned in our purpose, we were originally trying to create a simple, low-budget method, but it seems that such a method is not feasible unless the problem is approached in a different manner.

Spring Approach

The results show that our device works in principle, because the mean accelerations decrease steadily as the measured mass increases. However, our measurements are not consistent or precise enough to be used for medical purposes. The variation of calcium concentration in blood is too small to be accurately determined using our device. Our results may not reflect the capabilities of our device because we did not collect good data during our flight due to one of the partners having motion sickness. A device operating along the same principles as ours could yield much better results with better equipment. We used a very basic accelerometer and a box that was not built for this device.

REFERENCES

Buckey, J. C. Jr. Personal correspondence: October 2005.

Buckey, J. C. Jr. "Preparing for Mars: The Physiologic and Medical Challenges*." *European Journal of Medical Research* (1999) 4: 353-356.

Knaus, Darin. Personal correspondence: October 2005.

Ohanian, Hans C. *Physics*, 2nd edition, Volume 1. U.S.A: 1985.

Tipler, Paul A. and Gene Mosca**.** *Physics for Scientists and Engineers*, Volume 1A: Mechanics**.** U.S.A: Susan Finnemore Brennan, 2003.

PHOTOGRAPHS

JSC2006E 34765 to JSC2006E34771
JSC2006E 34781
JSC2006E 34784 to JSC2006E 34786
JSC2006E 34792 to JSC2006E 34794

VIDEO

- Zero G flight week August 15 -16, 2006, Master: 721666

Videos available from Imagery and Publications Office (GS4), NASA/JSC.

CONTACT INFORMATION

Thierri Callier: Callier@dartmouth.edu
Abdallah Chammas: Abdallah.Chammas@dartmouth.edu
Edward Chien: Edward.D.Chien@dartmouth.edu
James T. Preston: James.T.Preston.jr@dartmouth.edu

TITLE
Vestibular Adaptation in Parabolic Flight

FLIGHT DATES
August 22 – 25, 2006

PRINCIPAL INVESTIGATOR
Mark Shelhamer, Johns Hopkins University

CO-INVESTIGATOR
Faisal Karmali, Johns Hopkins University

GOAL

To determine the neural mechanisms of human adaptation to parabolic flight.

OBJECTIVES

The purpose of this research study was to examine the ability of human subjects to adapt various behaviors (reflexive eye movements and orientation perception) to different conditions of gravitoinertial force (g level). The resulting information will be of value in determining how the brain processes gravity information, in learning how humans can maintain different adapted states in different g levels simultaneously, and in aiding the design of future spaceflight programs.

This set of flights was the fourth out of four planned weeks of flights for this NIH-funded project. We are now analyzing data from all the flights and preparing follow-up studies.

INTRODUCTION

On their first exposure to parabolic flight, many people experience motion sickness. Some subjects have been known to consider not returning to fly the next day. Their experience the second day, however, is usually considerably better than that of the first day; motion sickness is much less prevalent. The adaptation process is dramatic and rapid, and some of it seems to occur during the period between flights. This phenomenon demonstrates aspects of adaptation and consolidation. One question that immediately arises is this: does adaptation to parabolic flight involve adaptation to each separate gravity level (context-specific), or is there a more generalized adaptation to the overall flight experience (implying, for example, a non-g-specific change in sensory weighting)? We are studying this with a series of measurements before, during, and after flight, on sets of first-time fliers and experienced fliers.

This study consists of multiple related experiments to learn more about how the human nervous system adapts to different gravity levels. We are particularly interested in adaptation of responses mediated by the vestibular system, such as orientation perception and reflexive eye movements. These adaptive processes are important because impairments in sensorimotor performance might occur when astronauts undergo transitions between gravity levels. Some of these changes, and the adaptive processes that counteract them, may be similar to vestibular changes in aging and ill people on Earth. To investigate these changes, we measured oculomotor and perceptual responses in subjects exposed to various gravity levels, as provided by parabolic flight.

Our most prominent findings to date involve changes in torsional eye position. During the g-level changes of parabolic flight, changes occur in torsional eye position (ocular counterrolling, OCR). These changes can be markedly asymmetric [Markham & Diamond 1993, Markham et al. 2000]. Changes in torsional alignment may be caused by a decompensation of otolith asymmetry in unusual g environments; on Earth, the nervous system presumably compensates for natural asymmetries in otolith organ properties, but in hyper-g and hypo-g this compensation is inappropriate and produces torsional misalignment. A similar disconjugate change has been found during spaceflight [Diamond & Markham 1998].

METHODS AND MATERIALS

We carried out a mix of sensorimotor and perceptual measures designed to examine a range of physiological responses, from low-level reflexive through high-order perceptual. Each test is carried out in 1g flight and in both g levels of parabolic flight, early and late in each flight. Experienced fliers are tested for one flight, since they are expected to exhibit almost immediate adaptation. New fliers are tested over the course of three or four consecutive flights to monitor adaptive changes. All subjects fly without benefit of motion-sickness medication. There are six main tests:

1. Ocular counterrolling (torsion) with the head upright and tilted. Torsional position of each eye is measured with a high-resolution digital camera.
2. Translational vestibulo-ocular reflex (TVOR) during transient lateral head motions. Lateral head motions are imposed by the experimenter, and the resulting reflexive eye movements are measured with a head-mounted video system.
3. Pitch angular vestibulo-ocular reflex (AVOR). The oculomotor response to pitch head movements at about 0.1 to 1.0 Hz is measured with a head-mounted video system.
4. Vertical alignment (skew). Vertical alignment of the eyes is assessed with a high-resolution digital camera.
5. Subjective vertical. The subject's sense of "down" (percept of vertical) is assessed in two ways. For subjective visual vertical, the subject sets a small line on a pair of goggles to the perceived vertical. For "postural" vertical, the subject sets a small indicator rod to the subjective vertical while seated.
6. Roll vection. The subject views a large rotating disk, which produces a sensation of self-rotation in a direction opposite to that of disk motion. The head-mounted video system measures torsion and the subject reports the subjective sense of self-rotation (vection) with a joystick and a verbal rating.

RESULTS

Early results center on three of the six measures, in six subjects who had not previously flown in parabolic flight. The results confirm our earlier findings, as previously reported.

The first result involves static torsional (roll) eye position at different g levels. A general reduction in disconjugate torsion occurs from the beginning of the first flight to the end of the last flight, for each subject. The disconjugacy depends on g level, and this g dependence decreases with experience, but more slowly with the head tilted than with it upright. These results show that torsional disconjugacy is initially high but is reduced within the first flight, and the adaptation that occurs is recalled at the start of subsequent flights. Vertical disconjugacy (skew) exhibits a similar adaptive pattern.

The second result involves compensatory eye movements (VOR) during pitching motions of the head. During active sine-like head movements (~0.9 Hz, 20 deg), eye movements were recorded with a head-mounted video system and head movements with a rate sensor. Gain was computed as the total eye excursion divided by head excursion for each movement. The gain of this pitch VOR during active head movements depended on the instantaneous g level, but this dependence decreased with experience. Gains early in flight were reduced in 0g and increased at 1.8g. These

differences between 0g and 1.8g decreased with experience, showing that the system had adapted a proper response to each gravity state.

All responses showed a g-level dependence early in flight that decreased with experience. The rate of adaptation was different for each measure: ocular alignment (torsion and skew) adjusted the most rapidly, followed by the pitch VOR, then vection. Disconjugate torsion and skew rapidly decreased on exposure to parabolic flight, and adaptation was retained between flights. This reduction occurred at both 0g and 1.8g , suggesting that a central compensation for otolith asymmetry was operating at each g level. Pitch VOR gain initially decreased in 0g and increased at 1.8g , consistent with an otolith contribution to this response. The difference in gain between the g levels decreased with experience and eventually disappeared, showing that the different otolith contributions at the different g levels were correctly processed after adaptation. Adaptation was also faster for active than for passive pitch movements. Upon adaptation (and in experienced fliers), torsion, skew, pitch VOR, and vection were more properly calibrated at each g level, supporting the hypothesis that each response has a context-specific adaptation.

In addition to these results from our primary experiment, we continued to evaluate an eye-movement measurement device that should be of use in future parabolic flight investigations. This device uses a magnetic search coil that sits on the eye. Head-mounted transmitter and receiver coils induce energy in the eye coil and detect its re-radiation. The relative intensities of the voltages detected by the three orthogonal receiver coils reveal the orientation of the eye coil, and hence the position of the eye. A larger version of this device is used in many clinics and labs, but this smaller unit has great potential for use in other experiment environments such as parabolic flight. In these flights, one subject wore the eye coil and performed various head movements while eye position was measured. This device is still in the prototype stage, but we were able to obtain useful eye-position data, which indicates the value of this method for future studies.

DISCUSSION AND CONCLUSION

Although we have now flown all four out of a planned four weeks in this study, the data analysis is still in its early stages. Current analysis suggests that, in accord with the time course of overall adaptation to parabolic flight, the most low-level of the neural responses that we measured – torsion and skew – show adaptive changes very rapidly. Higher-level integrative responses – pitch AVOR and roll vection – show clear differences between g levels early in flight that become less distinct later or in subsequent flights. These results indicate that low-level responses such as ocular alignment and compensation for otolith asymmetry occur very rapidly, whereas responses that require integration of afferent information from several physiological sensors adapt more slowly. Furthermore, some of these adaptive effects take place in a context-specific manner, so that the responses are appropriate for each instantaneous gravity level, while remaining appropriate for 1g.

REFERENCES

A Berthoz, T Brandt, J Dichgans, T Probst, W Bruzek, T Vieville (1986) European vestibular experiments on the Spacelab-1 mission: 5. Contribution of the otoliths to the vertical vestibulo-ocular reflex. Exp Brain Res 64:272-278.

SG Diamond, CH Markham (1998) The effect of space missions on gravity-responsive torsional eye movements. J Vestib Res 8:217-231.

F Karmali, O Juhasz, M Shelhamer (2006) Adaptation due to repeated exposure to parabolic flight, of static torsional alignment and the pitch vestibuloocular reflex. Presented at the 2006 MidWinter Meeting of the Association for Research in Otolaryngology, Feb. 5-9, Baltimore MD.

JR Lackner, P DiZio (1993) Multisensory, cognitive, and motor influences on human spatial orientation in weightlessness. J Vestib Res 3:361-372.

JR Lackner, A Graybiel, WH Johnson, KE Money (1987) Asymmetric otolith function and increased susceptibility to motion sickness during exposure to variations in gravitoinertial acceleration level. Aviat Space Environ Med 58:652-657.

CH Markham, SG Diamond (1993) A predictive test for space motion sickness. J Vestib Res 3:289-295.

CH Markham, SG Diamond, DF Stoller (2000) Parabolic flight reveals independent binocular control of otolith-induced eye torsion. Arch Ital Biol 138:73-86.

DM Merfeld, LH Zupan, CA Gifford (2001) Neural processing of gravito-inertial cues in humans. II. Influence of the semicircular canals during eccentric rotation. J Neurophysiol 85:1648–1660.

DM Merfeld, LH Zupan (2002) Neural processing of gravitoinertial cues in humans. III. Modeling tilt and translation responses. J Neurophysiol 87:819-33.

MF Reschke, LN Kornilova, DL Harm, JJ Bloomberg, WH Paloski (1997) Neurosensory and sensory-motor function. In: CL Huntoon, VV Antipov, AI Grigoriev (eds), Space Biology and Medicine. Vol. III. Humans in Spaceflight. Reston VA: AIAA, pp. 135-193.

M Shelhamer, DS Zee (2003) Context-specific adaptation and its significance for neurovestibular problems of space flight. J Vestib Res 13:345-362.

ACKNOWLEDGMENT

This work was funded by NIH grant DC006090.

PHOTOGRAPHS

JSC2006E37656 to JSC2006E37684
JSC2006E37930 to JSC2006E37955
JSC2006E38010 to JSC2006E38011
JSC2006E38077 to JSC2006E38053
JSC2006E38282 to JSC2006E38292

VIDEO

- Zero G flight week August 21 - 25, 2006, Master: 721672

Videos available from Imagery and Publications Office (GS4), NASA/JSC.

CONTACT INFORMATION

Mark Shelhamer
Johns Hopkins University, School of Medicine
210 Pathology Bldg.
600 N. Wolfe St.
Baltimore MD 21287
mjs@dizzy.med.jhu.edu
410-614-6302

TITLE

Rapid Development of Colorimetric-Solid Phase Extraction Technology for Water Quality Monitoring: Evaluation of C-SPE and Debubbling Methods in Microgravity

FLIGHT DATES

August 22 – 25, 2006

PRINCIPAL INVESTIGATOR

Marc D. Porter, Arizona State University

CO-INVESTIGATORS

Torin McCoy, NASA, Johnson Space Center
April Hazen-Bosveld, Iowa State University
Bob Lipert, Iowa State University
John Nordling, Iowa State University
Chien-Ju Shih, Iowa State University
Lorraine Siperko, Arizona State University
Dan Gazda, Wyle
Jeff Rutz, Wyle
John Straub, Wyle
John Schultz, Wyle

NASA Photo: JSC2006E38269

GOALS

1. Develop procedures for manual manipulation of water sample collection bags to separate air/water mixtures effectively, thus enabling the collection of bubble-free 1 mL and 10 mL water samples in microgravity for the respective in-flight determinations of silver(I) and molecular iodine (I_2).
2. Verify the functionality of colorimetric solid-phase extraction (C-SPE) test methods in microgravity by demonstrating analyses for silver(I) and iodine using water samples consisting of dispersed air/water mixtures containing up to 50% air.
3. Begin to evaluate C-SPE procedures for total iodine and total silver analyses to be used on future C-9 test flights.

OBJECTIVES

Flight 1: Manual Bubble Mitigation and Syringe Filling

1. Evaluate manual bubble mitigation strategies for the 30 mL water sample collection bags used for silver(I) analysis and the 155 mL bags used for iodine analysis.
2. Determine a procedure for filling syringes with either 10.0 mL of bubble-free iodine water or 1.0 mL of bubble-free silver water from sample collection bags containing a dispersed 50/50 air/water mixture.
3. Evaluate the performance of bubble removal strategies by comparing the mass of liquid in 1 mL and 10 mL syringes filled in flight from sample collection bags with up to 50% air to that of the same syringes filled on the ground from bubble-free collection bags.

Flight 2: Silver(I) Analysis

4. Demonstrate agreement between ground and flight data from silver(I) C-SPE analyses.

Flight 3: Iodine Analysis

5. Demonstrate agreement between ground and flight data from iodine C-SPE analyses.

Flight 4: Evaluation of Reagent Introduction Procedures

6. Determine the amount of reagent drawn into a syringe from a reagent cartridge present in line between the sample collection bag and the syringe.

7. Determine the volume of air drawn into the syringe (that is, the effective dead volume of the reagent cartridge) and the volume of liquid drawn into the syringe when the plunger of the syringe is withdrawn to a pre-specified mark.

8. Evaluate procedures for removal of air from syringes filled by drawing liquid through an in-line reagent cartridge.

9. Determine the effectiveness of a variety of syringe filters in preventing air contained in the sample collection bag from entering the syringe.

MATERIALS AND METHODS

Instrumentation

Both in-flight and ground-based C-SPE measurements were made using BYK Gardener Color Guide spin d/8° diffuse reflectance spectrophotometers. All mass measurements were performed using a calibrated Mettler Toledo model AG205 analytical balance.

Silver(I)-Sensitive Membranes

A solution of 5-(4-(dimethylamino)benzylidene) rhodanine (DMABR) was prepared by dissolving 0.1523 grams (g) of DMABR in 50 mL of dimethyl formamide in a 250 mL volumetric flask. Solubilization required sonicating for ~5 min, after which the solution was brought to volume using methanol. A second solution was prepared by pipetting 3.073 g Brij-30 surfactant into a tared Nalgene bottle on a balance and bringing the total mass to 100.4 g with deionized water.

These solutions were used to impregnate 3M Empore SDB-XC (polystyrene-divinylbenzene) 47 mm extraction membranes. Each membrane was placed in an all-glass filter holder assembly (Millipore), and 10.0 mL of the DMABR solution was pipetted into the funnel. Next, a vacuum pump was used to apply a pressure differential across the membrane of ~1 inch of Hg to pull the solution through the membrane. After the DMABR solution had passed through the membrane, the pressure differential was maintained for another 10 s to remove residual liquid. The funnel then was separated from the filter holder and wiped clean with a methanol-wetted wipe to remove residual solution, which tends to form DMABR particulates when exposed to water. The cleaned funnel was reattached to the filter holder, and 5.0 mL of the Brij-30 solution was added via a pipette. A vacuum-derived pressure of ~3.5 inches of Hg was applied to pull this solution through the membrane. This pressure differential was subsequently increased to ~20 inches of Hg (the maximum attainable pressure differential) for 30 s to dry the membrane. After reagent impregnation, the membranes were allowed to dry further by storage for ~12 h in a closed drawer before being cut into 13 mm disks using a cork borer.

Iodine-Sensitive Membranes

A solution was prepared by dissolving 3.0112g poly(vinylpyrrolidone) (PVP; molecular weight = 10,000) in 50 mL of 1:1 methanol:water in a 100-mL volumetric flask. This solution was then brought to volume with 1:1 methanol:water. Iodine-sensitive membranes were prepared by passing 10.0 mL of this solution through an Empore SDB-XC membrane using the aforementioned vacuum filtration system. A pressure difference of ~3.5 inches of Hg was required to drive this solution through the membrane. Once the solution had passed, the pressure difference was maximized for 45 s to remove residual solvent and dry the membrane. These membranes were also stored for ~12 h in a dark drawer before being cut into 13-mm disks.

NaCl-Loaded Glass Wool and Paper Disks

Sodium chloride (NaCl) was used as a simulant for the introduction of reagent into water samples. Two different types of reagent disks were prepared. The first type, designed to simulate the Oxone-coated glass wool used in the analysis of total iodine [1], was prepared by evaporating

an aqueous solution of NaCl onto glass wool. A sheet of glass wool was cut to fit into a Petri dish 140 mm in diameter, and ~20 mL of a solution containing 4.00g NaCl in water was poured over it. The glass wool was then dried in a 105°C oven for ~2 h. The dried glass wool was subsequently cut into disks 13 mm in diameter, each containing ~34.5 mg NaCl.

The second type of NaCl disk was prepared from filter paper, which is used to introduce the colorimetric reagent in the analyses of formaldehyde [2] and nickel [3] by C-SPE. To prepare this type of disk, 50 µL of a solution containing 10.5 mg/mL NaCl (aq) was pipetted onto a 13 mm-diameter disk of Whatman #1 filter paper. The water was then dried at room temperature for ~12 h, yielding a NaCl-impregnated disk containing 0.5 mg NaCl.

C-SPE Cartridges

All C-SPE membranes and NaCl-coated media were prepared the day before their corresponding flight. A few hours before flight, the appropriate membranes or media were cut into 13 mm disks and loaded into Swinnex polypropylene filter holders. These filter holders have Luer fittings that readily form leak-tight connections with a syringe and waste collection bag. Additionally, the holders contain a Teflon gasket that defines the area of the membrane disk exposed to the water sample and forms an internal seal within the cartridge.

Silver(I) Solutions

Silver solutions were prepared in opaque Teflon bottles by diluting a silver(I) atomic absorption standard (Aldrich) with deionized water. Five solutions were prepared by pipetting a predetermined mass of the standard into a tared Teflon bottle on a balance and bringing the total mass to 100g. The actual silver concentrations, as determined by inductively-coupled plasma mass spectrometry (ICP-MS), were 0.000, 0.238, 0.478, 0.703, and 1.03 ppm.

Iodine Solutions

Iodine sample solutions were prepared gravimetrically by diluting the appropriate mass of a 100 ppm iodine stock solution (made by diluting a volumetric iodine standard solution [Fixanal, Riedel-de Haen] with deionized water) to 500g in a 500 mL opaque Teflon bottle. The actual iodine concentrations were determined by the Leuco Crystal Violet method [4] to be 0.000, 0.106, 0.302, 1.66, and 3.60 ppm.

PROCEDURES, RESULTS, AND DISCUSSION

Flight 1: Manual Bubble Mitigation and Syringe Filling

Procedures

Teflon sample bags (American Fluoroseal) were prepared to contain predetermined air/water mixtures. To mimic a silver(I) analysis, 30 mL-capacity bags were filled with 15 mL of air and 15 mL of water with two drops of red food coloring to enhance bubble visibility. To mimic an iodine analysis, 155 mL-capacity bags were filled with 20 mL of air and 60 mL of water with two drops of blue food coloring. During the microgravity portions of the first 10 parabolas, fliers worked in pairs to test various approaches for manipulating the sample bags (one type of bag per

pair) and to practice filling syringes using the method found to be the most effective. For simulating silver(I) analysis, 1 mL plastic, single-use syringes (Norm-Ject, Henke Sass Wolf) were filled from the 30 mL bags. For iodine, 10.0 mL samples were collected from the 155 mL bags using 10- and 25 mL glass syringes (SGE International Pty. Ltd.). If bubbles were observed, the syringe was overfilled and swung in an arc to drive bubble-free water to the plunger end of the syringe. The air was then pushed back into the sample bag as the plunger was adjusted to the 10.0 mL mark. During the second set of 10 parabolas, each pair of fliers debubbled bags and filled syringes, which were capped and returned to JSC for ground measurements of the collected water mass. The types of sample bags and syringes were then switched between the pairs of fliers and the process was repeated during the second half of the flight.

Each parabola began with dispersion of the air into the water phase, followed by a quick, vigorous fling of the bag in an arc to force liquid into the narrow tube at the exit valve. Then, various techniques of swinging the bag in arcs were tested to accumulate a bubble-free volume of liquid at the exit valve. These manipulations represent a manual form of centrifugation of the liquid in the bag. Extensions of this general theme included 1) attachment of plastic clamps to the bags that served to isolate the liquid from the gas phase after centrifugation; and 2) tests of an aspiration valve that was attached to a waste bag to remove the small plug of air introduced by the syringe inlet. All manipulations, from air dispersal through syringe filling, were performed in a single microgravity parabola. Figure 1 presents photographs from the in-flight fillings of 1- and 10 mL syringes from manually debubbled sample bags.

Figure 1. Left: 1 mL syringe filled in flight. Right: 10 mL syringe filled in flight.

Results

The accuracy and reproducibility of filling syringes from bags containing up to 50% air are given in Table 1. A total of twenty 1 mL samples were collected in flight, five by each flier. For the larger syringes, eight 10 mL and nine 25 mL syringes were successfully filled in flight out of a targeted 10 each. The missing samples resulted from the fact that each bag was only ~13% full when the final sample was collected, and obtaining a plug of liquid in bags with such a large void volume was a difficult task to accomplish in 25 s.

Table 1. Comparison of the mass of liquid in syringes filled in flight from bags containing air/water mixtures to the mass in syringes filled on the ground from bubble-free samples.

	1 mL syringe		10 mL syringe		25 mL syringe	
	Flight	Ground	Flight	Ground	Flight	Ground
Average Mass (g)	0.9932	1.0003	9.8983	9.9893	9.7680	9.9448
Std. Dev.	0.0177	0.0045	0.0686	0.0269	0.2503	0.0864
RSD	1.8%	0.45%	0.69%	0.27%	2.56%	0.87%
Error	-0.68%	+0.03%	-1.02%	-0.11%	-2.32%	-0.55%

As is evident from Table 1, manual bubble mitigation is very effective for the production of bubble-free water samples, facilitating the accurate and reproducible metering of liquids in microgravity. It is also important to note that these results were obtained when all manipulations were performed in a single, ~25-s microgravity period. We firmly believe that even closer agreement with ground data will be obtained on the International Space Station (ISS) or the Shuttle, where the relaxed time constraints will enable even more effective sample manipulation.

Discussion

The simplest procedures proved highly effective for the accurate and precise metering of liquids from sample bags containing air/water mixtures. We found that, although the aspiration valve assembly would generate bubble-free liquids in the syringes, the same results were obtained without the valve by rapidly pumping a filled syringe that contained a bubble back into the sample collection bag and refilling the syringe. Therefore, aspiration valves were not used to collect samples for the mass determination.

Clamps were also found to be effective for isolating a portion of bubble-free liquid in a section of the sample bag. However, good results were also obtained by simply making a clamp with one's fingers or by folding the bag. These procedures were found to minimize the time required for sample collection, ensuring that the entire process could be completed in the microgravity segment of a single parabola. We add that in each set of experiments, two fliers filled a single syringe. Since only one astronaut will be performing these tasks on the ISS or Shuttle, it may be preferable to use clamps to facilitate the withdrawal of samples without redispersing air into the liquid phase.

Flight 2: Silver Analysis

Procedure

Before this flight, 20 mL of each silver(I) solution was loaded into a 30 mL sample bag, followed by 15 mL of air. All sample bags, syringes (HSW 1 mL polyethylene syringes), and silver-sensitive membrane cartridges were color-coded for each concentration. Four replicate experiments were carried out at each sample concentration, both in flight and on the ground.

To identify the effects of microgravity on the analysis, ground and flight experiments were performed concurrently. The ground experiments mimicked both the thermal environment (~14-23 ºC) and the time constraints of the aircraft.

Notably, as the 1 mL samples were removed from each bag during flight, the liquid/air ratio in each bag decreased from ~57% when filling the first syringe to 53% when filling the last syringe.

Each flight consisted of four sets of ten parabolas. During the first few parabolas of each set, a 1-mL sample was collected from each bag. This task was accomplished by having one flier manipulate the bag to disperse air, and then manually debubble the sample bag in the manner determined during Flight 1. The same flier then held the bag while the partner flier attached a corresponding, color-coded syringe to the bag and filled it to the 1.0 mL mark. These syringes were capped and stored in a syringe holder firmly mounted to the flight table. With four fliers working in teams of two (Fliers 1 and 2 on Team 1 and Fliers 3 and 4 on Team 2), four syringes were filled in the first two parabolas.
On Parabola 3, the tasks changed. Team 1 stopped filling syringes and began the analyses of the syringe-loaded samples. Thus, Team 2 filled the fifth and final syringe for that particular set of ten parabolas, while Flier 1 passed one of the 1.0 mL samples through its corresponding color-coded cartridge. On Parabola 4, Flier 2 dried this membrane by using a syringe to pass 60 mL of air through the cartridge. On Parabola 5, Flier 3 opened the cartridge, mounted the bottom section, which contained the membrane, on the sample locator, and measured the spectrum of the disk with the hand-held diffuse reflectance spectrometer while Flier 4 recorded the sample number, cartridge color, and any observations about that sample.

This process was repeated until all five samples were analyzed, and the entire procedure was repeated for each of the four sets of ten parabolas. The data analysis of these results, which was completed on returning to JSC, included downloading the spectra to a laptop computer, converting reflectance data using the Kubelka-Munk function, *F(R)* [5], and plotting *F(R)* versus concentration.

Results

Four samples of each concentration were tested in both the ground and flight experiments. Figure 2 is a plot of all data collected, after Kubelka-Munk workup, in both sets of experiments. Table 2 lists the calibration equation, the correlation coefficient, and the calculated limit of detection (LOD) obtained from each experiment.

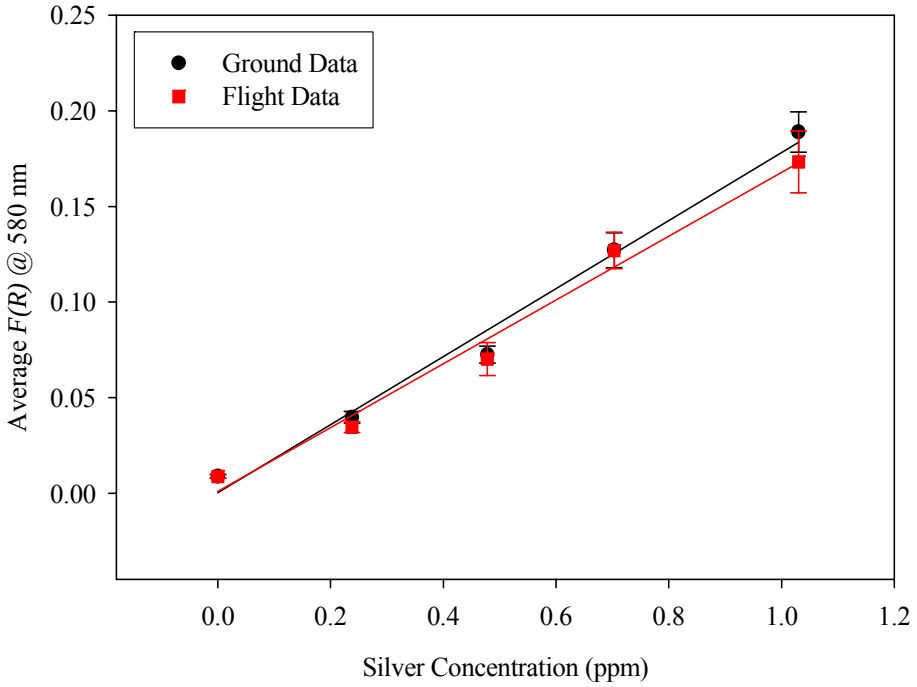

Figure 2. Comparison of the data from ground and flight testing of silver(I) by C-SPE.

Table 2. Comparison of the data from ground and flight testing of silver(I) by C-SPE.

	Calibration Equation	R^2	LOD (ppb)
Flight Data	[Ag+] = 6.00 *F(R)* – 0.0066	0.984	28.5
Ground Data	[Ag+] = 5.62 *F(R)* – 0.019	0.986	21.8

LOD, limit of detection.

Discussion

The agreement between the ground and flight results shown in Figure 2 for the analysis of silver by C-SPE is excellent. These results demonstrate that the entire analysis, from sample collection to data acquisition, can be reliably carried out in microgravity, thus indicating that the method is suitable for tests during spaceflight by deployment on the ISS or the Shuttle.

Although linear regressions were applied to the data for comparison purposes, a small, reproducible degree of non-linearity exists at the lower concentration range. The origin of this dependence is under investigation. As a consequence, the LOD was calculated by using the response of the blank and the lowest of the silver(I) concentrations tested, 0.238 ppm. Importantly, the ~30 ppb LOD for the in-flight data easily meets the limit imposed by NASA.

Flight 3: Iodine Analysis

Procedure

Before flight, five 155 mL color-coded sample bags were filled with different concentrations of iodine solutions. After preparation, each bag contained 60 mL of iodine solution and 20 mL of air, which enabled the collection of four 10 mL samples from each bag during the flight. During the course of the flight, the liquid/air ratio in each bag during the debubbling step ranged from 75% for the first sample to 60% for the fourth sample. In all other ways, the procedure for this experiment was identical to that used in the silver(I) flight.

Results

The data collected during the ground and flight experiments are plotted in Figure 3, while Table 3 shows a comparison between the ground and flight calibration equations. The limits of detection listed in Table 3 were calculated as described for the silver(I) experiment.

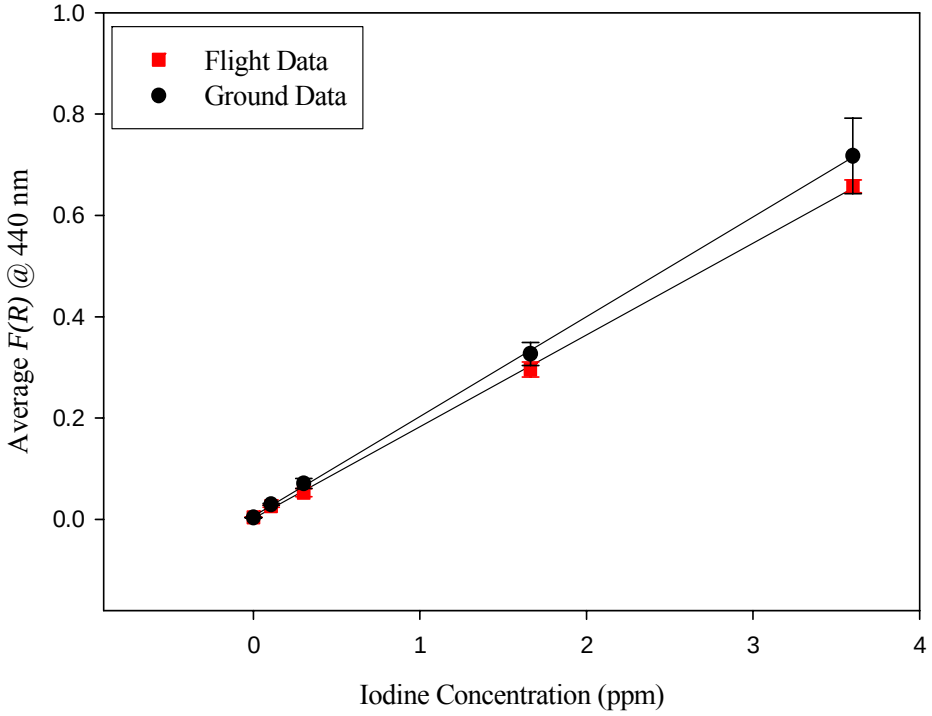

Figure 3. Comparison of the data from ground and flight testing of iodine (I_2) by C-SPE.

Table 3. Comparison of the data from ground and flight testing of iodine (I_2) by C-SPE.

	Calibration Equation	R2	LOD (ppb)
Flight Data	[I2] = 5.52 *F(R)* – 0.010	0.9996	7.3
Ground Data	[I2] = 5.09 *F(R)* – 0.033	0.9997	4.9

Discussion

As with the silver(I) results, the agreement between the ground and flight data for I_2 is excellent. The slight negative deviation in the data from the flight experiment, although well within the in-flight performance requirements, is attributed to two factors, acting alone or in concert. First, a very small, but not quantifiable, level of leakage of the iodine solutions from the cartridges was observed during flight. A loss of solution while metering the liquid through the membrane would, of course, result in a negative deviation in the response with respect to the ground data. We feel strongly, based on experiments carried out without the 25 s time limits imposed by C-9 testing, that this is an issue only when forcing the 10 mL liquid sample through the membrane at such a high rate. Second, the sample bags used for flight were filled before those used on the ground, thereby exposing the flight solutions to light for a longer period. Since iodine solutions are sensitive to light, the flight solutions may have degraded slightly more than the ground samples. Despite these concerns, which are of minimal importance given the excellent agreement between ground and flight data, these results indicate that the entire procedure for this analysis can be easily performed in microgravity with an extremely high level of effectiveness.

Flight 4: Evaluation of Reagent Introduction Procedures

Procedures

Filling Through Reagent Cartridges – The results from the first three flights have shown that bubble-free samples ranging from 1.0 mL to 10.0 mL can be collected into syringes from bags containing up to 50% air. However, some of the C-SPE methods we are developing for NASA, including those for total iodine, total silver, nickel, and formaldehyde [1-3,6], involve the use of a reagent cartridge in line between the sample bag and the syringe. The reagent cartridge contains an inert medium, such as glass wool or filter paper, that has been impregnated with, for example, an oxidizing agent, pH buffer, colorimetric reagent, or masking agent, which is then introduced into the solution as it enters the syringe. Because the reagent cartridge also contains an unknown dead volume of air, air enters the syringe even when samples are collected from a debubbled bag.

Several C-SPE analyses of this type are under development. These involve filling a 10 mL glass syringe (as for total iodine) or a 3 mL polyethylene syringe (as for total silver, nickel, and formaldehyde) through a Swinnex cartridge containing the reagent medium. For this flight experiment, several syringes were filled from debubbled sample bags through C-SPE cartridges containing either NaCl-impregnated glass wool or filter paper disks. The filled syringes were returned to the ground, where several performance metrics were determined, including the amount of NaCl dissolved by the liquid sample due to its in-flight passage through the reagent cartridge, and the amount of air introduced into the syringe by the cartridge dead volume.

During the first two sets of parabolas (parabolas 1-20), Fliers 1 and 2 filled 10 mL and 3 mL polyethylene syringes to the mark (3.0 or 10.0 mL) from debubbled sample bags containing deionized water. Five syringes of each volume were filled through NaCl-coated glass wool cartridges and five through NaCl-impregnated filter paper cartridges. Fliers 3 and 4 documented these proceedings with photographs and videos. These syringes were capped and returned to the ground-based laboratory where the amount of liquid collected in each syringe was determined

gravimetrically. This value was then used to calculate the cartridge dead volume, and the concentration of NaCl in each sample was determined by ICP-MS.

During parabolas 21-30, the four fliers broke into two-member teams to collect and debubble five samples through each type of cartridge. Fliers 1 and 2 collected five separate 10.0 mL samples using 10 mL glass syringes, while Fliers 3 and 4 collected 1.0 mL samples using 3 mL polyethylene syringes. To collect a sample, the flier first pulled the plunger well beyond the position marked for the intended sample volume. The syringe was then detached from the cartridge and swung in an arc to force the liquid away from the tip while forcing the entrapped air toward the tip. The air was subsequently expelled, along with excess liquid, into a waste bag by the forward displacement of the plunger. Finally, the debubbled syringe was capped and stored for ground analysis.

Debubbling by Filtration – For this set of experiments, a sample bag containing a mixture of air and water was connected to the outlet of a commercially available syringe filter, and the filter inlet was attached to a 5 mL syringe. During the microgravity portion of the flight, attempts were made to withdraw a 5 mL sample of water through several types of filters into the syringe. Photographs and video of the process were again taken to assess the effectiveness of each cartridge in preventing air from entering the syringe.

Results

Filling Through Reagent Cartridges – Results from the gravimetric analyses of the samples collected in flight are given in Tables 4 and 5. The average volume of liquid contained in the 3 mL and 10 mL syringes that were capped as filled (that is, not debubbled) are given in Table 4. The volume of liquid was calculated from its mass using the density of water (1 g/mL), and the volume of air introduced into each syringe by the reagent cartridge was obtained by subtracting the liquid sample volume from the total volume (either 3.0 or 10.0 mL). The results from samples that were manipulated to collect bubble-free 1.0 and 10.0 mL samples are presented in Table 5.

Table 4. Average volumes of liquid and air introduced into 3 mL and 10 mL syringes when filled to the mark through reagent cartridges.

	3 mL Syringes				10 mL Syringes			
	Glass Wool		Filter Paper		Glass Wool		Filter Paper	
	Liquid	Air	Liquid	Air	Liquid	Air	Liquid	Air
Average Volume (mL)	1.20	1.80	1.85	1.15	8.093	1.907	8.52	1.48
Std. Dev.	0.46	0.46	0.32	0.32	0.083	0.083	0.16	0.16

Table 5. Average volumes of 1.0 and 10.0 mL samples collected by filling 3 mL and 10 mL syringes through reagent cartridges and manually debubbling.

	3 mL Syringes		10 mL Syringes	
	Glass Wool	Filter Paper	Glass Wool	Filter Paper

Average Volume (mL)	1.016	0.999	9.807	9.60
Std. Dev.	0.016	0.034	0.078	0.40

As previously mentioned, the concentration of sodium in each sample collected during the flight was determined by ICP-MS analysis. The average concentration for each sample type is reported in Table 6.

Table 6. Results from ICP-MS analysis of sodium concentration in all samples collected through reagent cartridges in flight.

	3 mL Syringes				10 mL Syringes			
	Glass Wool		Filter Paper		Glass Wool		Filter Paper	
	As filled	Debubbled	As filled	Debubbled	As filled	Debubbled	As filled	Debubbled
Average [Na+] ppm	5184	4302	57	54	1165	1122	8.2	11.02
Std. Dev.	2238	1844	22	10	141	273	1.2	0.64

Debubbling by Filtration – No syringes were successfully filled through the syringe filters as the solution flow was either very slow or zero in all tests. These results are attributed to either the decreased ambient pressure in flight (which drives the water through the filter) or to the inability of the syringe filter to release the check valve on the sample bag.

Discussion

According to the data reported in Table 4, the addition of a reagent cartridge in line between the sample bag and the syringe introduces up to 1.9 mL of air during sample collection. In a few cases, the Luer slip fitting between the cartridge and the sample bag was not secure, causing those syringes to be filled with ambient air rather than liquid from the sample bag. This problem occurred with four of the samples, which were therefore excluded from the data reported in Tables 4–6. To avoid this problem in the future, cartridges with Luer-Lok fittings on both ends will be used.

Despite this minor issue, the data in Table 5 clearly show that, although filling through a cartridge introduces air into the syringe, it is possible to collect a bubble-free sample by removing the air from the syringe. Manually centrifuging the syringe by swinging it in an arc was a very effective method for removing air bubbles from a liquid sample in both the 10 mL and 3 mL syringes. Figure 4 shows the bubble distribution in a 3 mL syringe filled through a reagent cartridge containing glass wool, and the same syringe after manual centrifugation created a plug of air that could easily be passed into a waste bag, leaving a debubbled sample in the syringe.

The results of the ICP-MS analyses indicate that the glass wool introduces much more NaCl into the sample than does the filter paper. This is to be expected given that each glass wool disk contained about 70 times as much NaCl as a filter paper disk. However, the 3 mL syringes filled through the glass wool disks had NaCl concentrations 80–90 times higher than those filled through the filter paper disks. The difference in the 10 mL syringes was even greater, with the

glass wool producing NaCl solutions 100–140 times as concentrated as those produced by filter paper disks. Taken together, these data suggest that the glass wool is a more efficient means of reagent introduction than filter paper.

Figure 4. Left side: A 3.0 mL syringe after filling through a glass wool cartridge. Right side: Same syringe, after manual bubble manipulation, attached to waste bag for adjusting to 1.0 mL.

The variability in NaCl delivery, however, is also greater for glass wool than for filter paper. Two likely reasons for this increase in standard deviation are 1) the glass wool disks, which are prepared by the user, have far more variability in thickness, density, etc. than the filter paper, which can be used as received, and 2) the solution used to prepare the glass wool disks was a slurry and therefore not as uniform as the homogenous solution used to impregnate the filter paper. It is important to note also that syringes were filled at varying speeds to observe the effect, if any, on bubble introduction, and this could very well have contributed to the variation in reagent introduction with both types of media. It was determined that in future experiments, syringes should be filled slowly, as this increases reagent delivery and reduces bubble dispersion.

CONCLUSIONS

1. Manual manipulation of water sample bags is effective for air/water separation.
2. 1.0 mL and 10.0 mL samples of effectively bubble-free water can be collected in syringes in microgravity starting with water samples containing up to 50% air, the largest amount tested.
3. Silver(I) analyses performed in flight on samples collected from bags containing up to 47% air agreed with ground results obtained using bubble-free samples.
4. Iodine analyses performed in flight on samples collected from bags containing up to 40% air agreed with ground results obtained using bubble-free samples.
5. Both 3 mL and 10 mL syringes can be filled with bubble-free 1.0 mL and 10.0 mL liquid samples despite the introduction of up to 1.9 mL of air from a cartridge used to introduce reagents, an important first step in development of C-9 test procedures for total iodine, total silver, nickel, and formaldehyde analyses.

REFERENCES

1. D.B. Gazda, R.J. Lipert, J.S. Fritz, and M.D. Porter, *Analytica Chimica Acta* **2004**, *510*, 241-7.

2. A.A. Hazen-Bosveld, J.S. Fritz, and M.D. Porter, *35th International Conference on Environmental Systems, Rome, Italy,* SAE Technical Paper #2005-01-3063, **2005**.

3. D.B. Gazda, J.S. Fritz, and M.D. Porter, *Analytica Chimica Acta* **2004**, *508*, 53-9.

4. *Standard Methods for Examination of Water and Wastewater,* 18th ed., American Public Health Association: Washington, DC, 1992.

5. G. Kortum, *Reflectance Spectroscopy: Principles, Methods, Applications*, Springer: New York, 1969, pp. 106-16.

6. M.P. Arena, M.D. Porter, and J.S. Fritz, *Analytical Chemistry* **2002**, *74*, 185-90.

PHOTOGRAPHS

JSC2006E37595 to JSC2006E37655
JSC2006E37859 to JSC2006E37917
JSC2006E38012 to JSC2006E38052
JSC2006E38262 to JSC2006E38281

VIDEO

- Zero G flight week August 21 - 25, 2006, Master: 721672

Videos available from Imagery and Publications Office (GS4), NASA/JSC.

CONTACT INFORMATION

Marc D. Porter, Ph.D.
Arizona State University
The Biodesign Institute
1001 South McAllister
Tempe, AZ 85287
Email: marc.porter@asu.edu
Office: (480) 727-8598

TITLE
Experimental Microfluidic System

FLIGHT DATES
August 22 – 23, 2006

PRINCIPAL INVESTIGATORS
Steve Gonda, NASA Johnson Space Center
Christopher Culbertson, Kansas State University

GOAL

The ultimate goal of this project is to integrate microfluidic devices with NASA's space bioreactor systems. In such a system, the microfluidic device would provide real-time feedback control of the bioreactor by monitoring pH, glucose, and lactate levels in the cell media, and would provide an analytical capability to the bioreactor in extraterrestrial environments for monitoring bioengineered cell products and health changes in cells due to environmental stressors. Such integrated systems could be used as biosentinels both in space and on planet surfaces.

OBJECTIVE

To demonstrate the ability to interface bioreactor systems with microfabricated devices to repeatedly and reproducibly perform amino acid and cell media separations in 0, lunar, martian, and hypergravity (1.8g).

INTRODUCTION

Microfluidic, or Lab-on-a-Chip, devices are small platforms on which a complete chemical analysis can be performed. These devices consist of a series of small interconnecting channels (10μm deep and 40 to 200 mm wide) etched in glass or molded in polymers, through which fluids can be moved. The fluids can be controlled with electric potentials generating electric fields within the channels that move fluid electrokinetically, or by generating pressure differentials using a syringe pump or peristaltic pump that moves the fluid hydrodynamically. Using these two methods of controlling fluid flow, it is possible to generate devices that have multiple uses. For example, we have previously shown that it is possible to use hydrodynamic flow to rapidly move large numbers of cells or large particles, such as beads, through a focusing intersection much faster than if one were to use electrokinetic flow. On the other hand, electric fields allow the separation of differentially charged analytes using capillary electrophoresis, something hydrodynamic flow alone cannot accomplish. These devices provide many advantages over conventional benchtop-scale instrumentation as a result of their ability to integrate sample handling and sample processing operations with analyte detection on a single, monolithic substrate. Such integration allows the efficient automation of chemical analyses. In addition to automation and integration, microchips have several other inherent advantages over conventional chemical analysis instrumentation. These advantages include 1) the ability to perform faster separations with no loss in separation efficiency, 2) less reagent and sample consumption (< 1 mL / year), 3) less waste production, and 4) the ability to fabricate many parallel systems on the same device. Thus far, their performance has been either equivalent to or better than conventional laboratory devices in all cases investigated. They seem to offer the rare combination of better-faster-cheaper simultaneously, and their ability to manipulate reagents and reaction products “on chip” suggests the potential to perform virtually any type of “wet-chemical” bench procedure on a microfabricated device.

The advantages described above make these devices especially interesting for use in extraterrestrial environments where small, portable, rugged, and reliable devices capable of sustained remote automated operation will be required.

METHODS AND MATERIALS

The portable microfluidic device developed for these tests is contained in a Bud box enclosure (NBA10148), which has exterior dimensions of about 30 cm wide x 18 cm deep x 40 cm high. The microchips, in their custom-machined 2-part PMMA holder, were attached to an x-y positioning plate (ST1XY-S; Thor Labs Inc., Newton, NJ) and positioned above a microscope objective (CD-240-M40X; Creative Devices, Neshanic Station, NJ). This objective was used to focus the 473-nm excitation light of a diode pumped blue CrystaLaser (BCL-010; CrystaLaser; Reno, NV). The laser beam was reflected off a long-pass dichroic mirror (500 DRLP; Omega Optical, Brattleboro, VT) before being focused into the microchip channel by the microscope

objective. The fluorescence from the labeled amino acids was collected by the same microscope objective, passed through the dichroic mirror, a 1.0 mm pinhole, and a 545-nm band-pass filter (545ALP; Omega Optical, Brattleboro, VT) before being detected at a channel photomultiplier tube (PMT) (MD972; PerkinElmer, Fremont, CA). The PMT was powered by a 5-volt power supply. The gain was manually controlled by a potentiometer with a locking mechanism to prevent accidental change.

The high voltages used for making injections and performing the electrophoretic separations on the microchip were provided by two independent high-voltage power supplies capable of 125 mA outputs at up to 8 kV (C80; EMCO High Voltage Corp., Sutter Creek, CA). Each high-voltage (HV) power supply was powered by a 15-V DC source. The HV output was determined by a 0- to 5–V DC control signal provided by a National Instruments AO card (DAQ Card AO-2DC). Each power supply occupied only 19 cm^3 and weighed 51 g, making them very suitable for portable applications.

A mini-pump variable-flow peristaltic pump (Fisher Scientific) was used to provide pressure to decrease the time needed to completely switch samples. Sample switching was performed using flight-certified cell culture bags connected with a 4-port switching valve with PEEK tubing (UpChurch Scientific, Oak Harbor, WA) directly to the microchip.

The entire instrument was controlled and data were acquired using in-house written LabVIEW software operated on a Dell laptop computer.

Protocol

Amino acid solutions of arginine, serine, and glutamic acid were prepared at concentrations of 5 mM in 150 mM sodium bicarbonate buffer at pH 9. BODIPY® FL CASE ester dye (Molecular Probes, Eugene, OR) was diluted in dimethyl sulfoxide (DMSO) to a concentration of 10 mM. The amino acids were individually labeled by adding 900 µL of each amino acid solution to 100 µL of the reactive BODIPY® FL CASE dye solution. The run buffer was composed of 10 mM sodium borate. The reGFP (100 ng/mL) control medium was acquired from Dr. Steve Gonda's lab (NASA).

RESULTS

The first flight on August 22 was used to complete an experiment integrating a bioreactor with a microfluidic device to perform an on-line separation of amino acids within the bioreactor. Amino acid separations and sample switching was successfully performed. To demonstrate the switching between samples within the bioreactor, two cell culture bags were filled with dilute amino acid solutions. Sample bag 1 contained a 2-µM solution of the BODIPY®-labeled arginine, serine, and glutamic acid in 10 mM sodium borate. Figure 1 below shows an example of the separation of the 2-µM amino acids performed at 0.18 g. The data have not been normalized, so the acceleration reading is slightly larger than actual. After 20 parabolas sample bag 2, containing a 1-µM solution of arginine and serine, was introduced using the 4-port switching valve. The concentration was halved and glutamic acid was removed to emphasize the

sample exchange. Figure 2 shows an example of the separation from bag 2 at 0.16 g, validated by the complete removal of glutamic acid.

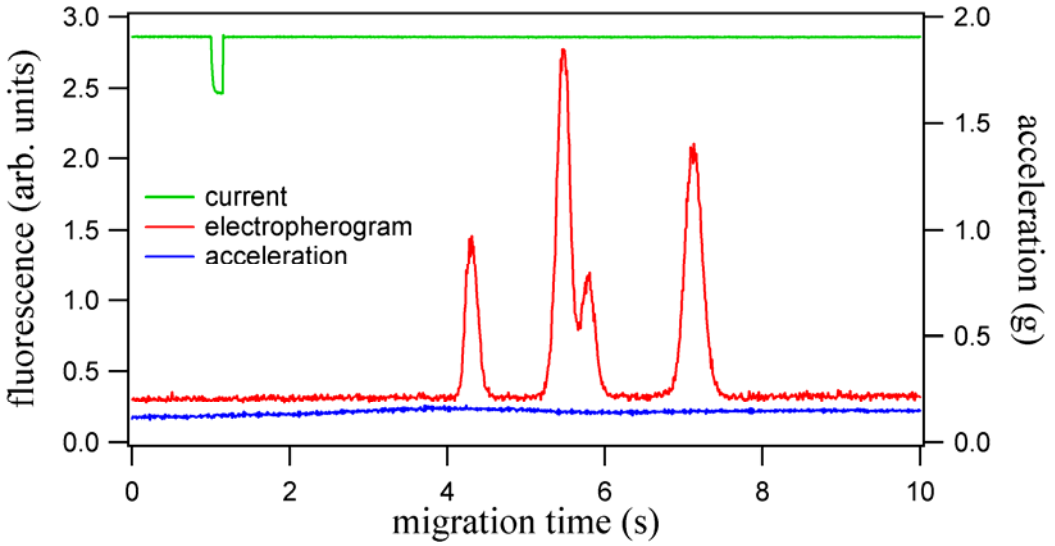

Figure 1. Amino acid separation at ~0.18g from the 22 August 2006 flight. The acceleration, current, and migration time are noted on the axis.

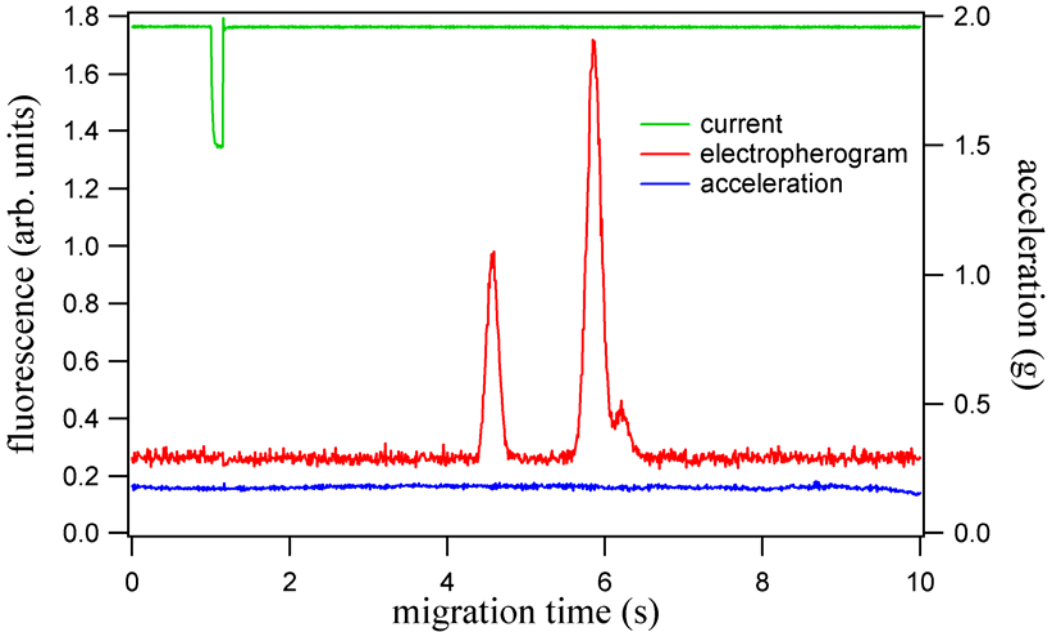

Figure 2. Amino acid separation at ~0.16g from the 22 August 2006 flight, showing the decrease in concentration and removal of glutamic acid.

The second flight on August 23 was to demonstrate the ability of the microfluidic device to sample from cell culture media and to detect nanomolar concentrations of reGFP from the media. The experiments were performed in a manner similar to that used on the first flight. Briefly,

flight bag 1 again contained a 2-µM solution of arginine, serine, and glutamic acid, similar to that depicted in Figure 1. Mid-flight, the 4-port switching valve was moved to sample from bag 2, which contained only the GFP control medium. Figure 3 shows the detection of the protein from NASA's cell culture media at 1.34 g. Due to surface adsorption before the second group of parabolas, we were unable to show a good quality 0g separation of GFP.

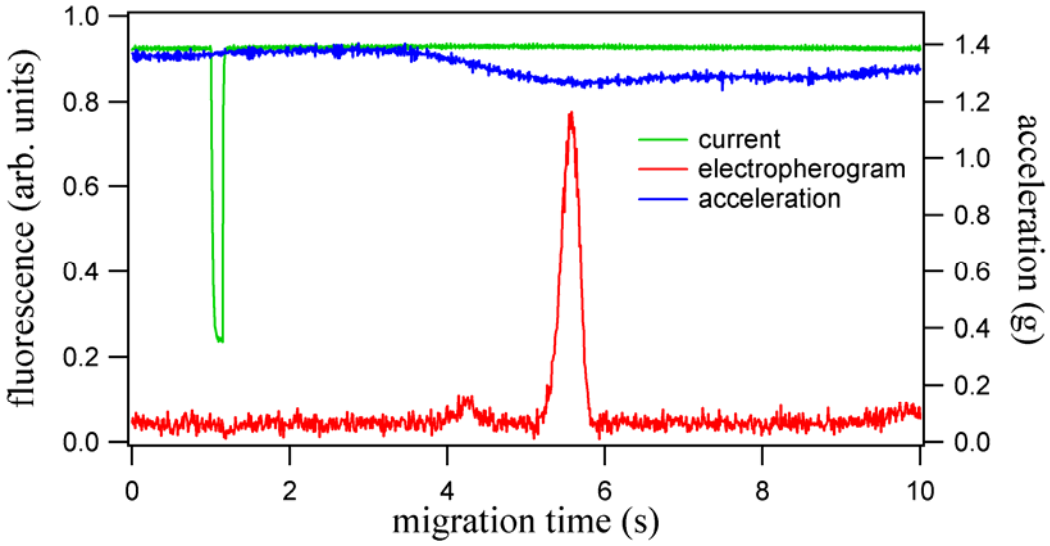

Figure 3. Separation and detection of reGFP control medium at ~1.34 g. Acceleration, current, and migration times are noted on the axis.

DISCUSSION

These data show that it is possible to integrate a bioreactor with a microfluidic device to perform an on-line separation of amino acids in the bioreactor in reduced-gravity environments. It has been demonstrated that the system can perform sample switching as well as nanomolar detection of green fluorescent protein (GFP) directly from cell culture media without performing any sample concentration. These results show progress toward the ability to monitor the media from living cells and get real-time feedback.

PHOTOGRAPHS

JSC2006E37548 to JSC2006E37562
JSC2006E37918 to JSC2006E37929
JSC2006E37992 to JSC2006E38009
JSC2006E38243 to JSC2006E38251

VIDEO

- Zero G flight week August 21 - 25, 2006, Master: 721672

Videos available from Imagery and Publications Office (GS4), NASA/JSC.

CONTACT INFORMATION

Dr. Christopher Culbertson
Kansas State University
Phone: 785-532-6685
Fax: 785-532-6666
culbert@ksu.edu

TITLE

Aerosol Deposition in Fractional Gravity: Risk Mitigation for Martian and Lunar Habitats

FLIGHT DATES

October 17 – 20, 2006

PRINCIPAL INVESTIGATOR

G. Kim Prisk, University of California-San Diego

CO-INVESTIGATORS

Chantal Darquenne, University of California-San Diego
I. Mark Olfert, University of California-San Diego

GOAL

The inhalation and deposition of small particles in the lungs is a health concern here on Earth, and future space travelers risk detrimental health consequences from particle inhalation. Because gravity affects the deposition of particles in the lung, in microgravity, or in the reduced gravity of the Moon and Mars, inhaled particles are left in suspension in the airways, and can be transported deeper into the lung where they reach the sensitive alveolar region. On the Moon and Mars it is believed that much of the dust is highly reactive, which may exacerbate its potential for lung damage. Because it is electrostatically charged, it sticks to space suits and could be tracked into habitats and subsequently inhaled.

OBJECTIVES

The deposition in the lung of aerosols from the environment presents a health risk. For particles larger than 0.5 μm, such deposition is strongly influenced by gravitational sedimentation. In microgravity, deposition by gravitational sedimentation is absent, and as a consequence, airway particle concentrations are higher than in 1g, enhancing aerosol transport to the alveolar region of the lung. The presence of previously unaccounted for complex mixing patterns in the periphery of the lung, combined with high alveolar aerosol concentrations, results in high deposition in this sensitive region of the lung in microgravity. Similar effects are expected in the fractional-gravity environments of the Moon and Mars.

The dust on the surface of Mars is highly oxidative, due to the ultraviolet (UV) light environment on the surface. Mars dust is also electrostatically charged, and so will tend to stick to the outside of space suits, and be tracked into habitats. The lung, with its huge exposed surface area, is highly vulnerable to adverse effects resulting from exposure to Mars dust.

The experiments performed on this series of flights was part of a multi-faceted approach involving human and animal experiments, combined with sophisticated modeling, to assessing the health risk of dust exposure in habitats on both the Moon and Mars, addressing Risk #7 in the Bioastronautics Critical Path Roadmap. Such an assessment has profound implications for the degree of engineering (and thus cost) that will be required to limit the risk of such exposure to the inhabitants of these habitats. We will address the following hypotheses and objectives:

1. That total aerosol deposition in the human lung in fractional gravity will be higher than predicted by existing models (as is the case in microgravity), and that a higher-than-predicted alveolar deposition will result in these circumstances. Using the NASA Microgravity Research Aircraft, we will non-invasively measure both the total and regional deposition of inert particles (0.5 to 2 μm) in humans in fractional g corresponding to that on the surface of the Moon and Mars.

2. That aerosol deposition in the lungs of spontaneously breathing rats in fractional g will be more peripheral (closer to the alveoli) than in 1g. We will expose spontaneously breathing rats to fluorescent- and magnetically-labeled particles of varying sizes (between 0.5 and 2 μm) in 1 g, and in fractional g corresponding to the surfaces of the Moon and Mars, and measure the specific sites of regional deposition in the lungs using both fluorescent confocal microscopy, and magnetic resonance imaging techniques.

3. We will couple existing sophisticated computational fluid dynamics (CFD) models of the upper airways of humans to our model of the alveolar region of the lung, to predict aerosol deposition under conditions matching those of the experiments performed in humans. In rats we will use detailed 3D images of the rat bronchial tree to develop an upper-airway CFD model which, used in conjunction with an appropriately scaled alveolar model, will predict aerosol deposition under conditions matching those of the experiments performed in rats.

METHODS AND MATERIALS

Human Studies in Fractional g

For details of the methods used in the human studies on this flight series, see the Appendix.

In the past we have measured both total and regional aerosol deposition in humans in 1g and in microgravity. The results of those studies highlighted the nonlinear nature of aerosol deposition of small (~ 1 μm) particles as a function of g level (2). Thus, to accurately determine particle deposition in fractional g, direct measurements are required.

Total Deposition

Protocol Overview – We measured total deposition of 0.5- and 1-μm particles in the lungs of subjects in 1 g, and at fractional g levels corresponding to the surface of the Moon and Mars (termed 1/6g and 1/3g for the sake of convenience). In the experiments reported here, deposition was measured only at 1/6g. Total deposition was measured during controlled tidal breathing, and as was the case in our previous studies in microgravity (2), we selected data during stable g-level periods after allowing sufficient time at those g levels for deposition to stabilize (2–3 breaths). We plan to have a total of six subjects for all parts of the human total deposition studies.

Equipment – Deposition data was collected by using equipment similar to that used in a previous study (2). The subject breathes from a reservoir through a non-rebreathing valve. Aerosol concentration and flow rate are measured at the mouth using a photometer and a pneumotachograph, respectively. A diffusion dryer is located between the photometer and the mouthpiece. The system is heated to body temperature to prevent water condensation. Data are recorded on a laptop PC equipped with a data acquisition subsystem.

Central and Alveolar Deposition (SA1b)

Protocol Overview – The proposed protocol will be the same as that used in our previous studies of bolus deposition and dispersion (1; 3; 4). The subject will perform a standardized maneuver and a 70-mL bolus will be inserted in the inspiration at one of the preselected penetration volumes (V_p) using the equipment described in the Equipment section. During the subsequent expiration, the exhaled bolus will be recorded.

We will measure deposition, dispersion (change in bolus half-width), and bolus mode shift. We can designate a volume below end inspiration for the bolus (the penetration volume, V_p), and propose to measure aerosol bolus parameters at each of 3 V_p (200, 500, and 1200 mL). We will use two particle sizes (0.5, 1 μm) at 1g and in 1/6 g. As was the case before, measurements will be performed in triplicate in a total of 6 subjects.

Equipment – The equipment will be the same as that used for previous studies and uses the same photometer and pneumotachograph system used in the total deposition studies. In brief, a pneumatically controlled sliding valve allows the subject to breathe filtered room air, or allows

inspiration through a tube pre-filled with a bolus of aerosol. By actuating the sliding valve at the appropriate point during inspiration, the operator can deliver the bolus at any desired penetration volume with an accuracy of ±100 mL. A full description can be found in previous publications (3).

Rat Studies in Fractional g

We propose to determine the degree of deposition and the location of inhaled particles in the lungs of spontaneously breathing rats, and compare the deposition patterns in 1g and in fractional g levels corresponding to the surface of the Moon and Mars. Our hypothesis is that in the fractional-g environments, total deposition may be somewhat reduced, but those particles that do deposit will do so more peripherally. In humans, more peripheral deposition results in particles avoiding the mucociliary system, and in the case of oxidative particles could increase oxidative damage to the lung.

After performing these studies in rats, we can use anatomical and state-of-the-art imaging techniques to determine the exact site and degree of deposition, providing otherwise unavailable validation for the CFD models. We expect to be able to experimentally demonstrate alterations in the heterogeneity of particle deposition between g levels.

Protocol – We propose to expose spontaneously-breathing, restrained rats to fluorescent-labeled and MRI-labeled particles during periods of fractional g corresponding to the surface of the Moon and Mars on the NASA Microgravity Research Aircraft. During 1g and during the hyper-g phase of parabolic flight, the animals will breathe filtered air, and while the aircraft is in fractional g they will be exposed to particle-laden air for head-only particle exposure for a cumulative exposure period of ~20 minutes. At the completion of the flight, the animals will be euthanized and the lungs preserved. The lungs will be returned to San Diego for magnetic resonance imaging (MRI) of particle location, and for slicing and confocal microscopy of fluorescent particle location (see below). We propose to use three different particle sizes (0.5, 1, and 2 μm), matching those used in the human studies (see above). We will require 2 flights per size and g level (10 rats per condition) for a total of 12 flights.

Exposure Techniques – Five rats (adult male Wistar, with body weight in the range 200–250 g) will be simultaneously restrained in head-out plastic cones (9) in individual sealed plethysmograph chambers. When the animal breathes, changes in box pressure occur as inspired air is warmed and humidified in the respiratory tract, allowing the calculation of tidal volume and breathing frequency (5; 6). An identical reference chamber will be used and differential pressure between the plethysmograph and the reference chamber will be measured (8). This will eliminate difficulties associated with changes in cabin pressure in the aircraft. The chambers will be ventilated continuously by drawing either filtered cabin air or particle-laden air through them at ~250 mL/min (9).

The inlet path for the ventilation will be such that it impinges directly onto the nose region of the restrained rats. This arrangement will allow us to rapidly switch the inlet flow between filtered (particle-free) air, and particle-laden air drawn from a reservoir into which particles in suspension

have been aerosolized during the period of hypergravity immediately preceding the fractional-g parabola. During 1g and during the hyper-g phase of parabolic flight, the animals will breathe filtered air, and while the aircraft is in fractional g they will be exposed to particle-laden air for head-only particle exposure. The fractional-g time available to us in the aircraft is ~35-40 seconds for 1/6g and ~45-50 seconds for 1/3g, giving a cumulative exposure period of ~20 minutes assuming 30 seconds (which will be recorded) of fractional-g exposure time can be used per parabola. Control studies on the ground (1g) will be performed after the fractional g studies, allowing us to match the timing of the exposures to that which occurred during the flights (a delayed synchronous control approach). Importantly in the context of this proposal, Pinkerton et al.(7) showed that in 1g exposure times of 15 to 30 minutes, deposition of 1.0μm microspheres occurred throughout the bronchial tree and alveoli of spontaneously breathing rats.

At the completion of the flight, the animals will be anesthetized by intra-peritoneal injection of pentobarbital and the trachea will be cannulated and connected to a pressure source to permit setting of intratracheal pressure. The caudal vena cava will be cannulated and the carotid arteries and veins cut to permit perfusion fixation. Physiological buffered saline will first be infused for 5 minutes to clear blood from the lungs, followed by fixative for 15 minutes as described by Pinkerton (7). Intra-tracheal pressure will be maintained at 9 mmHg, providing for a lung volume approximating functional residual capacity.

For the flights reported here, a 2-chamber prototype plethysmograph with no rat was flown as an engineering evaluation. An animal ventilator provided realistic signals for assessment of noise levels in the aircraft environment.

RESULTS

Combining data from these October 2006 flights with the data collected during the week of June 13-16, 2006, we now have a full data set of fractional and total deposition in 1/6g for six and four human subjects, respectively. Preliminary inspection of the data show good quality signals. Data analysis is in progress and no final results are yet available. Data analysis of fractional deposition in three subjects has been completed. These partial results have been compiled in an abstract that was submitted for presentation at the International Conference of the American Thoracic Society (ATS), to be held in San Francisco in May 2007. A copy of the submitted abstract is attached in the appendix.

DISCUSSION AND CONCLUSION

A preliminary discussion can be found in the abstract submitted to the ATS (see appendix).

REFERENCES

1. Darquenne C, Paiva M and Prisk GK. Effect of gravity on aerosol dispersion and deposition in the human lung after periods of breath-holding. J Appl Physiol 89: 1787-1792, 2000.
2. Darquenne C, Paiva M, West JB and Prisk GK. Effect of microgravity and hypergravity on deposition of 0.5- to 3-μm-diameter aerosol in the human lung. J Appl Physiol 83: 2029-2036, 1997.
3. Darquenne C, West JB and Prisk GK. Deposition and dispersion of 1 μm aerosol boluses in the human lung: Effect of micro- and hypergravity. J Appl Physiol 85: 1252-1259, 1998.
4. Darquenne C, West JB and Prisk GK. Dispersion of 0.5-2 mm aerosol in micro- and hypergravity as a probe of convective inhomogeneity in the human lung. J Appl Physiol 86: 1402-1409, 1999.
5. Jacky JP. A plethysmograph for long-term measurements of ventilation in unrestrained animals. J Appl Physiol 45: 644-647, 1978.
6. Jacky JP. Barometric measurement of tidal volume: effects of pattern and nasal temperature. J Appl Physiol 49: 81-86, 1980.
7. Pinkerton KE, Gallen JT, Mercer RR, Wong VC, Plopper CG and Tarkington BK. Aerosolized fluoresecent microspheres detected in the lung using confocal scanning laser microscopy. Microscopy Research and Technique 26: 437-443, 1993.
8. Steinbrook RA, Feldman HA, Fencl V, Forte VA, Gabel RA, Leith DE and Weinberger SE. Naloxone does not affect ventilatory responses to hypoxia and hypercapnia in rats. Life Sci 34: 881-887, 1984.
9. Sweeney TD, Leith DE and Brain JD. Restraining hamsters alters their breathing pattern. J Appl Physiol 70: 1271-1276, 1991.

PHOTOGRAPHS

JSC2006E45012 to JSC2006E45026
JSC2006E45267 to JSC2006E45274
JSC2006E45316 to JSC2006E45331
JSC2006E45873 to JSC2006E45890

VIDEO

- Zero G flight week October 17 -20, 2006, Master: DV0729

Videos available from Imagery and Publications Office (GS4), NASA/JSC.

APPENDIX

Abstract submitted to the International Conference of the American Thoracic Society held in San Francisco in May 2007:

Title: Aerosol Deposition in the Human Lung Is More Peripheral in Lunar Gravity than in 1G

G.K. Prisk, Ph.D., D.Sc.1 and C. Darquenne, Ph.D.1. 1Dept. of Medicine, University of California, San Diego, La Jolla, CA, United States.

Lunar dust is highly reactive and presents a potential toxic challenge to future explorers of the moon. The extent of the inflammatory response to lunar dust will depend on where in the lung the particles deposit. We performed bolus inhalations of 0.5 and 1 μm-diameter latex particles in three subjects on the ground (1G) and during short periods of lunar gravity (1/6G) aboard the NASA Microgravity Research Aircraft. An aerosol bolus of 70 mL was inhaled at a penetration volume (V_p) of 200, 500 and 1200mL. Inspiration was from residual volume (RV) to one liter above functional residual capacity at a flow rate of 0.45 l/s and was immediately followed by an expiration to RV at the same flow rate. Bolus deposition (DE) was calculated from aerosol concentration and flow rate continuously monitored at the mouth. For both particle sizes, DE increased with increasing V_p and was gravity-dependent, being 50% lower in 1/6G than in 1G. For the same level of deposition, particles were deposited more distally in lunar than normal gravity. For example, for d_p = 1 m, a level of 20% deposition was reached by V_p = 200mL in 1G but not until V_p = 700 mL in 1/6G. For d_p = 0.5 μm, a level of 20% deposition was reached by V_p = 250mL in 1G and by V_p = 800 mL in 1/6G. Thus in 1G, deposition in more central airways reduces the transport of fine particles to the lung periphery. These data suggest that in the fractional gravity environment of a lunar outpost, while inhaled fine particle deposition may be lower than on Earth, those particles that are deposited will do so in more peripheral regions of the lung, increasing the potential for an exaggerated inflammatory response.

ACKNOWLEDGMENTS

Funded by NSBRI/NASA #TD00701

CONTACT INFORMATION

G. Kim Prisk, PhD, DSc
Department of Medicine -0931
University of California, San Diego
9500 Gilman Drive
La Jolla, CA 92093-0931
kprisk@ucsd.edu

TITLE
NASA Explorer School Program: Chemical Reactions

FLIGHT DATES
February 8 – 9, 2007

PRINCIPAL INVESTIGATOR
Amy D'Andrea, Key Peninsula Middle School

CO-INVESTIGATORS
Kathy Tucker-Patton, Key Peninsula Middle School
Briana Randall, Key Peninsula Middle School
Ron Stark, Key Peninsula Middle School

GOAL

The purpose of this experiment is to determine how microgravity affects the reaction rate of baking soda and vinegar. For the purpose of this experiment, the reaction rate is the volume of carbon dioxide gas that is produced per second, determined by measuring the pressure in an enclosed container of carbon dioxide gas generated in the first 20 seconds of the reaction.

OBJECTIVE

We predict that combining baking soda and vinegar in normal gravity conditions and microgravity will result in slower chemical reaction rates in the reduced-gravity environment because there will be fewer collisions of the baking soda and vinegar molecules. Our prediction

is based on the assertion that in a reduced-gravity environment, the reactant molecules will be separated due to less gravitational force holding them to one common location within the test tubes.

METHODS AND MATERIALS

A syringe containing 5 mL of vinegar and a Vernier PS-DIN pressure sensor were attached to a 50-mL test tube containing 0.05g of baking soda. During freefall, the chemical reaction was initiated by injecting the vinegar into the test tube. As the reactants mixed, carbon dioxide gas was produced and the air pressure inside the test tube increased. Data were collected in one-second increments for 20 seconds.

The amount of carbon dioxide gas produced by the experiment was measured via the pressure sensor and a LabPro data interface, and reported via a TI-83 calculator. This experiment was repeated five times in five prepared test tubes housed in a test tube rack. A sixth trial was conducted using vinegar only and no baking soda to determine a baseline pressure for comparing the pressures of the five trials. The experiment was conducted and contained in an enclosed glove box on the C-9. See Figures 1 and 2.

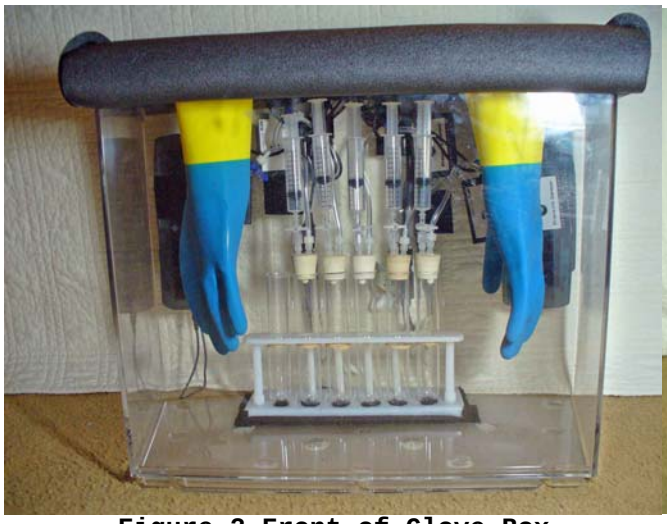

Figure 2 Front of Glove Box

Figure 1 Rear of Glove Box

Table 1 shows averaged trials for microgravity and gravity, plus pressure controls for microgravity and normal gravity conditions. Time was measured in seconds and pressure in kilopascals (kPa).

Table 1. Averaged chemical reaction pressure data and pressure control data.

Time	Microgravity Average (kPa)	Gravity Average (kPa)	Microgravity Pressure Control (kPa)	Gravity Pressure Control (kPa)
0	97.4	105.0	99.2	104.4
1	97.1	112.1	98.9	110.1
2	99.6	113.5	99.2	109.5
3	102.7	116.3	99.2	109.5
4	105.9	118.7	106.0	109.5
5	108.5	120.1	107.9	109.5
6	110.5	121.2	107.4	109.5
7	112.5	121.8	107.4	109.5
8	114.3	122.4	107.6	109.0
9	115.9	122.9	107.6	109.3
10	117.5	123.2	107.6	109.0
11	118.9	123.6	107.4	109.0
12	120.1	123.9	107.4	109.3
13	121.4	124.2	107.4	109.5
14	122.4	124.5	107.1	109.0
15	123.1	124.5	107.4	109.3
16	124.1	124.7	106.5	108.7
17	124.4	124.9	106.8	109.0
18	125.4	125.0	106.8	109.0
19	125.4	125.2	106.8	109.3
20	125.9	125.2	106.8	109.0

DISCUSSION

The data from the mixing of vinegar and baking soda in normal gravity conditions and in microgravity support the hypothesis that the reduction in gravity would have an effect on the chemical reaction measured by the change in pressure of CO_2 production. It was predicted that the Earth's gravity would keep the baking soda at the bottom of the test tube and that vinegar would fall to the bottom of the test tube as well, resulting in a complete mixing of the two reactants. In microgravity it was predicted that contact between the vinegar and baking soda would be reduced and, therefore, the rate of reaction would be slower.

The data show that the 20 seconds allocated for the reaction in normal gravity conditions and microgravity was sufficient time for the chemical reaction to be completed, but there was a notable difference in the rate of reaction between trials conducted in normal gravity conditions and those completed in microgravity. In normal gravity conditions, 80 percent of the chemical

reaction occurred in the first 6 seconds and the remaining 20 percent in the remaining 14 seconds. In microgravity, 46 percent of the chemical reaction occurred in the first 6 seconds and the remaining 54 percent in the remaining 14 seconds. This pattern was consistent over all trials. See Table 2.

The 6-second mark was selected because it appeared that after 6 seconds the reaction in normal gravity conditions began to increase less rapidly as measured by the rate of pressure change. If we look at the same data in 5-second increments, it is even more apparent that the rate of reaction in normal gravity conditions was faster than in microgravity over the range of time. (See Figure 5.)

Table 2. Rates of pressure change (kPa).

Microgravity		Normal-Gravity Conditions	
Total Pressure Change	28.5	Total Pressure Change	20.2
Change over first 6 sec	13.2	Change over first 6 sec	16.2
Change over last 14 sec	15.4	Change over last 14 sec	4.0
Average change over first 5 sec	2.2	Average change over first 5 sec	3.0
Average change over second 5 sec	1.8	Average change over second 5 sec	0.6
Average change over third 5 sec	1.1	Average change over third 5 sec	0.3
Average change over last 5 sec	0.6	Average change over last 5 sec	0.2
Total change over first 5 sec	11.1	Total change over first 5 sec	15.1
Total change over second 5 sec	9.0	Total change over second 5 sec	3.1
Total change over third 5 sec	5.5	Total change over third 5 sec	1.3
Total change over last 5 sec	2.8	Total change over last 5 sec	0.8

Table 3. Data analysis in 5-second increments.

Microgravity		Normal-Gravity Conditions	
Percent change over first 5 sec	39	Percent change over first 5 sec	75
Percent change over second 5 sec	32	Percent change over second 5 sec	15
Percent change over third 5 sec	19	Percent change over third 5 sec	6
Percent change over last 5 sec	10	Percent change over last 5 sec	4

The pressure control data were consistent with the chemical reaction data. The total increase in pressure for microgravity was 8.7 kPa at time 3 to 5 seconds, and the total increase in pressure for normal gravity conditions was 5.7 kPa at time 0 to 1 second. The remainder of the trial for each control showed minor fluctuations in pressure as expected. We noted that the delay in the first 3 seconds of microgravity control data was caused by the difficulty in applying enough force while in microgravity to push down the syringe to insert the vinegar. Pressure reached the maximum of 107.9 kPa in 2 seconds in the microgravity control and 110.1 kPa in 1 second in the gravity control.

CONCLUSION

The data provide evidence that chemical reaction rates were slower in microgravity than in normal gravity conditions. In the first 6 seconds, the reaction was 80 percent complete in normal gravity conditions and only 46 percent complete in microgravity. We conclude that our hypothesis was correct and, furthermore, that molecular collisions are about half as frequent in reduced-gravity conditions as in normal gravity conditions.

Several questions arose during the analysis of data:

1. Does surface tension (liquid versus solid) play a role in collision theory? Testing reaction rates of two liquids may help to clarify whether collision theory is affected by or occurs differently with similar states of matter.
2. Could reactant introduction methods affect the reaction rate? In other words, if the reactants were introduced in a more passive manner, would the reaction rates differ from those in our trials?
3. Did the seal on the test tube stopper affect the pressure data?
4. We also were curious about the totality of the chemical reactions taking place, especially given the small mass and volume of reactants used in these trials. We would like to be able to compare any remaining reaction after initial data readings are complete. This may tell us if reaction methods in microgravity conditions can be improved in space vehicles or in other microgravity environments or if chemical reactions are consistently inefficient in lesser gravity environments.

These questions and the answers to them have implications for life sciences in space travel and exploration, as well as colonization where gravity conditions are different than on the Earth, since chemical reactions are crucial in systems such as digestion of food or waste, or in the creation of products used for other purposes.

REFERENCES

Key Peninsula Middle School Test Equipment Data Package, January 2007.

Key Peninsula Middle School, Reduced Gravity Flight Program 2006-2007 Program Application September 2006.

PHOTOGRAPHS

JSC2007EO7943 to JSC2007EO7946
JSC2007EO7974
JSC2007EO7985
JSC2007EO7999 to JSC2007EO8009
JSC2007EO8053 to JSC2007EO8055
JSC2007EO8302 to JSC2007EO8310
JSC2007EO8232
JSC2007EO8240
JSC2007EO8284

VIDEO

- Zero G Student Campaign week Febuary 2 – 9, 2007, Master: DV0820

Videos available from Imagery and Publications Office (GS4), NASA/JSC.

CONTACT INFORMATION

Amy D'Andrea
5510 Key Peninsula Hwy KPN
Lakebay, WA 98349
253-530-4272
dandreaa@peninsula.wednet.edu

Kathy Tucker-Patton
5510 Key Peninsula Hwy KPN
Lakebay, WA 98349
tuckerpattonk@peninsula.wednet.edu
253-530-4240

TITLE
Locomotion Kinematics in Microgravity

FLIGHT DATES
February 27 – March 2, 2007

PRINCIPAL INVESTIGATOR
Donald Hagan, NASA Johnson Space Center

CO-INVESTIGATORS
John DeWitt, Bergaila Engineering Services
Gail Perusek, NASA Glenn Research Center

SUPPORTING PERSONNEL
Jason Bentley, Wyle
W. Brent Edwards, Wyle
Melissa Scott-Pandorf, National Space Biomedical Research Institute
Jason Norcross, Wyle
Cassie Wilson, JES Tech
Kirk English, JES Tech
Leah Zidon, Wyle
Grant Schaffner, Wyle
Meghan Everett, University of Houston

ABSTRACT

The purpose of this experiment was to measure the ground reaction forces, bungee external load magnitudes, and joint motions during locomotion in weightlessness. Five subjects (2 male and 3 female) completed locomotion trials in microgravity on board the NASA C-9 aircraft during parabolic flight. Subjects walked at 1.34 m s^{-1} and ran at 3.13 m s^{-1} while wearing a harness similar to that normally used during exercise on the International Space Station. Subjects performed locomotion with an external load of about 60% and 90% of body weight provided with bungees. Vertical ground reaction force data were collected during each trial with an instrumented treadmill. Joint kinematics were determined using a motion capture system. Joint kinematics were also recorded as subjects performed treadmill locomotion in normal gravity on a treadmill. There were no differences in contact time between normal and microgravity conditions. Stride time was not different between conditions during walking, but during running in microgravity it was greater with 60% of body weight loading than with 90% of body weight loading. Contact time and joint ranges of motion were similar for microgravity and normal gravity conditions. Ground reaction forces increased as external load increased. Our results indicated that joint kinematics are similar in microgravity and normal gravity during both walking and running.

INTRODUCTION

On board the International Space Station, astronauts perform treadmill locomotion to deter bone and muscle losses that occur during long-term microgravity exposure. Previous investigations have been performed during parabolic flight to examine the external load levels and ground reaction forces that occur during walking and running in weightlessness (Schaffner et al., 2005; De Witt et al., 2004; De Witt et al., 2003). However, few data have been available on joint kinematics due to the difficulty of collecting motion capture data during aircraft flight. The experiences gained during previous flights have allowed investigators to develop methods that make effective collection of motion capture data possible.

The purpose of this experiment was to determine how walking and running kinematics in weightlessness differ from locomotion in normal gravity. The secondary purpose was to obtain ground reaction force data to compare with data collected on a microgravity analog treadmill. We hypothesized that contact time, stride time, and hip, knee, and ankle range of motion would be different in microgravity and normal gravity environments. We further hypothesized that ground reaction forces would be affected by external load magnitude.

METHODS AND MATERIALS

Seven subjects completed locomotion trials in microgravity during parabolic flight on board the NASA C-9 aircraft. However, during post-processing, motion capture data for two subjects were found to be unusable. Therefore, data from five subjects (2 male and 3 female, age = 36.2 ± 2.6 y, mass = 61.3 ± 14.6 kg) were analyzed. Data were collected during four flights, and each flight consisted of 40 microgravity parabolas. This investigation was reviewed and approved by the NASA Johnson Space Center Committee for Protection of Human Subjects. Subjects provided written informed consent before participating in the study.

Data Collection

Parabolic Flight Locomotion Trials

On arrival at the C-9 aircraft hangar, each subject was provided with running shoes (Xccelerator TR, Nike, Inc, Beaverton, OR) and completed a health questionnaire. Subjects wore Spandex running tights. During flight, subjects walked at 1.34 m s^{-1} (3 mph) and ran at 3.13 m s^{-1} (7 mph) while loaded with bungees and wearing a prototype harness developed by NASA Glenn Research Center.

Subjects completed locomotion at each speed under two external load (EL) conditions. During the light EL condition, the bungee load was adjusted to about 57% of body weight (BW). During the heavy EL condition, the bungees were adjusted to about 90% of BW. Appropriate EL levels were obtained by adding carabiner clips in series with the bungees, and by using either single bilateral or parallel bilateral bungee configurations. EL levels were verified in microgravity as each subject stood still on the instrumented treadmill (see Table 1). Subjects completed multiple trials at each speed and EL condition. A single trial from each EL and speed condition was chosen for further analysis.

Table 1. Mean external load (% BW) for each subject during walking and running in microgravity.

Subject	Walk	Run
1	0.55	0.87
2	0.59	0.88
3	0.59	0.92
4	0.65	0.89
5	0.48	0.90
Group Average	0.57 ± 0.02	0.89 ± 0.06

Ground-Based Locomotion Trials

Each subject completed locomotion in normal gravity on a treadmill in the laboratory. Subjects walked for 1 minute at 1.34 m s^{-1} (3 mph) and ran at 3.13 m s^{-1} (7 mph) wearing normal exercise apparel without the harness. Lower-limb kinematics were recorded using a motion capture system (SMART Elite system, BTS Engineering, Padova, Italy).

Ground Reaction Forces

Vertical ground reaction force (GRF) data were collected during each trial with an instrumented treadmill (Kistler Gaitway, Amherst, NY) at 480 Hz for 25 s. For each trial, the mean of each variable was computed using multiple footfalls. Any partial footfall measurements were eliminated from the analysis.

Kinematics

Reflective markers were attached to the subjects' left side. Markers were placed arbitrarily on the lateral neck near the C5 vertebra, the lower trunk near the hip, the upper and lower thigh, the

upper and lower shank, and the heel and toe. The body was modeled as four rigid, linked segments (see Figure 1). This configuration allowed each segment to be represented as the vector connecting the proximal marker to the distal marker. Three-dimensional marker locations were found using the six-camera motion capture system with a sampling frequency of 60 Hz.

Figure 1. Marker positions during data collection.

All three-dimensional data were expressed relative to an inertial reference frame that was established during calibration. The inertial reference frame was arbitrarily oriented so that the vertical axis was normal to the treadmill surface. A treadmill reference frame was created so that the x-axis was oriented to approximate the fore/aft direction of the treadmill belt, the y-axis was perpendicular to the treadmill surface, and the z-axis was parallel to the fore-aft axis of the treadmill in the direction of locomotion.

Raw motion capture data were examined for missing points, which were replaced using cubic spline interpolation. The motion capture data were then filtered using a 4^{th}-order Butterworth low-pass filter with an optimal cutoff frequency for each marker determined using an autocorrelation procedure (Challis, 1999). The autocorrelation was executed independently for each coordinate of each marker, and the highest cutoff frequency determined for each coordinate was used for each marker. Cutoff frequencies ranged from 6 to 28 Hz (mean = 16.65 Hz).

Joint angle trajectories of the ankle, knee, and hip were found for each sample of each trial. Hip angle was defined as the angle separating the thigh and trunk. Knee angle was defined as the angle separating the shank and thigh. Positive hip and knee angles indicate flexion. Ankle angle was the angle separating the shank and foot segments. To relate the ankle angle to the anatomical angle, 90 degrees was subtracted from the computed ankle angle. Positive ankle angles represent plantar flexion. All joint angles were corrected relative to the anatomical position by subtracting joint angles found during a static (standing) trial.

Dependent Variables and Statistical Analysis

Contact time (CT), stride time (ST), kinematic, and GRF data were processed using custom software programmed in MATLAB v7.1 (The MathWorks, Inc., Natick, MA). Kinematic variables of interest included the range of motion (ROM) of the hip, knee, and ankle. GRF variables of interest included peak impact force (PI), average loading rate (LR), peak propulsive force (PP), and impulse (Imp). Differences in CT, ST, and kinematic means between conditions were tested using a repeated-measures analysis of variance (ANOVA). Differences in GRF variables were tested using paired *t*-tests since these data were collected only during microgravity trials. Separate analyses were conducted for walking and running. The significance level was set at $P < 0.05$.

RESULTS

Gait Parameters

CT and ST means are presented for each gait type (see Table 2). Gravity level had no effect on CT during either speed. However, subjects had significantly longer ST during walking and running in microgravity with the light EL than with the heavy EL.

Table 2. Mean CT and ST for microgravity trials with each EL level and in normal gravity.

			Speed	
Data	Gravity	Load	Walking	Running
Contact Time (s)	Micro	Light	0.65 ± 0.08	0.32 ± 0.06
	Micro	Heavy	0.63 ± 0.10	0.32 ± 0.06
	Normal	-	0.70 ± 0.07	0.32 ± 0.02
Stride Time (s)	Micro	Light	1.10 ± 0.07	0.78 ± 0.10*
	Micro	Heavy	1.01 ± 0.09	0.70 ± 0.07
	Normal	-	1.03 ± 0.08	0.71 ± 0.07

*Significantly different from the heavy EL condition, $P < 0.05$.

Kinematics

Means of the hip, knee, and ankle ROM are shown in Table 3. The repeated-measures ANOVA revealed no differences in ROM at any joint between conditions (microgravity under both load conditions and the normal gravity condition) during walking and running. Mean curves ensemble-averaged across all subjects are plotted in Figure 2. Except for the ankle during walking, time-history curves are very similar for all conditions for walking and running.

Table 3. Mean hip, knee, and ankle range of motion for microgravity trials with each EL level and in normal gravity.

			Speed	
Data	Gravity	Load	Walking	Running
Hip ROM (deg)	Micro	Light	55.12 ± 10.31	62.63 ± 6.94
	Micro	Heavy	59.37 ± 22.53	67.34 ± 6.72
	Normal	-	42.04 ± 1.58	58.43 ± 4.46
Knee ROM (deg)	Micro	Light	62.66 ± 7.93	79.72 ± 7.51
	Micro	Heavy	64.49 ± 17.09	78.48 ± 11.68
	Normal	-	65.80 ± 3.78	85.40 ± 18.29
Ankle ROM (deg)	Micro	Light	27.01 ± 6.19	50.32 ± 3.83
	Micro	Heavy	26.50 ± 5.11	46.32 ± 2.72
	Normal	-	29.60 ± 3.04	47.15 ± 9.25

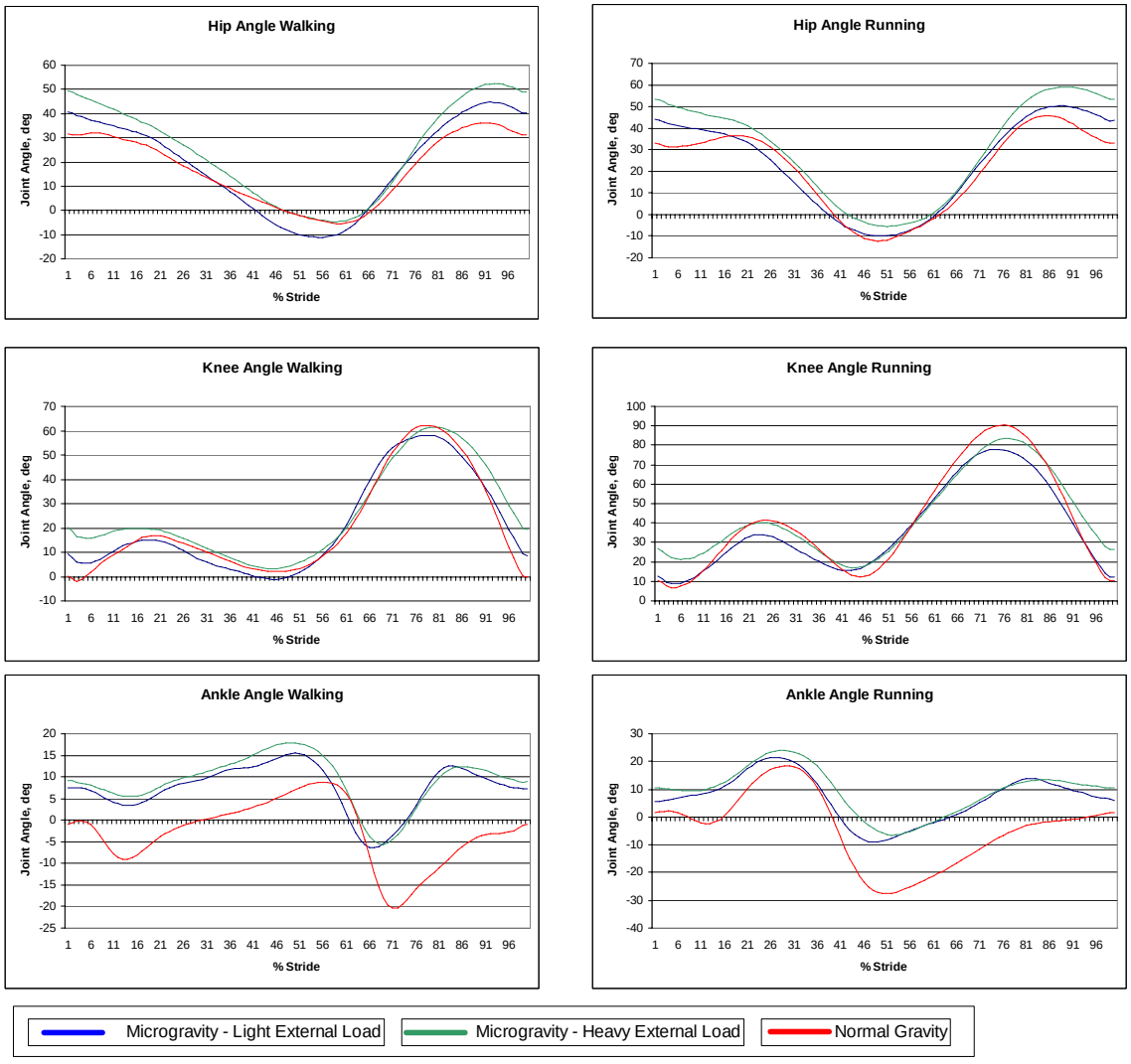

Figure 2. Mean ensemble-averaged joint trajectories for the hip, knee, and ankle during walking and running in normal gravity and in microgravity with light and heavy external loads.

Ground Reaction Forces

GRF means are presented in Table 4. All force measures were normalized to body mass. Except for loading rate, mean dependent-variable values for light and heavy external loading were significantly different from each other. Loading rates under the two loading conditions during walking were not significantly different.

Table 4. Mean peak impact force, propulsive force, loading rate, and impulse during walking and running in microgravity under light (57% BW) and heavy (90% BW) external loads.

		Speed	
Data	Load	Walking	Running
Peak Impact Force (N/kg)	L	7.58 ± .020*	10.79 ± 2.31*
	H	9.48 ± 0.86	12.90 ± 2.40
Peak Propulsive Force (N/kg)	L	6.30 ± 1.77*	14.34 ± 1.00*
	H	8.65 ± 1.45	16.71 ± 0.88
Loading Rate (N/kg/s)	L	77.20 ± 27.77	354.59 ± 153.26*
	H	75.16 ± 26.27	455.96 ± 179.47
Impulse (N/kg·ms)	L	3060.94 ± 603.67*	2139.32 ± 222.37*
	H	4072.65 ± 952.48	2487.65 ± 180.20

* Significantly different from heavy condition, $P < 0.05$.

DISCUSSION

During this investigation, subjects exercised on a treadmill in microgravity while loaded to about 55% and 90% of their body weight using bungees. Gait kinematics during locomotion were compared for microgravity conditions and normal gravity conditions. Our results suggest that gait kinematics are similar for microgravity and normal gravity conditions with the exception of an increase in running stride time during low loading (55% BW) in microgravity.

The increased stride time during low-loaded running in microgravity coupled with no differences in contact time between EL conditions and the normal gravity condition suggests that an increase in flight time occurred. This result makes sense because a decreased EL may allow the subjects to propel themselves farther vertically from the treadmill due to the lower resistive force. The lower force pulling the subjects back to the treadmill may therefore result in longer flight times. However, because joint ranges of motion were not different between these conditions, it is possible that the subjects scaled their strides to account for the increased stride time. Therefore, maintenance of the kinematic pattern of joint motion was a critical control factor.

Our data suggest that ground reaction forces during locomotion in microgravity are affected by external load. These results make sense and are intuitive, given that a subject should have to produce greater forces to overcome a greater EL.

CONCLUSION

Our findings suggest that locomotion kinematics during 55 and 90% BW external loading in microgravity are very similar to locomotion kinematics during normal gravity. A slight increase in stride time occurs during running with a low EL, but joint ranges of motion are not affected. Ground reaction forces are affected by EL level, with higher EL resulting in larger ground reaction force magnitudes.

REFERENCES

Challis, J.H. (1999) A procedure for the automatic determination of filter cutoff frequency for the processing of biomechanical data. *Journal of Applied Biomechanics* 15:303-317.

Schaffner G, DeWitt JK, Bentley JR, Yarmanova E, Kozlovskaya I, Hagan RD. (2005). Effect of subject loading device load levels on gait. NASA Technical Report TP-2005-213169.

DeWitt JK, Schaffner G, Laughlin MS, Loehr J, Hagan RD. (2004). External load affects ground reaction force parameters non-uniformly during running in weightlessness. Presented at the 2004 Annual Meeting of the American Society of Biomechanics, Portland, OR.

DeWitt JK, Schaffner G, Blazine K, Bentley JR, Laughlin MS, Loehr J, Hagan RD. (2003). Loading configurations and ground reaction forces during treadmill running in weightlessness. Presented at the 2003 Annual Meeting of the American Society of Biomechanics, Toledo, OH.

PHOTOGRAPHS

JSC2007E11849 to JSC2007E11868
JSC2007E11885 to JSC2007E11903
JSC2007E12058 to JSC2007E12067
JSC2007E12084 to JSC2007E12099
JSC2007E12453 to JSC2007E11475

VIDEO

- Zero G flight week 02/27 – 03/2/07 17 -21, 2006, Master: 300205

Videos available from Imagery and Publications Office (GS4), NASA/JSC.

CONTACT INFORMATION

John DeWitt
c/o Wyle
1290 Hercules Suite 120
Houston, TX 77058
281-483-8939
john.k.dewitt@nasa.gov

TITLE
Predicting and Assessing Postural Reentry Disturbances

FLIGHT DATES
February 27 – March 2, 2007

PRINCIPAL INVESTIGATORS
James R. Lackner, Brandeis University
Paul DiZio, Brandeis University

OBJECTIVES

The experiment we conducted February 27 – March 2, 2007 in parabolic flights on board the C-9 was a continuation of our effort to measure how exposure to spaceflight-like environments of weightlessness (0 g) and increased gravity (1.8g) affect a flier's localization of the subjective vertical and perceived angular self-displacement. The new specific aims of this experiment were 1) to assess perceptual cross-talk in the subjective vertical during static tilts and 2) to determine if responses to rapid tilt transitions lead to perceptual responses with slower dynamics.

BACKGROUND

Our interest in perceptual cross-talk is motivated by the desire to test and expand a mechanistic model of static orientation that we have developed (Bortolami et al. 2006). Past parabolic flight experiments have confirmed a novel prediction of this model, that localization of the subjective vertical during recumbent yaw axis tilts is not influenced by increases in gravitoinertial force (gif) background above 1g. This finding contrasts with the well-known influence of gif on

subjective vertical estimates for pitch and roll tilts (Correia et al. 1968). A further prediction of our model is that tilt about one axis will cause systematic variations in estimates of the subjective vertical not only about the physical axis of head tilt but also about the orthogonal axes. The first specific aim of the present experiment was to expose recumbent subjects to static tilts about their yaw axis and to measure the errors in their localization of the subjective vertical both in the yaw axis and in the pitch axis.

Our model of static orientation does not include any dynamic perceptual mechanism, but recent theoretical (Bos and Bles 2002; Kaptein and Van Gisbergen 2004) and empirical (Bos and Bles 2002; Kaptein and Van Gisbergen 2004) studies have suggested such a mechanism exists. If such a dynamic response to static tilt does exist, we would like to incorporate it into our model. It would also be critical to account for response dynamics in the design of future experiments performed under time constraints. Therefore, our specific aim was to examine whether localization of the vertical immediately after a physical tilt differed from the response 15 seconds later, at the end of the constant force periods available in parabolic flight.

METHODS

Each of 8 subjects was tested in 20 consecutive parabolas. Seven of the subjects had previous experience in parabolic flights and one subject was tested in parabolas 21-40 of his first day of flight. The participation of human subjects was approved by the Brandeis Institutional Review Board for the protection of human subjects as well as by the Johnson Space Center Committee for the Protection of Human Subjects.

The apparatus included a motorized bed that could tilt recumbent subjects about their long (yaw) axis. A gimbaled joystick that could move about an axis parallel to the bed axis (yaw) and an axis running medial-lateral to the subject (pitch) was affixed to the bed and positioned for easy manipulation. Sufficient friction was added to the gimbals' bushings to oppose the tendency for it to fall into an anti-pendant position, which would otherwise have provided an undesired cue about the gravitoinertial vertical.

Each subject was tested during 20 consecutive parabolas of a 40-parabola flight, and during periods of straight and level flight preceding and following the parabolas. Subjects were blindfolded and tightly restrained in the bed. They wore earplugs and noise-canceling earphones and listened to white noise to mask the sounds of the aircraft, which otherwise would have served as orientation cues. The white noise could be interrupted by programmed, computerized audio commands or by the experimenter. Trials were conducted in both the 1.8-g and 0g phases of each parabola. Before each 1.8-g force phase, the bed was set to the desired starting angle, and the experimenter triggered a bed movement as soon as the force transition occurred, by viewing computer readout of the aircraft g_z. The starting and final tilt angles of the bed were 6°, 18°, 30°, 42°, or 54° tilted left or right. The velocity of bed movements followed a raised cosine profile with a peak velocity of 45°/s, durations of 0.85 to 4.25 s, and displacements of ±12° to ±60°. As soon as bed movement was complete, the subject heard a computer-generated command to point to the vertical direction. Subjects had been trained to pay attention to the yaw and pitch axes. Five seconds later they received a command to slew the stick to either the left or right, selected randomly. Ten seconds later (about 5 seconds before the end of the constant force

period) they were told again to point to the vertical. After another five seconds (just before or during the force transition into 0 g) the bed moved to a new starting position, and when the transition to 0g was complete the bed moved to a new final position and the subject pointed to the subjective vertical on command, immediately and again 15 s later. Seven subjects completed a 20-parabola session in which each final bed position was repeated twice in 1.8g and twice in 0g. One subject had to be removed after 10 parabolas because of motion sickness and completed only one repetition of each angle.

For subjects tested in parabolas 1-20, the 1g straight and level flight trials were conducted before the parabolas, and for subjects tested in parabolas 21-40, they were conducted afterward. The timing of trials was matched to the average cadence of the parabola trials. A ground-based 1g test session consisting of 4 repetitions per tilt angle was performed the morning before flight for each subject.

RESULTS

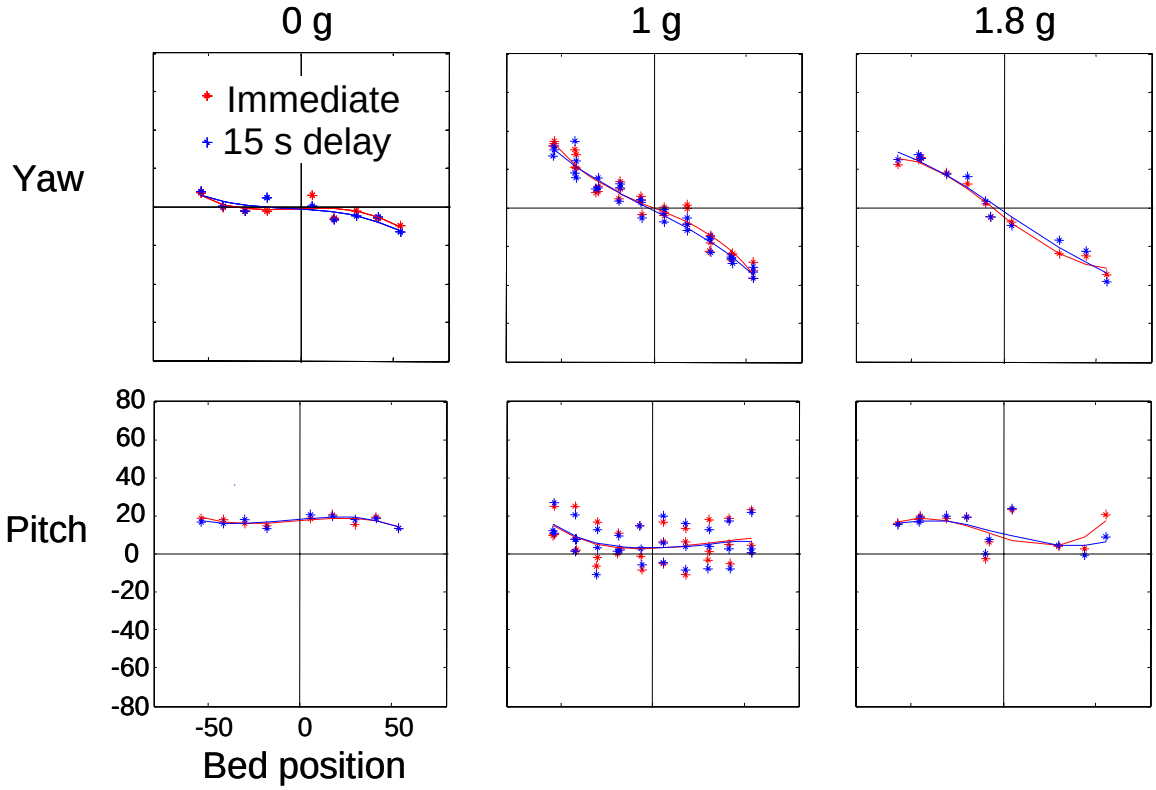

Figure 1. Subjective vertical estimates by one subject in the yaw and pitch axes plotted against head tilt (Bed position). Estimates were made immediately after the bed angle changed or 15 s later.

Preliminary analysis of the flight data has been completed for some subjects. A summary of these findings is given below. In Figure 1, subjective vertical estimates are plotted against head tilt (Bed position) in 0 g, 1 g, and 1.8g , for one subject. Blindfolded, recumbent subjects pointed a rod to the perceived vertical. All head tilts were about the yaw axis. The top row of plots

represents pointing direction in the yaw axis, and the bottom row indicates pointing direction in the pitch axis. The red symbols represent settings made immediately after the bed angle changed and the blue symbols represent settings made 15 s after the bed angle changed.

Effects of Force Background on Yaw Axis Judgments during Yaw Axis Tilts

Visual comparison of the top row of plots indicates that the function of subjective vertical versus head tilt is the same in 1g and 1.8g , confirming our previous results. The 0g plot in the top row shows that subjects always indicate that the subjective vertical is perpendicular to their torso, and they report they always feel supine. This is also consistent with our previous findings.

Cross-Talk: Pitch Axis Judgments during Yaw Axis Tilts

Visual inspection of the bottom row of plots indicates that pitch axis judgments were modulated by yaw axis tilt in 1g and 1.8g , but not in 0g. Our model predicts different cross-axis effects in 1g and 1.8g , but we have not yet done quantitative comparisons of model simulations and data.

Response Dynamics

Visual comparison of the red and blue symbols indicates there was no difference between judgments made immediately and those made 15 s after a change in orientation.

CONCLUSION

The preliminary findings appear to follow novel predictions of our model of static orientation. The findings confirm that dynamics, such as hysteresis, do not have to be included to make accurate predictions of perceived orientation. Such dynamic effects may be present for larger or slower tilts than those included in our stimulus set. The results also support the presence of gif-dependent cross-talk in subjective vertical judgments, in non-weightless environments. The essential feature of the model that leads to this prediction is that it represents the lumped three-dimensional otolith end-organ mechanics and neural encoding. The positive results suggest this aspect of the model merits further investigation. The ultimate goal of this modeling and experimental approach is to make accurate predictions of orientation in aerospace environments.

REFERENCES

Bortolami SB, Rocca S, DiZio P, Lackner J (2006) Mechanisms of human static spatial orientation. Exp Brain Research 173: 374-388.

Bos JE, Bles W (2002) Theoretical considerations on canal-otolith interaction and an observer model. Biol Cybern 86: 191-207.

Correia MJ, Hixson WC, Niven JI (1968) On predictive equations for subjective judgments of vertical and horizon in a force field. Acta Otolaryngol (Stockh.) Suppl. 230: 1 -20.

Kaptein RG, Van Gisbergen JA (2004) Interpretation of a discontinuity in the sense of verticality at large body tilt. J Neurophysiol 91: 2205-2214.

ACKNOWLEDGMENT

This work was funded by NASA Grant NNJO4HJ14G.

PHOTOGRAPHS

JSC2007E11869 to JSC2007E11884
JSC2007E111904 to JSC2007E11916
JSC2007E12054 to JSC2007E12083
JSC2007E12476 to JSC2007E12509

VIDEO

- Zero G flight week 02/27 – 03/2/07 17 -21, 2006, Master: 300205

Videos available from Imagery and Publications Office (GS4), NASA/JSC.

CONTACT INFORMATION

Dr. James R. Lackner, Director lackner@brandeis.edu
Dr. Paul DiZio, Associate Director dizio@brandeis.edu

Ashton Graybiel Spatial Orientation Laboratory
Brandeis University MS 033
Waltham MA 02454-9110
Tel: 781-736-2033
Fax: 781-736-2031

TITLE

Chest Compression Efficacy for CPR in Microgravity: Instrumented Mannequin Pilot Study

FLIGHT DATES

March 20 – 21, 2007

PRINCIPAL INVESTIGATOR

George M. Pantalos, Ph.D., University of Louisville

CO-INVESTIGATORS

M. Keith Sharp, Sc.D., University of Louisville

INTRODUCTION

The ability to deliver advanced cardiac life support in the event of a crew member's cardiac arrest must be available on the International Space Station as well as for lunar base operations and Mars expeditions. Advanced cardiac life support depends in part on the ability of chest compressions (CC) during cardiopulmonary resuscitation (CPR) to generate survivable blood pressure and flow to the heart and brain until cardiac function can be restored. Chest compression effectiveness in humans in microgravity has yet to be demonstrated and the delivery of chest compressions optimized. Previous data indicate that central venous pressure, intrathoracic pressure (as indicated by intraesophageal pressure), and plasma volume are reduced in spaceflight, which may reduce the effectiveness of CPR, thus requiring the maximum CC efficacy possible.

OBJECTIVE

To investigate the effectiveness of two existing and two newly proposed techniques to deliver CC for CPR during parabolic flight.

GOAL

To guide the evaluation of CC techniques for effective CPR in the spaceflight environment. These data are critical to performing effective CPR should the need arise during emergencies in space.

METHODS AND MATERIALS

Ultimately, healthy, instrumented human test subjects will be used in a cross-over study design to evaluate the ability of CC to augment cerebral artery blood flow, cerebral oxygenation, arterial blood pressure, coronary perfusion pressure, and intraesophageal pressure in a ground-based investigation. Metered, partial CC will be delivered on alternate heartbeats during systole with the test subject in the supine posture using standard CPR sternal CC with the NASA Crew Medical Restraint System and using a newly proposed modification adding over-the-shoulder straps to oppose "chest compression recoil." A third CC method, newly proposed herein, using circumferential CCs at the sternal level (modified Heimlich maneuver or "backward bear hug") will be investigated with the test subject in the upright posture (see figure below). Vertical or "hand-stand" CPR will be the fourth technique evaluated.

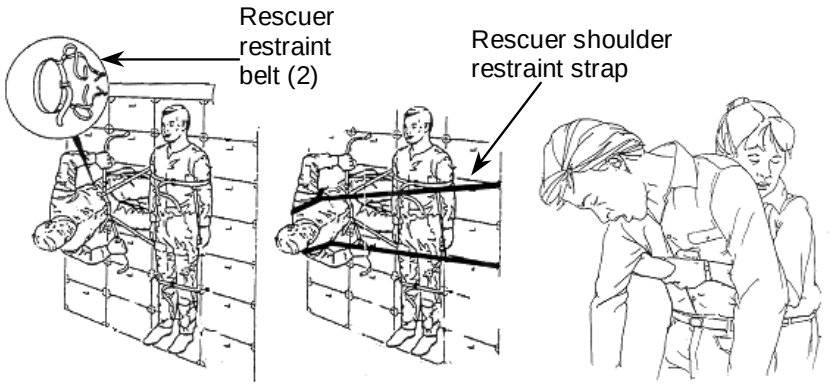

Figure 1. Three of the four techniques for delivering CCs for CPR in this investigation are shown. *Left*: Standard technique for delivering CCs using the NASA Crew Medical Restraint System (CMRS). *Middle*: Modified standard technique for delivering CCs using the CMRS with the rescuer shoulder restraint straps added to counter CC recoil. *Right*: Modified Heimlich maneuver (backward bear hug) with the rescuer approaching the victim from behind with hands grasped at the lower sternal level of the heart.

Assessment of CC efficacy for CPR will be based on the ability to augment cerebral artery blood flow, cerebral oxygenation, arterial blood pressure, coronary perfusion pressure, and intraesophageal pressure for heartbeats when CCs have been delivered compared to heartbeats without CC. Observations on how to operationally initiate and maintain the delivery of CC in a rapid and realistic manner will also be made.

To date, we have made the above-described measurements during ground-based studies on an instrumented mannequin and on three volunteer human test subjects, with favorable results. Before initiating parabolic flight studies with instrumented human test subjects, parabolic flight experiments were performed using an instrumented mannequin while evaluating the four candidate CC techniques as performed by four certified CPR rescuers. The force and depth of the CCs were recorded digitally and on FM data tape to give each rescuer the opportunity to deliver each CC technique during at least five 0g periods. Anecdotal assessments of the CC techniques were also made during lunar-g and martian-g exposures. Data were evaluated for each CC technique to determine the peak chest compression force (CCF) and residual force of each CC technique and the peak and residual chest compression depth (CCD) of each CC technique.

RESULTS

As shown in the figures below, no difference in the peak force or depth of compression or the residual force or depth of compression was found between the four techniques evaluated by the four rescuers.

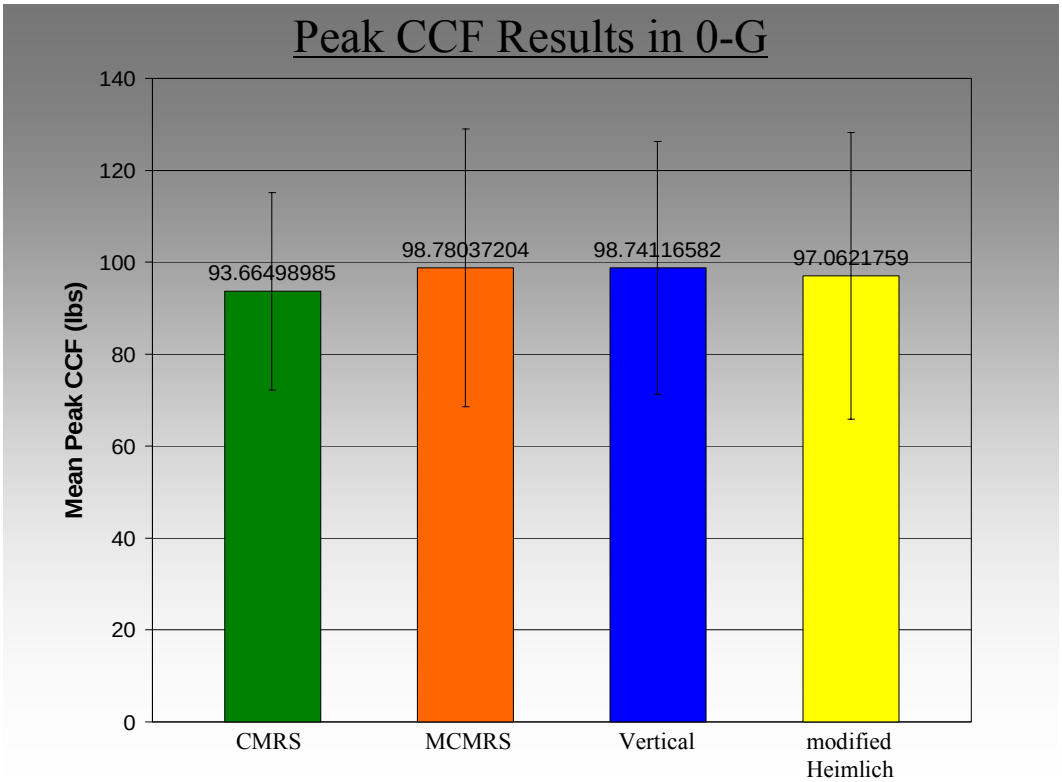

Figure 2. Peak chest compression force in four CPR techniques performed in microgravity.

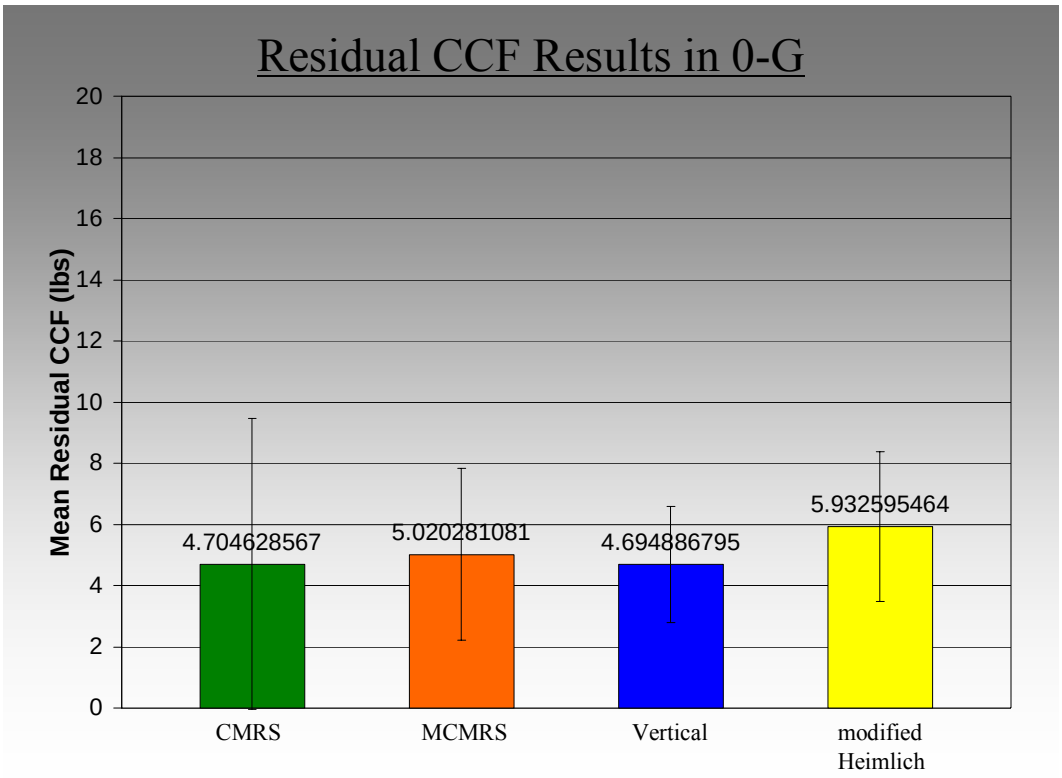

Figure 3. Residual chest compression force in four CPR techniques performed in microgravity.

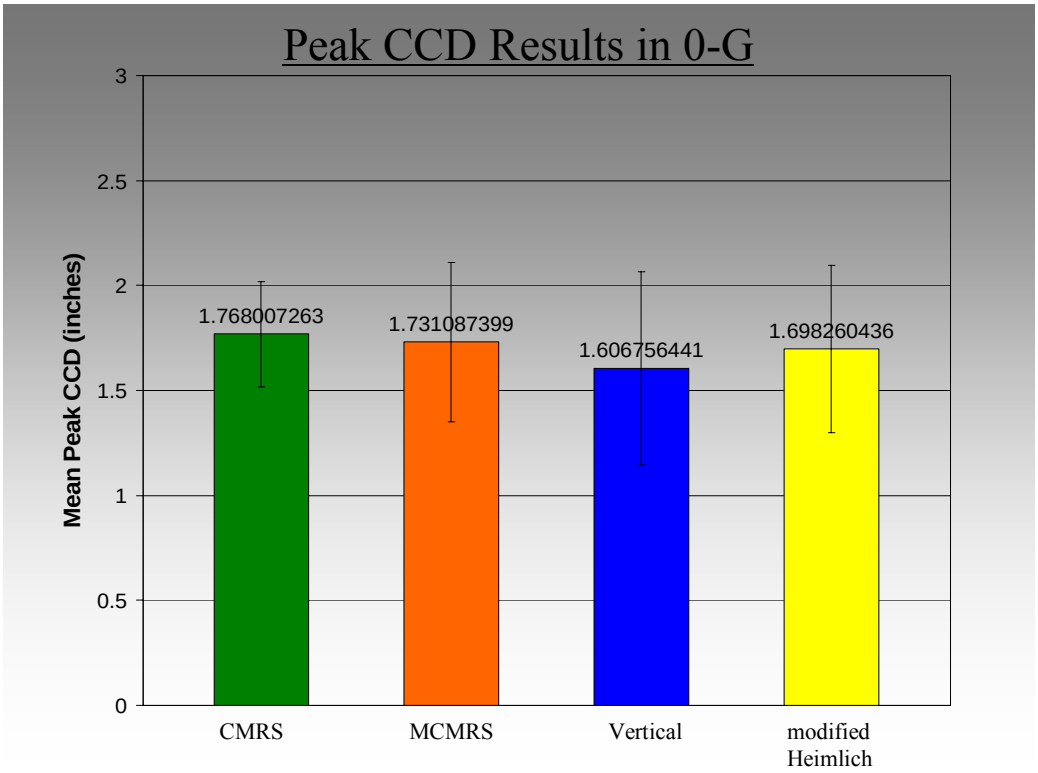

Figure 4. Peak chest compression depth in four CPR techniques performed in microgravity.

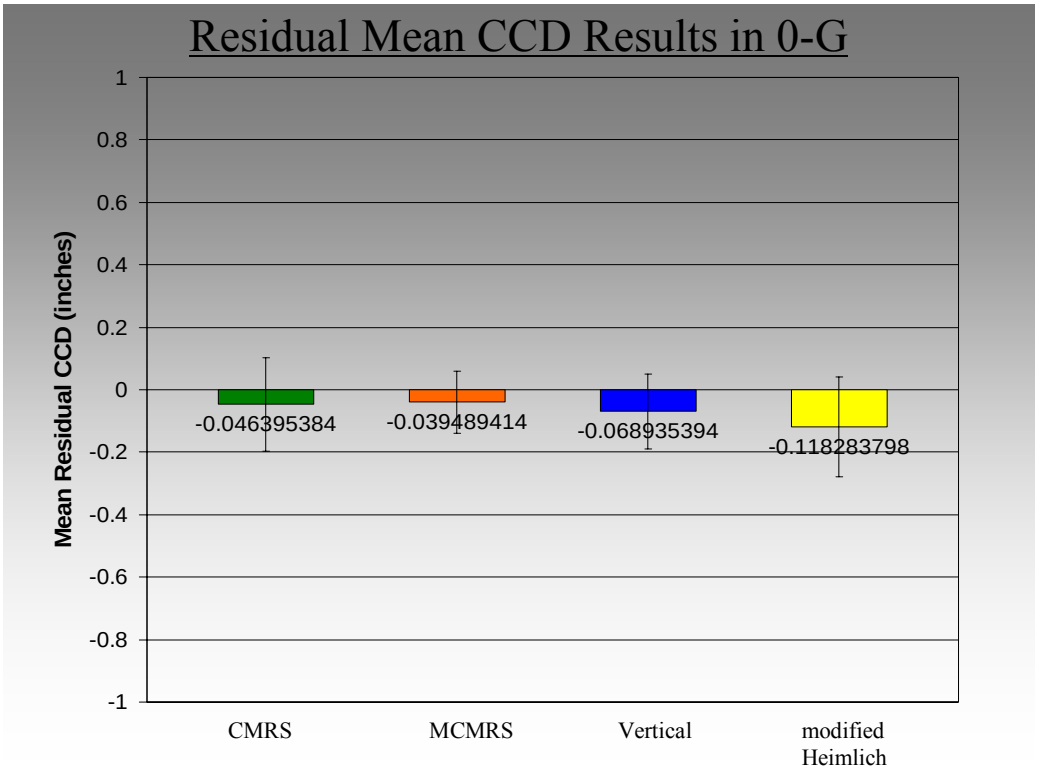

Figure 5. Residual chest compression depth in four CPR techniques performed in microgravity.

Note that since the calibration of the CCD sensor was conducted in 1 g, slightly negative residual depth represents real chest expansion of the mannequin in 0g under the residual force. We also note that compared to the 1g reference data for each technique for each rescuer, in 1g it was possible to deliver a significantly greater CCF than could be delivered in 0g. Limited measurements in lunar g and martian g were consistent with the measurements made in 0g. It was the subjective assessment of the four rescuers that the modified Heimlich or "backward bear hug" technique would be the CC technique easiest and most rapidly to implement.

CONCLUSION

We conclude that each of the four candidate techniques for chest compressions was capable of delivering the same peak force and depth of compression in 0g. We further conclude that the results from 1g investigations may not correspond directly to the results that can be achieved in 0g. Since the techniques evaluated did not differ in force and depth of chest compression, and the subjective assessment of the four rescuers was that the modified Heimlich or "backward bear hug" technique would be the easiest and most rapidly implemented at this phase of the investigation, we conclude that the backward bear hug chest compression would be the preferred chest compression technique for CPR in 0g.

PHOTOGRAPHS

JSC2007E14610 to JSC2007E14709
JSC2007E14885 to JSC2007E14930
JSC2007E15726 to JSC2007E15742

VIDEO

- Zero G flight week 3/20 -23, 2007, Master: DV0857

Videos available from Imagery and Publications Office (GS4), NASA/JSC.

CONTACT INFORMATION

George M. Pantalos, Ph.D., Professor
Departments of Surgery & Bioengineering
University of Louisville
Cardiovascular Innovation Institute
302 East Muhammad Ali Blvd.
Louisville, KY 40202
Tel: (502) 852-4345, e-mail: gmpant02@louisville.edu

TITLE

Lab-on-a-Chip Application Development Portable Test System (LOCAD-PTS)

FLIGHT DATES

March 22 – 23, 2007

PRINCIPAL INVESTIGATORS

Jake Maule, Carnegie Institution of Washington and NASA Marshall Space Flight Center
Norm Wainwright, Charles River Laboratories, Inc.

CO-INVESTIGATORS

Andrew Abercromby, Wyle

OBJECTIVE

Evaluate second and third generations of LOCAD-PTS cartridges.

INTRODUCTION

LOCAD-PTS is a hand-held device on board the International Space Station (ISS) for monitoring biological and chemical substances in the cabin environment. Results are obtained on board, thereby reducing reliance on ground-based laboratories for analysis and removing the need to return samples to Earth.

LOCAD-PTS contains multiple interchangeable cartridges for the detection of a variety of molecular targets. The first generation of cartridges, currently on board the ISS, detects bacteria and fungi (specifically, lipopolysaccharide [LPS] and beta-1,3-glucan). The second generation, scheduled for launch on STS-123 in 2008, detects only fungi (just beta-1,3-glucan). The third generation, scheduled for launch on STS-126, detects gram-positive bacteria (specifically, lipoteichoic acid).

This study evaluated the mixing, incubation, and optical absorbance measurements of the second and third generations of LOCAD-PTS cartridges under microgravity conditions. Swabbing, mixing, and dispensing procedures were tested further to develop new techniques to improve the efficiency of on-orbit operations.

METHODS AND MATERIALS

The dimensions and appearance of LOCAD-PTS and cartridges are shown in Figure 1 below.

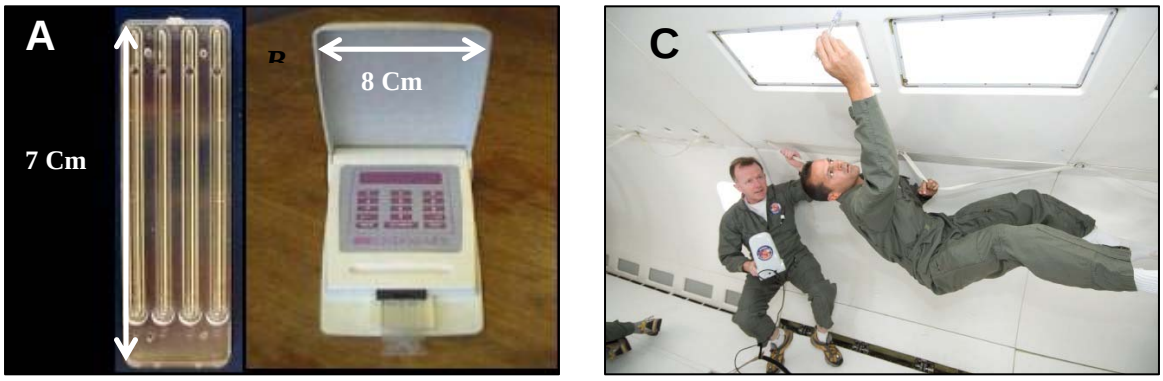

Figure 1. A, LOCAD-PTS cartridge. **B**, LOCAD-PTS (weight 2 lbs) with cartridge inserted. **C**, Norm Wainwright (left) holds LOCAD-PTS, while Jake Maule (right) swabs surface in 0g.

RESULTS AND DISCUSSION

1. *Both second (beta-glucan) and third (lipoteichoic acid) generations of LOCAD-PTS cartridges functioned effectively in microgravity*. Although a complete LOCAD-PTS test takes 5 to 15 minutes and cannot be performed in the 20 to 25 seconds of a parabola, we make an assumption that if nominal function is observed in the 0-g–2g fluctuating conditions of parabolic flight, function will also be nominal in the somewhat calmer zero-g conditions on the ISS.

2. *Bubbles can be removed from the dispensing tip after mixing and before the dispensing step*. The LOCAD-PTS cartridge contains 4 sample wells, into each of which the operator must dispense one notch of the swabbing unit, that is 25 µl. Variation in the volumes across the 4 sample wells can lead to some discrepancies in the test readings. This "cross-well" volume variation may be caused by the dispensing of incomplete droplets, due to presence of air bubbles in the dispensing tip. We found that the most

efficient method to ensure dispensing of consistent volumes was to remove air bubbles completely from the dispensing tip, as follows. The operator should: i) pipet down to notch 6 to expel all air bubbles, ii) detach the water cartridge from the swabbing unit, iii) return the swabbing unit knob to position 1 or 2, iv) reattach the water cartridge to the swabbing unit, and v) continue dispensing.

3. *Media slides were more likely to remain attached in 0g than in 1g*. A minor concern was detachment of media slides from surfaces, especially the slides for detection of fungi. All media slides tested on vertical surfaces of the aircraft cabin were less likely to detach in 0g than at 1g.

4. *LOCAD-PTS procedures, from swabbing to analysis, were nominal in lunar (0.16 g) and martian (0.38 g) gravity.*

CONCLUSIONS

1. The next two generations of LOCAD-PTS cartridges function nominally in microgravity.
2. A new step was developed to remove air bubbles from the dispensing tip. It has now been incorporated into on-orbit ISS procedures.
3. Lunar gravity will not be a constraint to operation of LOCAD-PTS on future lunar missions.

PHOTOGRAPHS

JSC2007E15274 to JSC2007E15294
JSC2007E15746 to JSC2007E15754

VIDEO

- Zero G flight week 3/20 -23, 2007, Master: DV0857

Videos available from Imagery and Publications Office (GS4), NASA/JSC.

CONTACT INFORMATION

Jake Maule, Ph.D., Project Scientist – LOCAD-PTS
Carnegie Institution of Washington, Geophysical Laboratory
5251 Broad Branch Road NW, Washington, DC 20015
202 478 8993
jmaule@ciw.edu

Norman R. Wainwright, Ph.D.
Charles River Laboratories, Inc.
1023 Wappoo Rd., Suite 43-B, Charleston, SC 29455
843 327 7080
norm.wainwright@crl.com

TITLE

The Effects of Microgravity on the Kinetics of Alkaline Phosphatase and Acetylcholinesterase

FLIGHT DATES

March 20 – 23, 2007

PRINCIPAL INVESTIGATOR

Vince LiCata, Louisiana State University

CO-INVESTIGATORS

Chin-Chi Liu, Louisiana State University
Sujatha Muralidharan, Louisiana State University
Daniel Deredge, Louisiana State University

GOAL

The overall goal was to determine if microgravity alters enzyme kinetics and equilibria.

OBJECTIVES

The objective of these flights was to test microgravity effects on two rapid protein + substrate kinetic reactions: alkaline phosphatase and acetylcholinesterase.

METHODS AND MATERIALS

Materials

Alkaline phosphatase was purified in house using published procedures (Simpoulos 1994). Acetylcholinesterase and all other standard reagents were purchased from Sigma Chemical (St. Louis, MO).

Over the course of several parabolic microgravity flights, we measured the following:

1) Ligand concentration dependence for the enzyme kinetics of the alkaline phosphatase reaction. Six data points were collected, in duplicate, for each full Michaelis-Menten (MM) curve. Each full parabola yielded one 0g data sequence (kinetics collected for 10 seconds) and one 1.7-g data sequence. Each data sequence was analyzed linearly (see below) to obtain the rate of reaction at that substrate concentration. Each rate point was then plotted against substrate concentration to obtain a full MM curve. Full MM curves were collected at 0%, 10%, 20%, and 30% glycerol concentrations.

2) Ligand concentration-dependence experiments were also performed for the enzyme kinetics of acetylcholinesterase (AChE). Eight data points, in duplicate, per full MM curve were collected for AChE kinetics. AChE was examined at 0% glycerol only.

Data Analysis

The initial portion of each kinetic trace was fitted to a linear equation to obtain the effect rate at that substrate concentration. A plot of rate (slope) vs. [substrate] yields a standard Michaelis-Menten kinetics curve:

$$v = V_{MAX}[S] / K_M + [S] \quad \text{(Equation 1)}$$

The curve (v versus [S]) is then nonlinearly fitted to determine the V_{max} and K_m parameters.

RESULTS

All reactions were measured during both the microgravity and 1.7-g portions of each parabola. The 1.7-g measurements served as the control measurements in flight. All reactions were also measured at 1g in the laboratory or on the C-9 while it was parked in the hangar at Ellington Field.

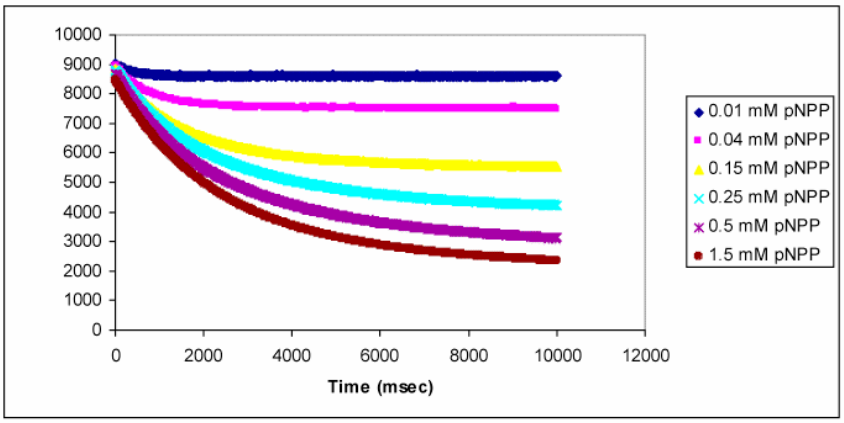

Figure 1. Representative kinetic data for alkaline phosphatase at different substrate concentrations on the ground.

A full series of kinetic reactions similar to that shown in Figure 1 was collected at both 0g and 1.8g at 0%, 10%, 20%, and 30% glycerol. Onboard data were significantly less precise than on-ground data (significantly greater random noise). Apparent differences between 0g and 1g are strongly suggested by the data, as shown in Figure 2, where the viscosity dependence of alkaline phosphatase is quite different in 0g and 1g. However, the in-flight data precision problem, and resultant low statistical significance of the differences require additional data collection from this system.

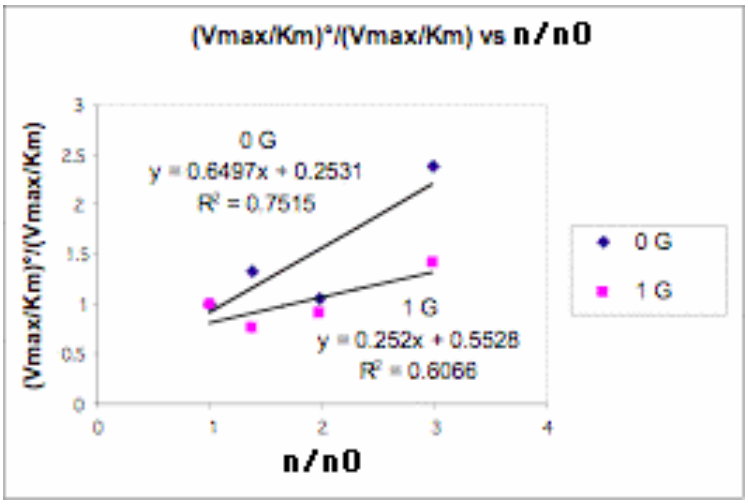

Figure 2. Catalytic efficiency (V_{max}/K_m) of alkaline phosphatase as a function of viscosity, at 0g (upper line) and 1g (lower line).

The data shown in Figure 2 indicate that the association kinetics for alkaline phosphatase may be different in microgravity versus macrogravity. The increased slope for V_{max}/K_m vs. n/n0 in microgravity suggests that in microgravity alkaline phosphatase is faster and controlled more directly by diffusion. Full statistical analysis of these data is still in progress.

DISCUSSION AND CONCLUSIONS

The goal of this project is to determine if microgravity alters the reaction rates of very rapid biological reactions. Small apparent effects of microgravity have been observed in several systems, but the harsh measurement conditions during flight consistently result in much higher random, and sometimes systematic, error rates for in-flight data. Continued redesign of the experimental equipment continues to improve data quality. Further data collection is necessary to confirm these conclusions.

REFERENCES

Cantor, C. R. and Schimmel, P. R. (1980) *Biophysical Chemistry, Part III, The Behavior of Biological Macromolecules*. W. H. Freeman and Company. San Francisco, CA. USA.

Hammes, G. G. (2000) *Thermodynamics and Kinetics for the Biological Sciences*. A. J. Wiley and Sons. New York, NY. USA.

Schoeffler, A.J., Ruiz, C.R., Joubert, A.M., Yang, X., and LiCata, V.J. (2003) Salt modulates the stability and lipid binding affinity of the adipocyte lipid binding protein, *J.Biol. Chem.* 278, 33268-33275.

Simpoulos, T.T. and Jencks, W.P. (1994) Alkaline phosphatase is an almost perfect enzyme. *Biochemistry* 33: 10375-10380.

PHOTOGRAPHS

JSC2007E14780 to JSC2007E14828
JSC2007E14931 to JSC2007E14964
JSC2007E15265 to JSC2007E15273
JSC2007E15743 to JSC2007E15745

VIDEO

- Zero G flight week 3/20-23, 2007, Master: DV0857

Videos available from Imagery and Publications Office (GS4), NASA/JSC.

CONTACT INFORMATION

Vince LiCata, Ph.D.
Department of Biological Sciences
Louisiana State University
Baton Rouge, LA 70803
Phone: (225) 578-5233
FAX: (225) 578-2597
email: licata@lsu.edu

TITLE
Space Medicine DC-9 Familiarization Flight

FLIGHT DATE
March 23, 2007

PRINCIPAL INVESTIGATOR
David Stanley, Wyle

CO-INVESTIGATORS
Melissa Rosse, Wyle
Michelle Schrenk, Wyle
Jerry Tiefert, M.D., University of Texas Medical Branch
Sean Wilson, Wyle

GOAL

To better understand the effects of microgravity on medical procedures, medical hardware, and medical training.

OBJECTIVE

To provide an opportunity for Medical Operations Branch personnel to become familiar with 0g by performing several medical contingency procedures—intravenous (IV) catheter insertion, cardiopulmonary resuscitation (CPR), and intubation (establishing an airway)—during parabolic flight. This familiarization exposes medical investigators to concerns associated with the

development of procedures used during flight and should make them more effective when interacting with crews preparing to live on board the International Space Station (ISS).

Several preflight activities were required. All medical investigators underwent an Air Force Class III Physical Examination and attended a physiological training session at the Sonny Carter Training Facility. One of the purposes of this physiological training session was to familiarize the investigators with each individual's specific hypoxic symptoms. This was accomplished at the Sonny Carter Training Facility in a hyperbaric chamber that increased the altitude, significantly decreasing oxygen and increasing carbon dioxide in the air. Medical investigators also attended a Familiarization Flight Training Session on site at Johnson Space Center, where general C-9 flight information was examined via a PowerPoint presentation and medical flight procedures were reviewed and practiced. On Monday, March 19, the medical investigators participated in the Test Readiness Review, a final safety review before flight that included an inspection of test equipment. The C-9 was loaded with the test equipment on Thursday, March 22, and all equipment was safely secured for takeoff. Loading the plane provided first-time fliers with the opportunity to gain situational awareness and insight into some of the challenges to be expected when completing specific tasks in microgravity.

Once in flight, the medical investigators immediately began to set up the three experiment stations so that the medical procedures could be performed when in 0g. The three stations—IV insertion, CPR, and intubation—were rotated among the medical investigators. Postflight activities consisted of unloading the C-9 plane, returning test equipment items to their appropriate locations, and writing a final report of research findings.

INTRODUCTION

The primary responsibility of an ISS Biomedical Flight Controller (biomedical engineer, BME) is to ensure astronaut health and safety by providing operations and engineering support to flight surgeons and representatives of other mission-support disciplines in the Mission Control Center. One of the most challenging aspects of being a flight controller is responding to new situations as they arise on board the ISS. Situational awareness and system knowledge, then, become the vital keys to successfully solving any unexpected situation. In the case of the BME, system knowledge revolves around any factor that could affect the health of the crew, ranging from mechanical or software malfunctions of countermeasure hardware to environmental or physiological changes. Thus, system knowledge also refers to the BME's ability to respond to any type of medical contingency situation and provide support for flight surgeons.

ISS Biomedical Flight Controllers (BMEs) undergo rigorous training to prepare for these types of predicaments. It is essential that the BME gains an understanding of what the crew might be experiencing, that is the type of environment the crew is exposed to when executing a recovery procedure. Utilization of this type of knowledge enables the BMEs, flight surgeons, and instructors to better relate to the crew. For this reason, the C-9 Familiarization Flight provides invaluable training for these job responsibilities. For example, the introduction of microgravity with the implementation of procedures learned on the ground gives the student an insight into how first-time fliers in space might feel with respect to orientation and coordination. Dynamic training experiences like the C-9 Familiarization Flight make a difference; the experience

enhances situational awareness and provides the tools to more effectively utilize system knowledge to determine the best course of action.

METHODS AND MATERIALS

Several onboard ISS procedures were used to perform IV insertion, CPR, and intubation. An *Intravenous Fluid Cue Card* from the U.S. SODF: Medical Checklist Book was attached to the workstation with the IV equipment, and an *Intubating Laryngeal Mask Airway: ILMA Cue Card* from the US SODF: Medical Checklist Book was attached to the intubation workstation.

RESULTS

All objectives and goals were achieved on this C-9 flight. Each station provided insight for interacting with the crew on board the ISS. Exposure to the crew's microgravity environment offered an awareness of factors overlooked on Earth. Some examples of these factors were orientation, control, dexterity, and foreign object debris (FOD) in the air. Medical investigators gained a better perspective of challenges the crew faces and must overcome to accomplish many tasks on a timeline. This was accentuated by the constantly transitioning environment that was going from 0g to 2g while the investigators were performing the different medical contingency procedures. Although this environment is different from the one the crew experiences on board the ISS, the environment introduced the medical investigators to dynamic situations where one must prepare for and expect a multitude of results and challenges.

DISCUSSION

At the CPR station, the first activity completed was deployment of the Crew Medical Restraint System (CMRS). With gravity, the CMRS is heavy to carry and position; however, in microgravity, it was easy to move and attach to tracks. This observation made it easier to visualize the crew quickly deploying the CMRS in less than 2 minutes if a medical contingency were to occur on board the ISS. The next activity was securing the mannequin to the CMRS. This presented a challenge and definitely required 2 individuals to keep with the time criticality of the contingent situation. Another challenge encountered was using the CMRS strap for restraint so that side-by-side chest compressions could be performed on the mannequin. It was difficult to locate the female end of the CMRS strap connector while trying not to float away from the mannequin, preventing immediate assistance to the "injured crew member." Using inverted CPR was the easiest approach to delivering immediate chest compressions in microgravity. The CPR station directed attention to the dexterity of the crew medical officer (CMO) who would be performing these procedures in space, trying to maintain time efficiency. The investigators better realized the significance of the BME's role at the Mission Control Center with the need for straightforward, immediate hardware guidance to ensure crew safety.

Figure 1. CPR station.

For IV insertion, several steps on the IV Fluid Cue Card had to be followed. Under the circumstances of microgravity and a medical contingency, remembering all of these steps after glancing at a cue card once would not be easy. These steps seemed not to be as intuitive as the steps for CPR or intubation. The need for ground assistance to direct the crew was appropriate, especially for providing concise directions on technique. Positioning oneself in microgravity to insert the IV without penetrating the entire vein was a challenge. Furthermore, assembling the injector and then inserting the needle into the Y-type catheter for drug administration was tricky. The needle appeared to bend more in microgravity on insertion into the catheter, and more force had to be applied for needle insertion. Disposal of the needle into the sharps container required a more conscientious effort in microgravity than on Earth. Reminders provided by the ground to the crew, such as to dispose of the needle and where to locate the sharps container, would be advantageous for the crew member's efficiency. The importance of communication between the ground and the crew member performing the procedure was recognized as integral to time and technique efficiency. As a result of completing this task, the investigators will be able to provide better technical support to crew members, along with predicting crew call-downs and possible crew challenges with medical contingency procedures.

Figure 2. IV administration station.

At the intubation station, two different intubating techniques were practiced. One technique utilized the Intubating Laryngeal Mask Airway (ILMA) equipment, while the other approach used the laryngoscope and its associated hardware. Each technique required the use of various pieces of equipment for intubation. It quickly became apparent how easily equipment floats away and how crew members must concentrate on following procedures as well as being cognizant of the consequences of their actions and movements. In microgravity, any subtle movement caused equipment to be effortlessly misplaced, propelled across a "room" or released from one's grasp. Use of the ILMA equipment for intubation was challenging as it did not function properly on these flights. An attempt was made to use the damaged ILMA hardware; however, inserting the tube was difficult and no positive outcome resulted. Thus, this experience emphasized the need for alternative options as well as the support expected from a BME in providing immediate technical assistance, that is readiness to give location and availability of alternative hardware found in medical kits, Ambulatory Medical Pack (AMP), and Advanced Life Support Pack (ALSP). The use of the laryngoscope was actually easier in microgravity than with gravity. A successful intubation and tube insertion occurred on the first attempt, providing air to the mannequin's lungs, which was seen with lung inflation. The findings from this station gave valuable insight into the crew member's world of "multi-tasking" in an unfamiliar environment.

Figure 3. Intubation station.

CONCLUSIONS

All objectives and goals were achieved on this C-9 flight. By performing the medical contingency procedures for IV insertion, CPR, and intubation, medical investigators gained a better understanding of the effects of microgravity on medical procedures, medical hardware, and medical training. For Biomedical Flight Controllers, this situational awareness enhances the BMEs' ability to better aid the crew and flight surgeons in the event of a contingency, better communicate the potential dangers to the Flight Director and Capsule Communicator, and better resolve unexpected problems.

PHOTOGRAPHS

JSC2007E15726 to JSC2007E15742

VIDEO

- Zero G flight week 3/20 -23, 2007, Master: DV0857

Videos available from Imagery and Publications Office (GS4), NASA/JSC.

CONTACT INFORMATION

David Stanley
Wyle
1290 Hercules Suite 120
Houston, Tx 77058
dstanley@wylehou.com

TITLE

Undergraduate Program Flights – Dynamics of a Planar Arm Model with Servo-regulated Viscoelastic Muscles in a Microgravity Environment

FLIGHT DATE

April 27, 2007

PRINCIPAL INVESTIGATORS
Jared Durden, Drury University
Drew DeJarnette, Drury University
Benjamin Taylor, Drury University
Adam Scott, Drury University
Gregory Ojakangas, Drury University

CO-INVESTIGATOR

Josh Petitt, Drury University

GOAL AND OBJECTIVES

1) Predict the motion of a two-degree-of-freedom mechanical arm, designed to simulate the behavior of a human arm in planar motion, under normal laboratory conditions and under microgravity conditions, by using kinematics.

2) Analyze and compare data of actual motion of the arm in laboratory and microgravity conditions.

3) Utilize the NASA microgravity flight experience and apparatus to foster interest in the physical and biophysical sciences in K–12 students as well as the general public by using our project as an outreach program.

4) Expose physics classes at Drury University to aspects of mathematical modeling, electronic hardware, computer programming, and construction of a research device, as a "real-world" class project.

METHOD AND MATERIALS

Equipment

We used the S5801 model sail control (winch) servos from Futaba Corporation. These servos can create 136 oz-in of torque and a speed of 360 degrees/0.5 sec, with a power requirement of about 7.2V. They are capable of about 720 degrees of rotation – more than enough for our application. The forearm and shoulder disks of the arm were cut from an acrylic sheet. The upper arm and the elbow disks of the experimental apparatus are made of a light-weight Plexiglas. To help guard against damage to our apparatus as well as to keep strain on the servos to a minimum, we mounted 4 of the servos on an acrylic mount. We included two accelerometers attached to our experiment platform to record and give us an inertial coordinate system from which to begin our analysis. These accelerometers are capable of measuring ± 2g and so were adequate for our experiment in microgravity.

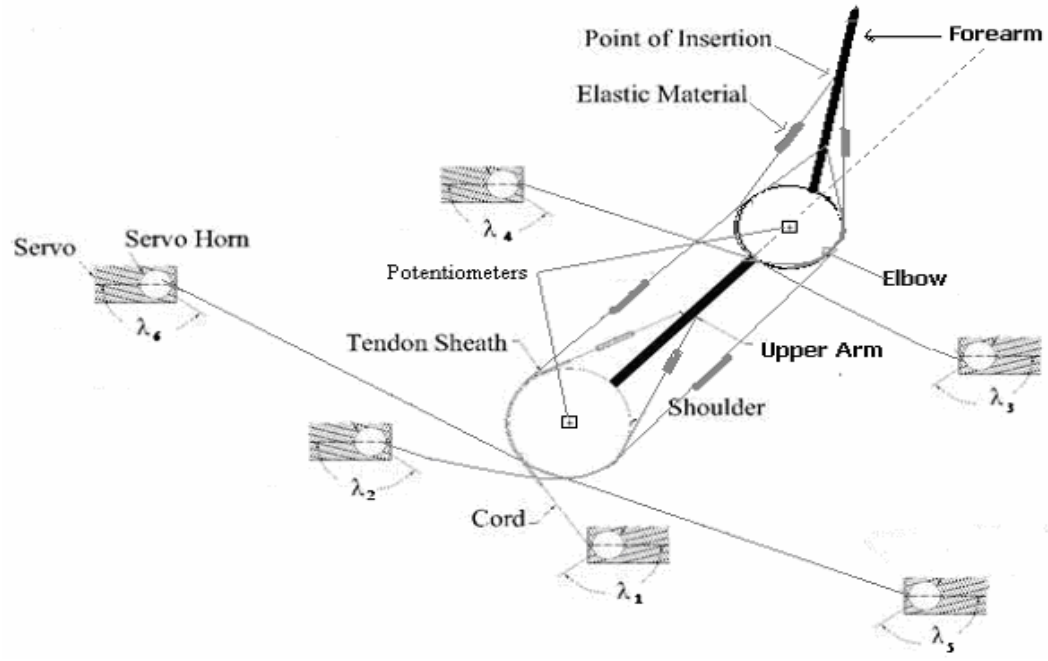

Figure 1. Design of arm apparatus with servos and connections.

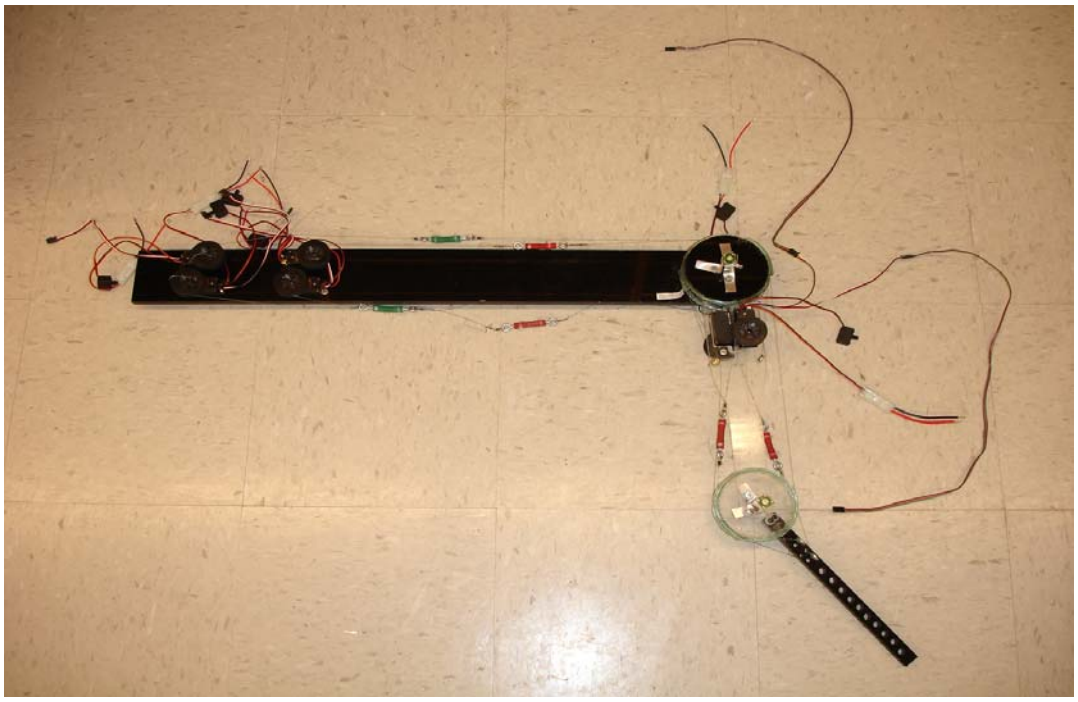

Figure 2. A photo of our experimental (arm) apparatus with tendon connections, servos, and potentiometers.

The servos were controlled by using two BrainStem® GP 1.0 microcontroller modules from Acroname Incorporated. This module supports five 10-bin analog-to-digital (A/D) inputs, five flexible digital outputs, a GP2D02 port, and four high-resolution servo outputs. The two Brainstem modules were connected via an IIC (inter-integrated circuit) cable. Using a USB port connection, we could send commands to the servos directly from a laptop computer. The angles of rotation of the shoulder and elbow joints were continuously monitored using angular motion sensors (potentiometers) attached directly to the elbow and shoulder joints. The potentiometers were obtained from the Piher Corporation. They are the 100-Kohm Trimmer potentiometers with a power rating of 0.5 W. Their analog outputs were digitized using the Brainstem's onboard A/D converter and have been calibrated to measure elbow and shoulder angles.

Preflight Laboratory Procedures

The first step in the experiment was to design proposed arm trajectories that we hoped to approximate in flight, shown in Figure 3. The angular positions were measured by the potentiometer and saved as functions of time by our trajectory routine program. The same routine initiated data collection from the accelerometer during each experiment. Care was taken to ensure that the angular positions and microgravity data were saved in distinct files after each experiment.

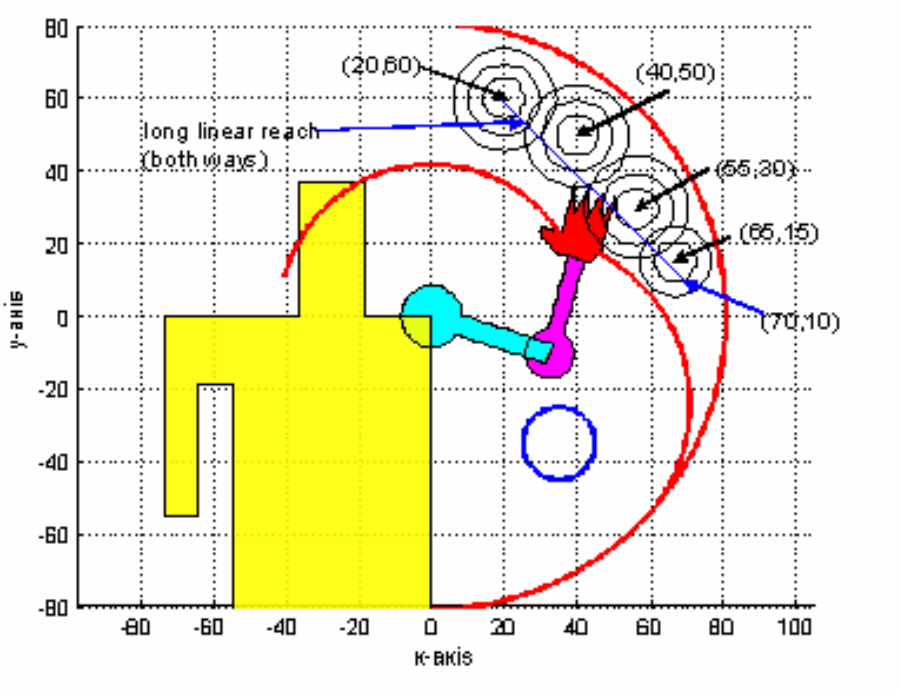

Figure 3. Trajectories executed during flights.

The bold red lines in Figure 3 show the workspace that our design allowed. The black circles show the chosen circular trajectories. The blue diagonal line extending from point (20,60) to point (70,10) was also chosen as a trajectory (this was traced from top to bottom and in another routine, from bottom to top). Although the tracings are not shown, we chose to trace linear reaches from the center of each circular set at 0, 45, 90, 135, 180, 225, 270, and 315 degrees. To execute these trajectories we had to convert the Cartesian position of the end effector, the point that traces the trajectory, to shoulder and elbow angles (θ_1, θ_2) at each time (cf. Hollerbach and Flash, 1982). The shoulder pivot is at the origin of the (x,y) coordinate system. In Figure 4, counterclockwise from the upper left panel are examples of the desired Cartesian end-effector trajectory, x and y versus time, θ_1 and θ_2 versus time, and the trajectory of the angular coordinates. The solid curves represent paths with constant linear speed along the circle, and the dashed curves represent smoother, more physically reasonable motion in which accelerations are not immediate at the beginning and end of motion. To create these smoother motions, we performed a simple parameterization of smooth movement along the (x,y) trajectory, using an inverse tangent function (details are omitted here for brevity). The bottom left graph of Figure 4 shows the kinematics for a typical circular end-effector trajectory, in which we have used the standard inverse-kinematics equations to convert Cartesian positions of the end effector to trajectories in θ_1 and θ_2 versus time.

The second step was to estimate the elastic torques τ_{1e} and τ_{2e} (that is, the torques transmitted by the tension in the muscle tendons) at the shoulder and elbow that were necessary to produce the desired motions. This was done using the equations of motion for the planar arm.

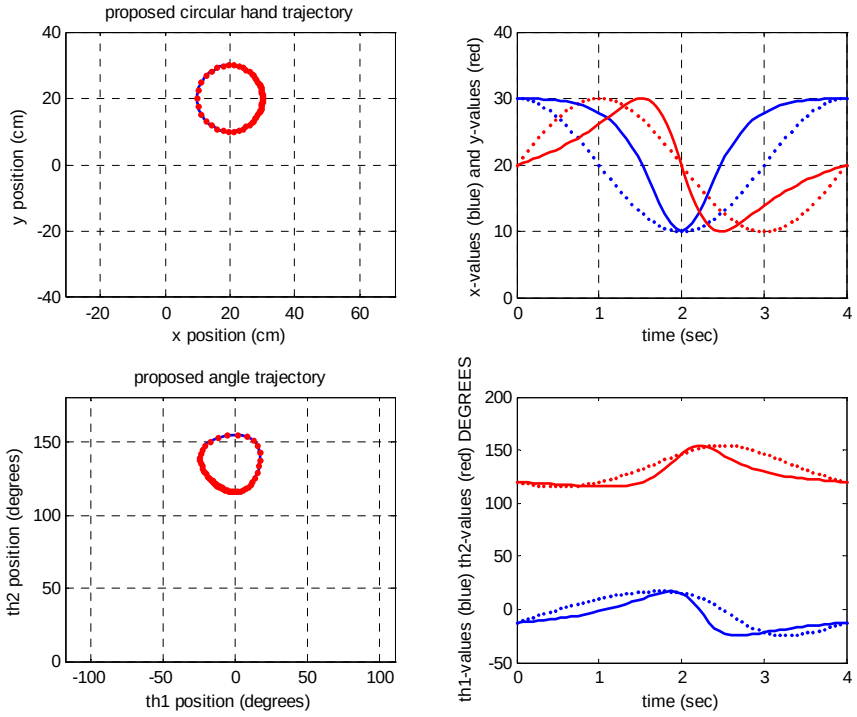

Figure 4. Kinematics for a simple circular end-effector trajectory.

Finally, we can derive values for all of the other terms on the left-hand side of our equations of motion by using numerical derivatives of the shoulder and elbow angles for each desired trajectory, together with inertial properties (masses, center-of-mass locations, rotational inertias, arm segment lengths) that we have measured for all components of the mechanical arm.

Once the required elastic torques were modeled, the next step was to determine a set of muscle forces that would generate these torques. Because we had 6 muscles and only 2 torque components, the computation of required muscle forces was an under-determined problem – there are infinitely many ways to generate the required torques with the available muscles. We had to choose to initially constrain the muscle forces so that the mean-squared value of the muscle forces at any time was minimized. This solution is provided by the generalized linear inverse method for under-determined systems of equations (cf. Strang, 1980). The torque vector can be written as $\vec{\tau} = J\vec{f}$, where J is the (2x6) Jacobian matrix of muscle moment arms and $\vec{f}$ is the (6-dimensional) vector of elastic muscle forces, which we wrote in terms of the spring constants, shoulder and elbow and servo horn radii, servo angles, and shoulder and elbow angles. We then computed our chosen muscle forces as $\vec{f}^{\,*} = J^t (JJ^t)^{-1}\vec{\tau}$. However, the result of this computation gives some forces that are negative, which cannot be generated by our elastic muscles. To counteract this problem, we added a constant force component to each muscle pair, so that all muscle forces remain nonnegative at all times (otherwise our muscles would "droop" and possibly fall off the arm during the experiments). Figure 5 shows the result for the case of the circular trajectory described above.

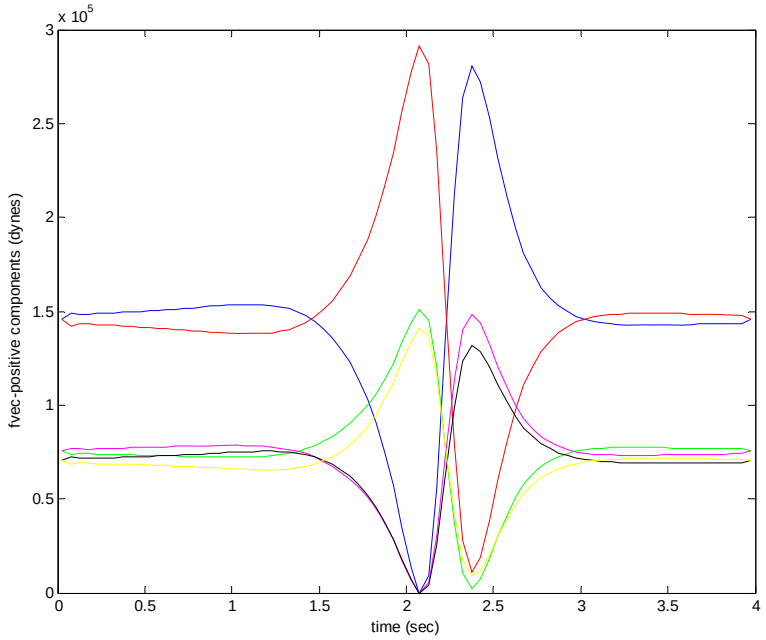

Figure 5. Elastic muscle forces versus time, derived from pseudo inverse method.

Finally, we converted the muscle forces into servo angles using simple Hooke's law relationships between the synthetic muscle force and degree of stretch:

$$\begin{bmatrix} f_1(\Delta l_1) \\ f_2(\Delta l_2) \\ f_3(\Delta l_3) \\ f_4(\Delta l_4) \\ f_5(\Delta l_5) \\ f_6(\Delta l_6) \end{bmatrix} = \begin{bmatrix} k_1(R_h\lambda_1 - R_s(\theta_1 - \theta_{11})) \\ k_2(R_h\lambda_2 + R_s(\theta_1 - \theta_{12})) \\ k_3(R_h\lambda_3 - R_e(\theta_2 - \theta_{23})) \\ k_4(R_h\lambda_4 + R_e(\theta_2 - \theta_{24})) \\ k_5[R_h\lambda_5 - R_s(\theta_1 - \theta_{15}) - R_e(\theta_2 - \theta_{25})] \\ k_6[R_h\lambda_6 + R_s(\theta_1 - \theta_{16}) + R_e(\theta_2 - \theta_{26})] \end{bmatrix}$$

where λ_j, θ_{ij}, R_s, R_e, R_h, and k_j are the servo angles, the equilibrium values of θ_j (shoulder or elbow angles for which the muscles are unstretched when the corresponding servo angle is zero), the shoulder, elbow, and servo horn radii, and the elastic constants for the jth muscle, respectively. Note that because we have adjusted all muscles so that their tensions remain positive throughout the motion, we are assured that their degrees of stretch will remain positive throughout each experiment.

The results for the nominal circular trajectory discussed above are presented in Figure 6.

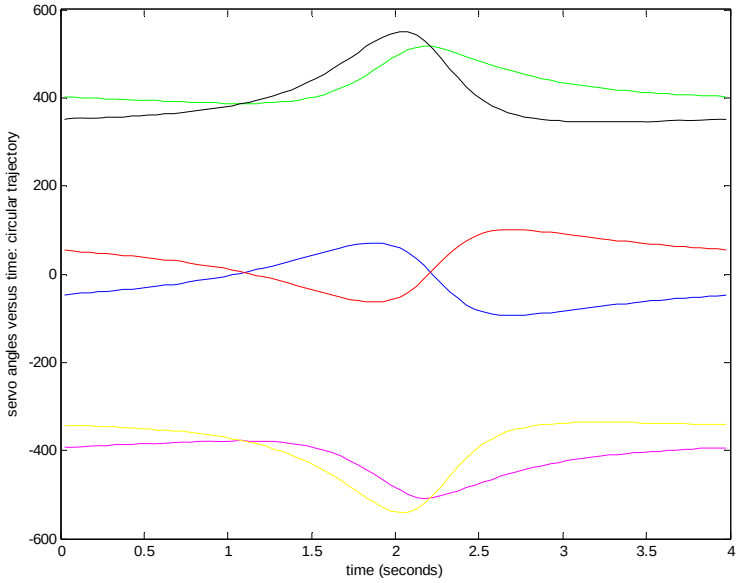

Figure 6. Servo angles versus time for the example discussed in the text.

Servo angle data sets for each proposed experiment (circular and linear reaching motions) will be converted into unsigned integer data ranging from 0 to 255, which is the format required for operation of typical hobby servos such as those that we have used in our experiment.

In-flight Procedures

With the preflight preparations completed, the procedures we needed to perform in flight were relatively simple:

1) Before each parabola: We prepared the arm for its intended motion by moving it to its angle (θ_{ij}) equilibrium state, the orientation corresponding to zero shoulder and elbow angles (that is, the arm fully extended at a right angle to the floor of the aircraft) and zero servo angles. In this orientation the muscle tendons can be adjusted as necessary, so we have nearly zero stretch, as possible, without slack or "sagging."

2) Once a microgravity environment was experienced, we executed a MATLAB/C software routine that moved the arm to the starting position of the intended trajectory.

4) We then executed a MATLAB routine that sent commands (specific to each experiment) to the servos as computed during our preflight preparations.

5) Data were recorded by the potentiometers and accelerometers directly through programming and the motion of the arm was recorded by digital camera.

RESULTS AND DISCUSSION

Unfortunately, because of equipment problems data analysis has not been completed. The potentiometer responsible for recording angular motion in the elbow joint did not report accurate data due to an unknown malfunction. Therefore, it has become necessary to utilize video footage taken on the flight. We are in the process of analyzing the video on Video Point software. This process is quite time-consuming and not yet completed. However, from observations made during flight experimentation, we definitely saw the desired motion from almost all of the trajectories and expect quite successful results from video analysis. Most importantly, throughout our work on this project it was the unforeseen complications that made the project so beneficial to us as students and as colleagues. The experience we gained in teamwork and troubleshooting could not be achieved in a classroom setting and has made us more efficient and precise research scientists.

REFERENCES

Hollerbach, J. M., Flash, T. (1982). Dynamic interactions between limb segments during planar arm movement. *Biological Cyberkinetics* 44, 67-77.

Strang, G. (1980). *Linear algebra and its applications*, second edition, Academic Press, London.

PHOTOGRAPHS

JSC2007E20882
JSC2007E20869
JSC2007E20899
JSC2007E20939 to JSC2007E20944

VIDEO

- Student Campaign Flight Week 4/24 -27/2007, Master: 726296

Videos available from Imagery and Publications Office (GS4), NASA/JSC.

CONTACT INFORMATION

Dr. Gregory Ojakangas
Drury University
900 N. Benton Ave.
Springfield, MO 65802

Jared Durden
(417) 838-1469
jdurden@drury.edu

TITLE
Transgenic Arabidopsis Gene Expression System (TAGES)

FLIGHT DATES
May 22 – 25, 2007

PRINCIPAL INVESTIGATORS
Robert J. Ferl, Ph.D.
Anna-Lisa Paul, Ph.D.

GOALS

The Transgenic Arabidopsis Gene Expression System (TAGES) experiment is currently part of a spaceflight payload, in development for deployment on the International Space Station (ISS) in late 2008 or early 2009, titled "Advanced Plant Experiments on Orbit-Cambium" (APEX-Cambium). The payload is being managed by the Sustainable Systems Division at the Kennedy Space Center (KSC). The purpose of the APEX-Cambium payload is to continue the development of state-of-the-art transgenic plant technology to answer important questions about plant biology in microgravity environments. The Principal Investigator (PI) team has developed a series of plants that contain specific environmental response genes designed to register and report the plants' perception of their environment, and are referred to as TAGES plants. *Arabidopsis thaliana* (Arabidopsis) plants have been genetically engineered with various gene promoters driving both the green fluorescent protein (GFP) and β-glucuronidase (GUS) reporter genes. KC-135 and C-9B flights have been performed in the past to quantify reporter gene

activity and survey changes in gene expression patterns. This reduced-gravity flight campaign continues to be performed as requested in the PI's NASA Research Announcement (NRA) proposal # 98-HEDS-02-299 for a spaceflight experiment entitled "Biomonitors of Spaceflight Exposure." Previous parabolic flight experiments have proven to be useful indicators of spaceflight performance, as demonstrated by the success of the Plant Growth in Microgravity (PGIM) payload on STS-93.

The goals of the May 2007 C-9B experiments included performing specific tests to further refine and identify the behavior of these reporter gene constructs before the spaceflight experiment is performed. Molecular genetic tools used throughout include reporter genes for GFP (the expression of this reporter gene can be captured with specialized imaging equipment in real time) and GUS (a sensitive enzymatic reporter that is monitored by fixing tissue in histochemical stain that reacts with the enzyme encoded by the reporter gene).

OBJECTIVES

The first objective was to test a new TAGES fluorescent imaging system. These experiments utilize Arabidopsis engineered with both GFP and GUS gene reporters so real-time images that are collected telemetrically (monitoring GFP gene expression) can be compared directly with the GUS expression patterns visualized through subsequent histochemical staining.

The second objective was to obtain a replicate data set characterizing the extent of thermal variation on the surface of Arabidopsis leaves during parabolic flight. The C-9B parabolic flight experiments conducted in 2006 were very successful in this endeavor; these experiments demonstrated that if air is not allowed to circulate, the surface leaf temperature can vary by 2-4 °C between the 0g and 2g segments of the parabola. It was our goal to repeat these experiments using the Fluke thermal imaging device in conjunction with plants engineered with gene reporters that are designed to reveal changes in gene expression in response to heat-induced stress. Data were collected in the form of digital images and tissue-specific reporter gene expression patterns.

The third objective was to develop further the genome-level genetic analyses initiated with the April 2003 KC-135 experiments. The results from the April 2003 data indicated that numerous genes associated with auxin metabolism are upregulated in response to parabolic flight (22,000 gene array chips from Affymetrix™). Several of these genes have been implicated in gravity sensing. The genetic analyses on the current C-9B flight will contribute to the dissection of this response. Plants engineered with gene reporters designed to respond to variations in auxin metabolism were used to gather tissue-specific gene expression data.

METHODS AND MATERIALS

The plants utilized for the above experiments were flown as seedlings (9- to 20-day-old plants) on Petri plates. All plants were contained in BioTransporter (BT) containers. The BTs were placed inside a duffel bag for takeoff and landing.

On each flight, required harvests were performed during the breaks that occur during 10-parabola plane turnarounds. Plants being harvested during the turnarounds were removed from their growth support medium using forceps and placed in capped tubes of stain (x-gluc) or preservative (RNAlater) solution. The sealed tubes were stowed in an additional level of containment (the BT) during all phases of the flight except when harvesting occurred.

Plants that did not require in-flight harvesting remained contained within their respective BTs or imaging or monitoring devices. GFP plants were inserted into the TAGES GFP imaging system, which consists of a fixed camera, LED (light-emitting diode) illumination, power supply, and controller board. Images were taken during the entire flight at a pre-programmed, regular interval. The entire system was assembled and initiated before takeoff, and was not disassembled until landing. The only other action required was to connect the laptop computer to the imaging system before parabolic flight began. The operator initiated imaging using the laptop software.

In addition, some free-float experimentation was conducted. The free-float equipment included a thermal imager attached to a 24-inch acrylic tube that, on the opposite end, was attached to a Petri plate lit on four sides by LEDs. Some plant tissue was removed from the Petri plate during turnarounds. Plants being harvested during the turnarounds were removed from their growth support medium using forceps and placed in capped tubes of stain (x-gluc) or preservative (RNAlater) solution. The sealed tubes were stowed in an additional level of containment during all phases of the flight except when harvesting occurred. On each of the four flights, up to four vials were used.

RESULTS

Good data sets were collected on each flight. The hardware functionality for the TAGES GFP imaging system and for the accessory thermal imaging system remained essentially intact for all flights. Initial examination of the data indicates that data quality is high and that the experiment goals are very likely to have been attained. Some thermal imaging issues may have a negative impact on analysis of leaf temperature on the lunar parabolas.

One flight was lost due to operational limitations, and this flight was to have included the martian gravity parabolas. The analyses of the lunar parabolas will be set aside until the martian parabolas are complete and the partial gravities can be analyzed together. These analyses include the molecular characterization of the plants as well as the image analyses from both the thermal and GFP imagers.

DISCUSSION

It is the nature of our C-9B flight experiments that significant downstream analyses are required to fully assay the results. However, it is reasonably clear from the initial examination of the data that the following statements can be made:

1) The thermal imaging experiments have fundamentally confirmed that leaf temperature is affected by the microgravity portion of the parabolic flights. Analysis of the lunar parabolas is

tentative and it is likely that full analysis of the lunar parabolas should await the acquisition of data from the postponed martian parabolas. Full analysis of thermal imaging data sets should be complete by the time the last flight of the series is rescheduled for this fall.

2) The TAGES GFP imaging system proved fundamentally functional in the parabolic flight environment. Analyses of the biological responses in the TAGES GFP imaging system will require significant downstream image processing. Analysis of images obtained during the lunar-gravity parabolas will await acquisition of the martian partial gravity data on the rescheduled flight opportunity.

The larger analysis awaits the completion of the flight set.

CONCLUSION

Analyses support no scientific conclusions as yet. The biological samples returned from the flights will be analyzed over the coming months, as will the images collected from both the thermal and GFP imaging systems. Full analyses of the lunar data sets and biological samples will await completion of the martian parabolas for comparison.

REFERENCES

Paul, A.L., H.G. Levine, W. McLamb, K.L. Norwood, D. Reed, G.W. Stutte, H.W. Wells, and R.J. Ferl. Plant molecular biology in the space station era: utilization of KSC fixation tubes with RNAlater. Acta Astronaut 2005; **56**(6):623-8.

Paul, A.L., and R.J. Ferl. Molecular aspects of stress-gene regulation during spaceflight. J Plant Growth Regul 2002; **21**(2): 166-76.

Paul, A.L., M.P. Popp, W.B. Gurley, C. Guy, K.L. Norwood, and R. Ferl. Arabidopsis gene expression patterns are altered during spaceflight. J Adv Space Res 2005.

PHOTOGRAPHS

JSC2007E25719 to JSC2007E25733
JSC2007E25990 to JSC2007E26003
JSC2007E26174 to JSC2007E26187

VIDEO

- Zero G flight week 5/23-24, 2007, Master: 727441

Videos available from Imagery and Publications Office (GS4), NASA/JSC.

CONTACT INFORMATION

Robert J. Ferl, Ph.D.
Anna-Lisa Paul, Ph.D.
Dept. of Horticultural Sciences
University of Florida
Gainesville, FL 32611-0690
Phone: (352) 392-1928 x 301 / x 331
Fax: (352) 392-4072
Email: robferl@ufl.edu
alp@ufl.edu

David Reed
Space Life Sciences Lab
BIO-3, Bldg M6-1025
KSC, FL 32899
Phone: (321) 861-2980
Fax: (321) 861-2226
Email: David.W.Reed@nasa.gov

TITLE
Medical Operations C-9 Familiarization Flight

FLIGHT DATE
May 24, 2007

PRINCIPAL INVESTIGATOR
Bob Tweedy, Barrios Technology

CO-INVESTIGATORS
Lindsey Turns, Wyle
Elisca Hicks, Futron
David Hoellen, Wyle
Bruce Nieschwitz, Wyle

GOAL

To familiarize Medical Operations personnel with the effects of microgravity on situational awareness, handling medical equipment, and executing emergency medical procedures.

OBJECTIVES

1. To successfully execute two methods of establishing an airway for a non-breathing victim
2. To successfully restrain an unconscious victim to the Crew Medical Restraint System (CMRS)
3. To successfully execute three methods of delivering cardiopulmonary resuscitation (CPR)
4. To successfully insert an intravenous (IV) catheter into the arm of a patient

METHODS AND MATERIALS

Three work stations were set up to execute the various emergency medical procedures: intubation (establishing an airway), CPR, and IV insertion.

Intubation

This work station was prepared so participants could practice various techniques for establishing a direct airway to the trachea. A mannequin that had all relevant upper respiratory features was deployed along with the medical kit that contained all of the necessary instruments. The first procedure required the insertion of the Intubating Laryngeal Mask Airway (ILMA) device and inflation of the cuff to ensure a good seal between the ILMA and tracheal airway. An Ambu bag was then attached directly to the ILMA and breaths were administered. Next, an intubation procedure was performed by inserting an endotracheal (ET) tube along the path of the ILMA and into the trachea. Once the ET tube was in place, the ILMA was removed. The Ambu bag was then attached directly to the ET tube and breaths were administered.

Another technique of establishing an airway involved inserting the ET tube with the aid of a laryngoscope. The laryngoscope blade was placed between the base of the tongue and the epiglottis to expose the vocal cords and a clear view of the trachea. The next step was to insert the ET tube directly into the trachea to establish the airway. With the ET tube in place, the Ambu bag was attached to the ET tube and breaths were administered.

Materials: Mannequin, ILMA, Ambu bag, endotracheal (ET) tube, stabilization rod, syringe, and laryngoscope.

CPR

This work station required the participants to first unstow the life-sized mannequin and secure him to the Crew Medical Restraint System (CMRS). Once the mannequin was secured, CPR was performed using three techniques: (1) kneeling beside the victim using the Crew Medical Officer (CMO) restraining straps, (2) straddling the CMRS and victim using the CMO restraining straps, and (3) performing inverted CPR, utilizing the ceiling of the plane for restraint and leverage to administer chest compressions.

Materials: CMRS, CPR mannequin.

IV Insertion

A single procedure was executed to start an IV via catheter. Using a needle as a guide, the participant inserted a Teflon catheter into the mannequin's vein. Once the catheter had been inserted, the needle was removed, leaving the catheter, and was promptly discarded into a sharps

container. A Y-type catheter was then attached to the Teflon catheter, and the IV tubing was secured to the arm with tape. No fluids were transferred into the vein during this procedure.

Materials: Mannequin arm, 16G Teflon catheter, IV administration kit, sharps container, tourniquet, and tape.

RESULTS

Airway

Each airway procedure was successfully executed with little or no trouble. During the first procedure, the ILMA was unstowed and the integrity of the cuff was verified by inflating it with 8 cc of air from a syringe. Once cuff integrity was verified, it was deflated, lubricated, and inserted into the mannequin's mouth and down into the trachea. Once positioned in the trachea, the cuff was inflated to form a seal and open the airway. Next, the Ambu bag was attached and breaths were introduced. The ILMA seal with the trachea was confirmed as both lungs rose with the introduction of each breath provided by the Ambu bag.

After the Ambu bag was disengaged, another technique for establishing an airway could begin. The first step was to unstow the ET tube, lubricate it, and insert it into the ILMA metal shaft. Once in place in the trachea, the ET tube cuff was inflated to seal its position. Then the ILMA cuff was deflated, the tracheal tube connector removed, and the ILMA assembly removed from the mannequin. The ET tube connector was then reattached and breaths were delivered with the Ambu bag.

Another method for establishing an airway was accomplished by inserting the ET tube with the aid of a laryngoscope. The blade of the laryngoscope was maneuvered into the space between the base of the tongue and the epiglottis until the tongue was displaced and the vocal cords were exposed. The ET tube was then inserted into the trachea and the laryngoscope subsequently removed. To seal its position, the ET tube cuff was inflated. Finally, the Ambu bag was attached and breaths were administered.

All instruments were stowed after the procedures were accomplished.

Overall, it seemed that the absence of gravity helped to more efficiently insert the ET tube with both the ILMA and the laryngoscope. Fighting the forces normally produced by the jaw on the ground was not needed in the 0g environment. Consequently, it was easier to confirm line of sight to the airway, making the entire process less taxing and more streamlined.

CPR

Three procedures were executed at the CPR station with little difficulty. The first group in the rotation was tasked with securing the mannequin to the CMRS, which was secured via seat tracks to the aircraft before flight.

The first CPR technique was similar to the conventional ground method of kneeling beside the patient and administering compressions from the side. The preferred Caregiver stabilization was to route the CMO side straps behind the back for support and leverage. Once the participant was

secured with the CMO straps, compressions could be administered perpendicular to the long axis of the patient's body.

The second CPR technique involved straddling the mannequin and delivering compressions in parallel with the long axis of the body. The preferred method of stabilization was to secure each leg with a CMO strap on each side of the CMRS.

The last CPR technique was the inverted method, in which the caregiver essentially does a handstand on the patient's chest and gives compressions with leverage gained by pushing from the ceiling of the plane.

Performing CPR revealed the unique conditions and challenges that a 0g environment presents. Securing the mannequin, for example, was particularly challenging because every part of his body had to be secured; any body part not secured would obstruct a direct path to the chest area where compressions were needed. Furthermore, it was difficult to quickly discern where to secure each strap, since some were intended for CMO restraint while others were for patient restraint. As for CPR procedures, it quickly became evident that kneeling beside the patient or using the straddle method would prove to be very difficult due to the challenge of staying in a secure and firm posture. Consequently, holding the needed leverage to deliver quality chest compressions was a battle. A more effective method was to use the inverted technique. This method provided the most stability and leverage so effective chest compressions could be achieved.

IV Insertion

The mannequin arm was prepped by tightly applying a tourniquet to the upper area of the arm. A 16G catheter was then removed from the IV kit and the seal broken by twisting the casing containing the needle and catheter. Using the thumb and index finger of the non-dominant hand, the vein was captured and then the needle (beveled side up) was inserted into the vein using the dominant hand. Once the needle entered the vein, the needle entry angle was dropped slightly before it and the catheter were pushed another 2 mm into the vein to the final position. Once they were in position, the needle was carefully removed and discarded into the sharps container, leaving only the Teflon catheter in the vein. The next step was to attach the Y-type catheter to the Teflon catheter and secure the IV tubing using a chevron pattern with tape.

The most challenging part of this activity was keeping track of and securing the relatively small instruments in the IV kit and ensuring the needle (sharps) was controlled at every moment once it was exposed. Inserting the needle into the vein and inserting the catheter were straightforward and not difficult. Furthermore, it was relatively easy to restrain oneself while performing the task.

DISCUSSION

It is important for anyone who interfaces with astronauts in space to understand the potential difficulties encountered with performing time-critical advanced life support procedures in 0g. In a broader sense, it is important to understand how the nature of the ISS environment may make simple tasks very difficult and vice versa. The more clearly instructors, engineers, and medical

personnel understand this environment and gain situational awareness, the more effective they can be for mission success.

CONCLUSION

The familiarization flight is fun, beneficial, and, mostly, educational. The only way to fully comprehend working in a weightless environment is to actually experience it firsthand. Goals accomplished with this flight included gaining a greater understanding of the crew environment and determining if tasks were easier or more difficult to accomplish in the absence of gravity. Participants found that some tasks were easier and some were more difficult. Furthermore, the zero-g environment allows superior economy of movement. It takes no physical effort whatsoever to translate and/or move hardware from one point to another. However, to successfully manage your movements without injury requires limited body movements, greater situational awareness, and a higher level of concentration. These factors are extremely important when you consider the complex tasks we ask Space Station crews to perform. Consequently, in our roles within Space Medicine, it is extremely important to remember and consider this special environment because a task that is generally easy to execute on the ground will require additional skills and thought when this task is executed on orbit. To ignore the added dimension of weightlessness during preflight training would result in inadequate training, something none of us want.

PHOTOGRAPHS

JSC2007E26123 to JSC2007E26163

VIDEO

- Zero G flight week 5/23-24, 2007, Master: 727441

Videos available from Imagery and Publications Office (GS4), NASA/JSC.

CONTACT INFORMATION

Bob Tweedy
c/o Wyle
1290 Hecules, Suite 120
Houston, Tx 77058
281-212-1400
robert.tweedy-1@nasa.gov

TITLE

The Effects of Microgravity on a Fast Enzyme Kinetics Reaction

FLIGHT DATES

May 22 – 24, 2007
June 19, 2007

PRINCIPAL INVESTIGATOR

Vince LiCata, Louisiana State University

CO-INVESTIGATORS

Chin-Chi Liu, Louisiana State University
Allison J. Richard, Louisiana State University

GOAL

The overall goal of this investigation was to determine if microgravity alters protein kinetics and equilibria.

OBJECTIVES

The objective of this flight week was to test microgravity effects on two enzyme kinetic reactions: fast and slow acetylcholinesterase.

METHODS AND MATERIALS

Materials

Acetylcholinesterase and all other standard reagents were purchased from Sigma Chemical (St. Louis, MO).

Over the course of several parabolic microgravity flights, we measured ligand concentration dependence for the enzyme kinetics of the acetylcholinesterase reaction. Two different acetylcholine variants were examined: fast (from electric eel) and slow (bovine). Six to eight data points were collected, in duplicate, for each full Michaelis-Menten (MM) curve. Each full parabola yields one 0g data sequence (kinetics collected for 10 seconds) and one 1.7-g data sequence. Each data sequence was analyzed linearly (see below) to obtain the rate of reaction at that substrate concentration. Each rate point was then plotted against substrate concentration to obtain a full MM curve. Full MM curves were collected at 0%, 10%, 20%, and 30% glycerol concentrations for fast AChE only.

Data Analysis

The initial portion of each kinetic trace was fitted to a linear equation to obtain the effect rate at that substrate concentration. A plot of rate (slope) vs. [substrate] yields a standard Michaelis-Menten kinetics curve:

$$v = V_{MAX}[S] / K_M + [S] \quad \text{(Equation 1)}$$

The curve (v versus [S]) is then nonlinearly fitted to determine the V_{max} and K_m parameters.

RESULTS

All reactions were measured during both the microgravity portion and the 1.7-g portion of each parabola. The 1.7-g measurements served as the control measurements in flight. All reactions were also measured at 1g either in the laboratory or on the C-9 while it was parked in the hangar at Ellington Field.

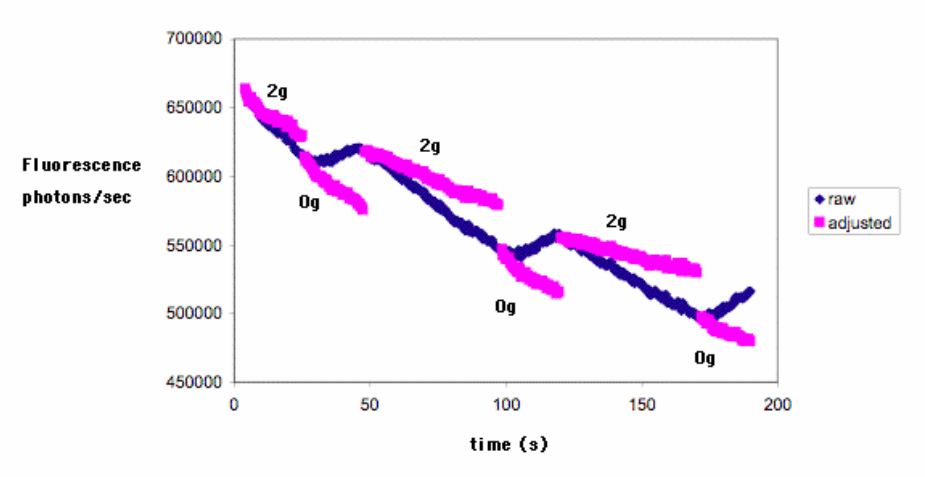

Figure 1. Representative kinetic data for slow (bovine) alkaline phosphatase over the course of 3 parabolas. Blue lines show the raw data, pink lines show the data after subtracting spectrophotometer drift. The difference in slope (reaction rate) between 2g and 0g is clearly visible in the data.

Significant spectrophotometer drift occurs while parabolas are being flown. The drift is linear, and the slope of the drift at 0g is different from its slope at 1.8g . However, drift slopes are highly consistent from one parabola to the next, and so raw kinetic data are processed by subtracting the spectrophotometric drift, as shown in Figure 1.

A full series of kinetic reactions similar to that shown in Figure 1 was collected at several different substrate concentrations, to construct full Michaelis-Menten curves for AChE at 0g and 2g, as shown in Figure 2.

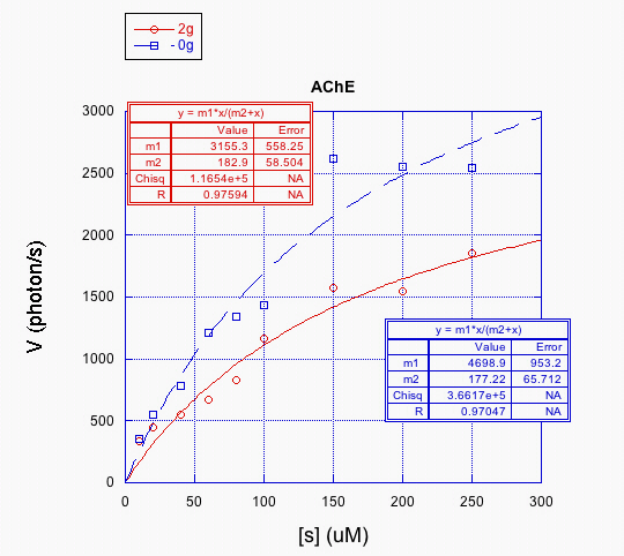

Figure 2. Michaelis-Menten kinetic curves for AChE at 0g (upper curve) and 1.8g (lower curve).

The data of Figure 2 indicate that the enzyme kinetics for AChE may be different in microgravity versus macrogravity. The increased V_{max} in microgravity suggested that acetylcholinesterase is faster in microgravity. Full statistical analysis of these data is still in progress.

DISCUSSION AND CONCLUSIONS

The goal of this project is to determine if microgravity alters the reaction rates of very rapid biological reactions. Small apparent effects of microgravity have been observed in several systems, but the harsh measurement conditions during flight consistently result in much higher random, and sometimes systematic, error for in-flight data. Continued redesign of the experimental equipment continues to improve data quality. Further data collection is necessary to confirm these conclusions.

REFERENCES

Cantor, C. R. and Schimmel, P. R. (1980) *Biophysical Chemistry, Part III, The Behavior of Biological Macromolecules*. W. H. Freeman and Company. San Francisco, CA. USA.

Hammes, G. G. (2000) *Thermodynamics and Kinetics for the Biological Sciences*. A. J. Wiley and Sons. New York, NY. USA.

Schoeffler, A.J., Ruiz, C.R., Joubert, A.M., Yang, X., and LiCata, V.J. (2003) Salt modulates the stability and lipid binding affinity of the adipocyte lipid binding protein. *J.Biol. Chem.* 278, 33268-33275.

PHOTOGRAPHS

JSC2007E25697 to JSC2007E25718
JSC2007E25982 to JSC2007E25989
JSC2007E26164 to JSC2007E26173
JSC2007E030171 to JSC2007E030180

VIDEO

- Zero G flight week 5/23-24, 2007, Master: 727441
- Zero G flight week 6/19-22, 2007, Master: 306303

Videos available from Imagery and Publications Office (GS4), NASA/JSC.

CONTACT INFORMATION

Vince LiCata, Ph.D.
Department of Biological Sciences
Louisiana State University
Baton Rouge, LA 70803
Phone: (225) 578-5233
FAX: (225) 578-2597
email: licata@lsu.edu

TITLE

Minimally Invasive Diagnosis and Therapy of Microgravity Medical Contingencies

FLIGHT DATES

October 17 – 20, 2006
June 19 – 22, 2007

PRINCIPAL INVESTIGATORS

Scott Dulchavsky, Henry Ford Hospital

CO-INVESTIGATORS

Shannon Melton, Wyle
Doug Hamilton, Wyle
Ashot Sargsyan, Wyle
Doug Ebert, Wyle

GOALS AND OBJECTIVES

To evaluate, in a flight experiment on healthy volunteers, acute changes in human physiology and anatomy associated with changes in gravity, using diagnostic ultrasound imaging devices, and to demonstrate feasibility of performing similar imaging protocols for operational space medicine purposes.

- Test and validate the following experimental protocols (modified and/or designed by the Primary Personnel) in whole or in part, for use in microgravity:
  a. Abdominal Renal/Pelvic Organ Morphometrics and Topography
  b. Cardiac Morphometrics, Physiology, and Topography
  c. Internal Jugular Vein Hemodynamics

- Identify specific limitations and modifications, if any, in imaging windows, scanning sequence, and scanning techniques, and other aspects requiring attention in microgravity.

- Identify vascular pressure, lumen, and/or flow changes related to gravity.

- Verify the applicability of basic terrestrial scanning protocols in the zero-g environment.

- Perform a pilot investigation of human factors and physiologic alterations associated with the Russian Bracelet Device using ultrasound.

INTRODUCTION

The feasibility of ultrasonic imaging in human spaceflight has already been demonstrated. Hardware has been flown aboard both NASA and Russian spacecraft, and successfully operated by both physician and non-physician astronauts. Previous success and promising research opportunities have motivated the installation of a sophisticated ultrasound system aboard the International Space Station (ISS) as part of the Human Research Facility (HRF). The HRF ultrasound system was successfully activated for autonomous use on the ISS on June 12, 2001, with no data transmission tested.

Ultrasound is the second most widely used clinical imaging modality in the United States. Its scope encompasses a large variety of medical and surgical conditions, many of which are considered possible in space. The diagnostic accuracy of this imaging modality is highly dependent on the professional knowledge, experience, and skills of the operator. Terrestrially, ultrasound data are acquired by a trained sonographer (technician or radiologist) and interpreted either during the process of examination (as in Europe, Russia, and Japan), or through review of standardized sets of still images (as in North America). In the ISS setting, a trained sonographer is not available on board; therefore, the essential expertise in both acquisition and interpretation is assumed to remain on the ground. Changes in anatomical norms and standard scanning "windows" can greatly affect the approach to diagnosis and treatment in a timely manner. This study attempts to identify some of these changes to better equip the experts on the ground for acquisition and interpretation. The acquired new knowledge is expected to be unique and valuable for future research programs concerned with human space physiology, space pharmacology, and other related disciplines. Certain products of these experiments may also be useful in the process of design and creation of the medical support systems for exploration-class missions.

METHODS AND MATERIALS

Eight C-9 microgravity flights were conducted using healthy volunteer human subjects for all procedures. Ultrasound experts used multiple ultrasound devices to capture images of the heart, vasculature, and abdominal organs.

Hardware

GE Logiqbook Ultrasound System (GE Medical Systems, Milwaukee, WI)
A portable ultrasound system approved for clinical use. Equipped with an abdominal (convex) and small parts (linear) probe.

Sonosite 180Plus Ultrasound System (Sonosite, Bothell, WA)
A portable ultrasound system approved for clinical use. Equipped with an abdominal (convex) and small parts (linear) probe.

Biosound MyLab30 (Biosound Esaote, Genoa, Italy)
A portable ultrasound system approved for clinical use. Equipped with a cardiac and vascular (linear) probe.

Airway Pressure Measurement and Biofeedback Regulation Device (Prototype, Wyle, Houston, TX)
A breathing device that continuously measures and displays actual pressures within the breathing orifice, allowing the subject to maintain required pressure through biofeedback and adjustment of their respiratory effort.

Inflatable Thigh Cuffs - Commercially Available Blood Pressure Cuffs.
Similar to blood pressure measurement devices used on the arms. Temporary venous occlusion is produced by an inflatable thigh cuff, and the venous volume response in the calf is measured during inflation of the cuff and for a few seconds after its release.

Bracelet (Kentavr-Nauka, Ltd., Moscow, Russia)
Bracelet-M Russian countermeasure device flown on ISS. The Bracelet is a strap that wraps around the upper thigh and is calibrated and fitted to the individual wearer.

Media Rack (Wyle, Houston, TX)
A flight-rated rack that contains five video channels with recording systems, 3 audio channels, and two real-time video monitors that can be switched between the multiple video sources. All video channels are mixed with overlays displaying flight time, g levels, and parabola numbers. A remote viewing station was set up in a separate area of the plane with two-way audio loops for communication and video feeds from either one of the ultrasound systems.

Procedures

Multiple imaging protocols were performed on normal human subjects by expert sonographers. In October, two scanning stations were set up on each flight, allowing two subjects to be scanned simultaneously. At one station the subjects were restrained supine. At the second station, the

subjects were given a reclined position in the aircraft seats, and restrained using straps and foot restraints. In June, only the reclined position in the seats was used.

Abdominal/Renal/Pelvic Organs (October)
The FAST exam was conducted on two normal human subjects in 0 g, 1/6g, and 1/3g to evaluate alterations in the ultrasound windows required for the examination. Preliminary analysis suggests that the RUQ and LUQ windows will need to be moved superiorly by 1 interspace for martian gravity and 2 interspaces for lunar gravity, similar to zero-gravity findings.

Non-Expert Ultrasound Operators
The ability of non-physician operators to perform ultrasound examinations during weightless conditions after a brief training period was assessed. Ultrasound scans of the jugular vein and greater saphenous vein were continuously evaluated during various flight phases during cuff occlusion with or without maneuvers.

Vascular (October/June)
Simultaneous real-time imaging of the heart and the internal jugular vein (IJV) was done in five reclined subjects. In October, inflatable thigh cuffs were used. In June, the Russian Bracelets were used on the legs. In June an additional ultrasound scan of the saphenous vein was included. The following conditions were evaluated:

2 g-0 g-2g transition with normal respiration, no thigh cuffs
2 g-0 g-2g transition with normal respiration, with thigh cuffs inflated or Bracelets applied
2 g-0 g-2g transition with subject inhaling at specific pressures at the breathing orifice
2 g-0 g-2g transition with subject exhaling at specific pressures at the breathing orifice
2 g-1/6 g-2g transition with normal respiration, no thigh cuffs
2 g-1/6 g-2g transition with normal respiration, with thigh cuffs inflated or Bracelets applied
2 g-1/6 g-2g transition with subject inhaling at specific pressures at the breathing orifice
2 g-1/6 g-2g transition with subject exhaling at specific pressures at the breathing orifice
2 g-1/3 g-2g transition with normal respiration, no thigh cuffs
2 g-1/3 g-2g transition with normal respiration, with thigh cuffs inflated or Bracelets applied
2 g-1/3 g-2g transition with subject inhaling at specific pressures at the breathing orifice
2 g-1/3 g-2g transition with subject exhaling at specific pressures at the breathing orifice

RESULTS AND DISCUSSION

Abdominal/Renal/Pelvic Organs

Imaging of the abdominal and retroperitoneal organs (liver, kidney, pancreas, spleen, gallbladder) was completed in all subjects, as described in the Materials and Methods section above. Data were verified post experiment. A comparison will be attempted between the data from this acute experiment and the information acquired in a similar fashion during long-term exposure to microgravity. Until such time, the data will be used to refine imaging protocols and measurement techniques, and to draw preliminary conclusions regarding the effects of microgravity and partial gravity on abdominal imaging data.

Cardiovascular Changes using Thigh Cuffs or Bracelet Device
Significant changes to the cardiovascular system and fluid redistribution occur during spaceflight, resulting in reduction in cardiac reserve. This reduction may have an impact on the ability of a crew member to respond to circulatory shock or any significant hypovolemic challenge. Symptomatic improvement with the application of the Bracelet has been consistently reported by the Russian cosmonauts, but the in-flight cardiovascular effects of the device have not been rigorously investigated. We hypothesize that the Bracelet-M device increases fluid sequestration in the extremities, reducing in-flight fluid shifts and inducing a temporary hypovolemia in the central circulation. The objective cardiac and vascular effects of the device may be variable because the limited current calibration and application techniques result in a narrow "therapeutic range."

On this series of C-9 flights, we developed the techniques needed to determine optimal device utilization of the Bracelet and measure if the effects can be reproduced using a standard inflatable thigh cuff. The effects were measured using simultaneous ultrasound imaging of the heart and the jugular and saphenous veins. The flight data helped validate optimal probe position of the 3 ultrasound imaging systems during reduced-gravity periods. Furthermore, the effects of cardiopulmonary maneuvers were measured and confirmed to be significant enough to consider using them when evaluating the Bracelet device on the ISS during increment 16. The cardiopulmonary maneuvers were measured using a unique airway pressure measurement device that approximated intrathoracic pressure. The information gained during this flight will help provide essential information to answer operationally relevant cardiovascular issues for exploration-class missions.

Non-Expert Users Evaluation
Non-physician operators (Crew Medical Officer analogues) were able to obtain diagnostic quality ultrasound images of peripheral venous structures with minimal training.

CONCLUSIONS

The goals of the experiment were accomplished. New knowledge was acquired and documented. Data acquisition was designed to be compatible with the data from ground- and space-based experiments, allowing consideration of comparisons, correlations, and combined evaluation for protocol development purposes.

A new methodology of respiratory pressure biofeedback with complex imaging evaluation of cardiac and central vascular parameters was successfully tested and showed great promise. Further study in this direction seems to be warranted.

Demonstrable alterations in cardiovascular hemodynamics were noted with Bracelet applications during nominal and 0g, and during various respiratory maneuvers. Further data analysis is continuing.

Non-expert operators were able to perform peripheral cardiovascular ultrasound evaluations during 0g after minimal training. This paradigm may be useful for space medical use and provide useful information for research and medical use of ultrasound on the ISS in the future.

Secondary results include successful evaluation of the hardware used. The hardware and its setup, deployment, connectivity, and data acquisition did not exhibit any inadequacies, and fully supported the intended applications.

ACKNOWLEDGMENTS

The Primary Personnel highly value the essential contributions of the following individuals (equipment, experiment design, setup and support, logistics, serving as subjects, expertise):

- Dr. J. D. Polk, NASA Johnson Space Center, Houston, TX
- Dr. Buck Parker, Henry Ford Hospital, Detroit, MI
- Jack Butler and Sai Rao, Henry Ford Hospital, Detroit, MI
- Kathleen Garcia, Houston, TX
- Richard Pettys, Terry Guess, and Ashkhan Moghaddam, Wyle, Houston, TX
- Anousheh Ansari, Prodea Systems, Plano TX
- Dan Mulhern, State of Michigan. Lansing, MI
- James Adams, Grosse Pointe South High School, Grosse Pointe, MI
- Angela Ruggiero, Harper Woods, MI

PHOTOGRAPHS

JSC2006E45028 to JSC2006E45059
JSC2006E45275 to JSC2006E45304
JSC2006E45322 to JSC2006E45352
JSC2006E45891 to JSC2006E45920
JSC2007E030181 to JSC2007E30209
JSC2007E030708 to JSC2007E030730
JSC2007E031284 to JSC2007E031293
JSC2007E032132 to JSC2007E032336

VIDEO

- Zero G flight week October 17 -20, 2006, Master: DV0729
- Zero G flight week June 19-22, 2007 Master: 306303

Videos available from Imagery and Publications Office (GS4), NASA/JSC.

CONTACT INFORMATION

Shannon Melton
Wyle
1290 Hercules Suite 120
Houston, TX 77058
281-212-1435
SMELTON@Wylehou.com

TITLE

Exploration Medical Capability Group (ExMC): Evaluation of the ActiBelt® in a Microgravity Environment

FLIGHT DATES

June 19 – 22, 2007

PRINCIPAL INVESTIGATORS

Victor Hurst IV, Wyle
Martin Daumer, Sylvia Lawry Centre for Multiple Sclerosis Research (SLCMSR)

GOAL

Determine if the ActiBelt® can be used to quantify the activity profile and energy consumption of human participants while in a micro- or partial-gravity environment.

INTRODUCTION

The purpose of this study is to do a hardware validation of a device called ActiBelt®, a high-tech belt buckle developed by a team led by Martin Daumer, Ph.D. (Daumer Team, Sylvia Lawry Centre for Multiple Sclerosis Research (SLCMSR). The ActiBelt® uses integrated accelerometers

to quantify the activity profile and energy consumption of human participants. The NASA Johnson Space Center (JSC) Exploration Medical Capability group (ExMC; SD4) and Wyle's Advanced Projects group (AP; SD4), both of the NASA JSC Medical Informatics and Health Care Systems group (MIHCS; SD4), collected data for the Daumer Team to determine if the ActiBelt® was capable of measuring energy consumption by human participants in a microgravity environment.

Physical activity is of paramount importance for the health of human beings on Earth as well as for astronauts in space, on the Moon, and on Mars. This has led to a pressing need for reliable and valid measures of energy consumption in various activities, including tasks performed during spaceflight. The ActiBelt® is a high-tech belt buckle that contains a miniaturized autonomous chip consisting of a three-dimensional accelerometer (see Figures 1 and 2) that uses several energy consumption measuring algorithms developed by the Daumer Team. The ActiBelt® has been tested for its ability to successfully distinguish and quantify movement patterns in both healthy individuals and patients with multiple sclerosis while they perform such activities as walking, running, sitting, and lying down while in a normal gravity environment [1]. The success of the device with these two cohorts has led to the belief that the ActiBelt® could also be very useful to monitor and evaluate the activity pattern and energy consumption of humans performing tasks in micro- or partial-gravity environments (such as astronauts aboard the International Space Station [ISS]).

Figure 1. The ActiBelt® buckle

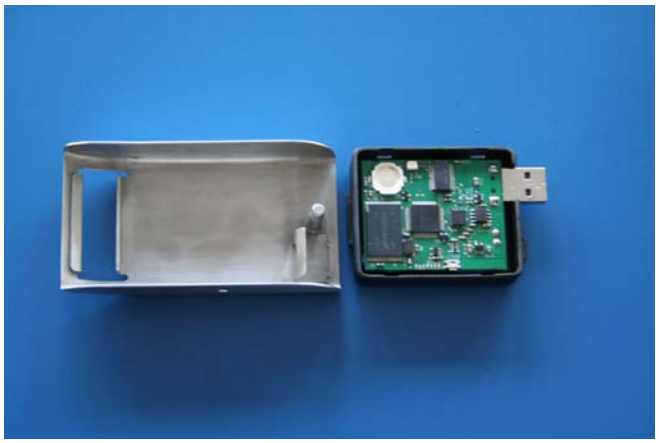

Figure 2. The circuit board and components within the ActiBelt® buckle.

In recent years, the space medical literature has indicated the importance of physical activity by astronauts during spaceflight for maintaining the responsiveness of their cardiovascular systems to orthostatic changes on their re-adaptation to gravity environments, especially after long-duration missions aboard the ISS [2]. The high performance of the ActiBelt®'s measurement system in combination with its wearing comfort, lightness, and small size—it does not constrain a person's mobility—makes the device an appropriate candidate for measuring the physical activity levels of astronauts during spaceflight.

OBJECTIVE

Determine if the ActiBelt® can be used to quantify the activity profile and energy consumption of human participants while they are in a micro- or partial-gravity environment.

METHODS AND MATERIALS

Human Subjects

On 24 May 2007, the investigators for this evaluation received approval to use humans as participants in this study from the NASA JSC Committee for the Protection of Human Subjects (CPHS). The proposal was titled "Evaluation of the Actibelt for Measuring Energy Consumption of Human Participants in a Micro/Partial Gravity Environment."

Experimental Approach

The protocol for the evaluation had members of the ExMC/AP flight team perform predefined movements (deep knee bends and push-ups) while wearing the ActiBelt® in the microgravity environment they experienced during the first 10 parabolas aboard the C-9 aircraft. The ActiBelt® data were compared with the oxygen intake, carbon dioxide production, and heart rate data collected from a commercial-off-the-shelf spiroergometer (Model K4b2; COSMED, Rome, Italy) that was also worn by the same ExMC/AP flight team members during the same parabola set (Figures 3 and 4). The data from the spiroergometer acted as a standard to validate the energy consumption data from the ActiBelt®. For reference measurements, ActiBelts® without spiroergometers were 1) worn by other members of the ExMC/AP flight team who were not performing predefined movements and 2) fixed within the cabin of the aircraft.

Figure 3. A participant wearing ActiBelt® with a spiroergometer while doing deep knee bends during the microgravity portion of the flight.

Figure 4. A participant wearing ActiBelt® with a spiroergometer while doing push-ups during the microgravity portion of the flight.

RESULTS, DISCUSSION, AND CONCLUSION

Preflight data were successfully collected from all four participants wearing both the ActiBelt® and the spiroergometer while doing the predefined movements. Data collection from all four participants during the flight was also successful, along with the collection of reference data from participants not wearing spiroergometers and the static ActiBelts® fixed within the cabin of the aircraft. Preliminary review of the data indicates that the ActiBelt® may be sufficient for collecting energy consumption data in a microgravity environment; however, a formal analysis of the data needs to be completed before conclusions regarding the ActiBelt®'s functionality in a microgravity environment is finalized. The data will be formally analyzed and written up by the Daumer Team for peer review.

ACKNOWLEDGMENTS

The ExMC project would like to acknowledge the following groups for their support with flight preparation and execution for this evaluation: NASA JSC Medical Informatics and Health Care Systems, Advanced Projects at Wyle, NASA JSC Flight Surgeon Office and the Medical Training Group at Wyle. Finally, the ExMC project also acknowledges the valued support and guidance they received from the NASA JSC Reduced Gravity Office (RGO) for these as well as previous experiments aboard RGO aircraft.

REFERENCES

1. Daumer M, Thaler K, Kruis E, Feneberg W, Staude G, Scholz M. Steps towards a miniaturized, robust and autonomous measurement device for the long-term monitoring of the activity of patients – ActiBelt. Accepted for publication June 2006, *Biomedical Engineering*

2. Meck JV, Reyes CJ, Perez SA, Goldberger AL, Ziegler MG. Marked exacerbation of orthostatic intolerance after long- vs. short-duration spaceflight in veteran astronauts. *Psychosom Med*. 2001 Nov-Dec;63(6):865-73

PHOTOGRAPHS

JSC2007E030734
JSC2007E030740
JSC2007E031312

VIDEO

- Zero G flight week 6/19 – 22, 2007, Master: 306303

Videos available from Imagery and Publications Office (GS4), NASA/JSC.

CONTACT INFORMATION

Victor Hurst IV, Ph.D.
Senior Scientist, Advanced Projects (AP)
Wyle
1290 Hercules
Suite 120 (MC:W1A)
Houston, TX 77058
(281) 212-1460
vhurst@wylehou.com

Martin Daumer, Ph.D.
Director, Sylvia Lawry Centre for Multiple Sclerosis Research (SLCMSR)
Hohenlindener Str. 1
D-81677 Munich
Germany
Tel: +49 89 2060 269 50
daumer@slcmsr.org

TITLE

Exploration Medical Capability Group (ExMC): Evaluation of the EZ-IO® Intraosseous Device in a Microgravity Environment

FLIGHT DATES

June 19 – 22, 2007

PRINCIPAL INVESTIGATORS

Richard Scheuring, NASA Johnson Space Center
Victor Hurst IV, Ph.D., Wyle

GOAL

To determine if the usability of the EZ-IO® device is sufficient for minimally-trained caregivers (that is, CMO analogues) to establish intravenous (IV) access during emergent medical situations in a microgravity environment.

INTRODUCTION

The purpose of this study is to do a hardware evaluation of the EZ-IO® device to determine if minimally trained caregivers, such as astronaut crew medical officer analogues (CMO analogues), are able to establish intravenous (IV) access during emergent medical situations in a microgravity environment. The NASA Johnson Space Center (JSC) Medical Informatics and Health Care Systems group (MIHCS) tasked both the NASA JSC Exploration Medical Capability group (ExMC) and the Advanced Projects group (AP) of Wyle to conduct this evaluation.

Astronaut crew medical officers (CMO) currently have one method for establishing vascular access in fellow crew members requiring IV fluid and/or medications; however, the successful establishment of vascular access using conventional IV access techniques is relatively slow and cumbersome, even in trained clinical hands. Anecdotal reports from astronaut physicians who have attempted vascular access in microgravity using conventional IV access state that it took 10-12 minutes to successfully establish an IV via the antecubital vein. The delay in establishing an IV route was due, in part, to the set-up time associated with the kit (needle catheters, prep pads, IV tubing, and fluid) in the microgravity environment. This finding is a concern considering that a majority of space missions do not have a physician on board.

Typically, a CMO has not received formal clinical training (as for a physician or nurse) and, thus, has had limited training in phlebotomy or vascular access. Consequently, it is believed that successful vascular access by non-clinician CMOs in microgravity during an emergent medical situation using the conventional IV access route will be difficult and time-consuming in the best-case scenario. Therefore, it is paramount to identify procedures and equipment that can facilitate establishment of IV access on a sick crew member by a CMO.

The technique of intraosseous (I/O) infusion was first described in humans in 1934 and it became increasingly popular in the 1940s. In recent years it has regained popularity as being one of the quickest ways to establish access for the rapid infusion of fluids, drugs, and blood products in emergency situations as well as for resuscitation. The procedure takes advantage of the fact that the marrow cavity in bones is in continuity with the venous circulation and thus can be used to infuse fluids and drugs, and to take blood samples. Briefly, the caregiver inserts a needle near the tibial tuberosity at the top of the lower leg (top of the tibia bone); below the knee to establish IV access (Figure 1). One can also use this technique at the base of the tibia (top of ankle) and at the top of the humerus (shoulder).

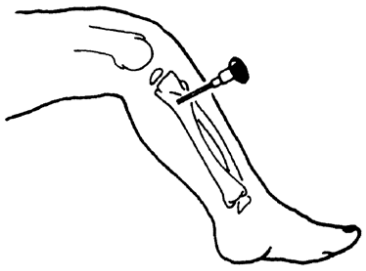

Figure 1. Insertion of intraosseous needle in the right tibia.
(Figure from Vreede et al. [1])

To assess the viability of IO access devices as an adjunct or alternative means to the conventional IV method for establishing emergent vascular access by minimally trained caregivers (such as CMO analogues) in microgravity, the ExMC and AP groups evaluated the usability of the EZ-IO® device by CMO analogues.

METHODS AND MATERIALS

Thirteen participants attended preflight training to become familiar with the EZ-IO device and associated equipment. Each participant was able to review the experiment protocol, including practice of EZ-IO needle insertion into each of the three simulated bones (top of lower leg, top of the ankle, and shoulder) using the hand-crank manual driver and the battery motorized power driver. Each participant was also thoroughly briefed on the safety protocols for handling and disposing of EZ-IO needles during the flight. After a brief "refresher" on the day of the flight, teams of two participants, acting as CMO analogues, were assigned to the IO station in the aircraft to attempt insertion of the EZ-IO needles into the simulated bones during the microgravity portions of the flight. The primary CMO analogue would perform the actual needle insertion while the secondary CMO analogue would have two roles: 1) record the times needed for the primary CMO analogue to complete needle insertion and 2) be the Safety Monitor to ensure that the needle handling was conducted per the safety protocols taught during training. Once the primary CMO completed his or her EZ-IO needle insertion attempts with both the manual needle driver (Figure 2) and the power needle driver (Figure 3), he or she switched roles with the secondary CMO analogue to continue the evaluation. All actions by the CMO analogues were recorded for retrospective analysis. All CMO analogues completed a questionnaire after their flight.

Figure 2. Participant using the manual driver to insert the EZ-IO needle into a simulated bone.

Figure 2. Participant using the power driver to insert the EZ-IO needle into a simulated bone.

RESULTS, DISCUSSION, AND CONCLUSION

Preliminary review of the data (observational and questionnaire) indicate that the participants, acting as CMO analogues, preferred to use the power driver to insert the EZ-IO needle into the simulated bone while in a microgravity environment rather than the manual driver in the same environment; however, a formal analysis of the data needs to be completed before conclusions regarding the use of this protocol and the EZ-IO device in a microgravity environment can be finalized. The data will be formally analyzed and written up by the ExMC and AP groups for peer review.

ACKNOWLEDGMENTS

The ExMC project would like to acknowledge the following groups for their support with flight preparation and execution for this evaluation: NASA JSC Medical Informatics and Health Care Systems, Advanced Projects at Wyle, NASA JSC Flight Surgeon Office, and the Medical Training Group at Wyle. Finally, the ExMC project also acknowledges the valued support and guidance they received from the NASA JSC Reduced Gravity Office (RGO) for these as well as previous experiments aboard RGO aircraft.

REFERENCES

1. Vreede E, Bulatovic A, Rosseel P, Lassalle X. Intraosseous infusion. *Update in Anaesthesia: Practical Procedures*. Issue 12 (2000), Article 10.

PHOTOGRAPHS

JSC2007E031304
JSC2007E032175
JSC2007E032180

VIDEO

- Zero G flight week 6/19 – 22, 2007, Master: 306303

Videos available from Imagery and Publications Office (GS4), NASA/JSC.

DISCLAIMER

The content of this report should not be considered final and binding. Formal review and evaluation of all data collected will be the subject of final reports and publications when deemed appropriate. The content of this report should permit the reader to become familiar with the procedures followed and the preliminary observations and lessons learned. This document neither endorses nor rejects the performance of the EZ-IO® Intraosseous Device by Vidacare, Inc. (San Antonio, TX).

CONTACT INFORMATION

Richard Scheuring, D.O.
Constellation Medical Operations Specialist
NASA Johnson Space Center
2101 NASA Parkway (MC: SD4)
Houston, TX 77058
(281) 483-9769
richard.a.scheuring@nasa.gov

Victor Hurst IV, Ph.D.
Senior Scientist, Advanced Projects (AP)
Wyle
1290 Hercules Avenue
Suite 120 (MC:W1A)
Houston, TX 77058
(281) 212-1460
vhurst@wylehou.com

TITLE

Exploration Medical Capability Group: Evaluation of the Revised International Space Station Advanced Cardiac Life Support Algorithm in a Microgravity Environment

FLIGHT DATES

June 19 – 22, 2007

PRINCIPAL INVESTIGATOR

Victor Hurst IV, Wyle

CO-INVESTIGATOR

Kieran Smart, Wyle

GOAL

Determine if the tasks in the revised International Space Station (ISS) Advanced Cardiac Life Support (ACLS) algorithm can be completed by astronaut crew medical officer (CMO) analogues in a microgravity environment. Please note that the tasks within the algorithm include steps for the newly manifested Automated External Defibrillator (AED) for the ISS.

INTRODUCTION

The purpose of this study was to do a protocol evaluation of the revised ISS ACLS algorithm using ISS astronaut CMO analogues in a microgravity environment. The tasks within the algorithm also include steps for the AED that has been recently manifested for use aboard the

ISS. The NASA Johnson Space Center (JSC) Exploration Medical Capability group (ExMC) and Wyle's Advanced Projects group (AP), both of the NASA JSC Medical Informatics and Health Care Systems group (MIHCS), collected performance and questionnaire data to determine if CMO analogues can execute the tasks within the ACLS algorithm while working in a microgravity environment.

The primary objective of the ACLS algorithm on the ISS is to provide an astronaut CMO the capability to autonomously manage a clinical situation on orbit using Advanced Life Support techniques while waiting for communication with a ground-based flight surgeon (FS). Representatives of the NASA JSC FS Office saw areas for possible improvement of the current ISS ACLS algorithm and generated a revised version of the algorithm with support from the Medical Simulation Laboratory Working Group (MSLWG) of the MIHCS group at NASA JSC. The MSLWG was then tasked by MIHCS and the FS Office to evaluate both versions of the algorithm for task completion, ease of navigation, and clarity. The main finding from this ground-based evaluation (conducted in the Medical Simulation Laboratory [MSL] at Wyle) was a preference among CMO analogues for using the revised version of the algorithm rather than the current version. To finalize the assessment of the revised version for spaceflight, MIHCS tasked the ExMC and AP groups to evaluate the revised version in the microgravity environment provided via parabolic flight aboard the C-9 aircraft to determine if CMO analogues can execute the tasks listed in the algorithm while working in a microgravity environment. [The ExMC, AP, and MSLWG groups are all part of the MIHCS group.]

OBJECTIVE

Determine if the tasks in the revised ISS ACLS algorithm can be completed by CMO analogues in a microgravity environment.

METHODS AND MATERIALS

Participants were selected for this study because they had received Health Maintenance System (HMS) training similar to that of ISS astronaut crew medical officers (CMOs). The participants assumed the role of CMO while completing the algorithm in this evaluation.

Fourteen participants took part in a "hands-on" evaluation of the revised ISS ACLS algorithm using equipment from the HMS System's medical packs (Advanced Life Support Pack (ALSP), Respiratory Support Pack (RSP), Automated External Defibrillator (AED), and Intubation Kit/Airway (IKA)). The participants were given a prebriefing before their flight regarding the expectations of the study, including directions to "Think Out Loud" as they went through the algorithm and to indicate when instructions were unclear and/or ambiguous. They were <u>not</u> shown the algorithm before participating in the evaluation. After they received a prebrief "refresher" on the day of the flight, teams of two participants, acting as CMO analogues, were presented with one of two specified paths of the algorithm to follow during the microgravity portions of the flight. The primary CMO would execute the tasks while receiving assistance from the secondary CMO per the primary CMO's direction.

Each evaluation used an Emergency Care Simulator mannequin (ECS; Medical Education Technologies, Inc., Sarasota, FL) as a test bed for executing procedures and applying equipment from the HMS medical packs as directed by the algorithm (Figure 1; please note that the ECS was neither powered up nor programmed to present a medical condition). All verbal data and actions by the participants as they executed the algorithm were recorded for retrospective analysis. Upon completing the flight, the participants completed a brief questionnaire.

Figure 1. Participants performing tasks listed in the revised Advanced Cardiac Life Support (ACLS) algorithm.

RESULTS, DISCUSSION, AND CONCLUSION

Preliminary review of the data (observational and questionnaire) indicated that the participants, acting as CMO analogues, were able to follow and execute the tasks of the revised ACLS algorithm within a microgravity environment; however, a formal analysis of the data needs to be completed before conclusions regarding the use of the algorithm in a microgravity environment can be finalized. The data will be formally analyzed and written up by the ExMC and AP groups for peer review.

ACKNOWLEDGMENTS

The ExMC project would like to acknowledge the following groups for their support with flight preparation and execution for this evaluation: NASA JSC Medical Informatics and Health Care Systems, Advanced Projects at Wyle, NASA JSC Flight Surgeon Office, and the Medical Training Group at Wyle. Finally, the ExMC project also acknowledges the valued support and guidance they received from the NASA JSC Reduced Gravity Office (RGO) for these as well as previous experiments aboard RGO aircraft.

PHOTOGRAPHS

JSC2007E031304
JSC2007E032175
JSC2007E032180

VIDEO

- Zero G flight week 6/19 – 22, 2007, Master: 306303

Videos available from Imagery and Publications Office (GS4), NASA/JSC.

CONTACT INFORMATION

Victor Hurst IV, Ph.D.
Senior Scientist, Advanced Projects (AP)
Wyle
1290 Hercules Avenue
Suite 120 (MC:W1A)
Houston, TX 77058
(281) 212-1460
vhurst@wylehou.com

Appendix:
Background Information about the C-9 and the Reduced-Gravity Program

The Reduced-Gravity Program, operated by the NASA Johnson Space Center (JSC), provides engineers, scientists, and astronauts alike with a unique opportunity to perform testing and training in a weightless environment but without ever having to leave the confines of the Earth's orbit. Given the frequency of Space Shuttle missions and the construction and habitation of the International Space Station, the Reduced-Gravity Program provides a truly ideal environment to test and evaluate space hardware and experimental procedures before launch.

The Reduced-Gravity Program was established in 1959 to investigate the reactions of humans and hardware during operations in a weightless environment. A specially modified C-9 turbojet, flying parabolic arcs, produces periodic episodes of weightlessness lasting 20–25 seconds. The C-9 is sometimes also flown to provide short periods of lunar (1/6) and martian (1/3) gravity. Over the last 35 years, about 100,000 parabolas have been flown in support of the Mercury, Gemini, Apollo, Skylab, Space Shuttle, and Space Station programs.

Excluding the C-9 Flight Crew and the Reduced Gravity Program Test Directors, the C-9 accommodates seating for a maximum of 20 other passengers. The C-9's cargo bay provides a test area that is about 45 feet long, 104 inches wide, and 80 inches high. The aircraft is equipped with electrical power, overboard venting system, and photographic lights. When requested and available, professional photography and video support can be scheduled to document activities in flight.

A typical flight lasts 2 to 3 hours and consists of 30 to 40 parabolas. The parabolas are flown in succession or with short breaks between maneuvers to allow time for reconfiguring test equipment.

For additional information concerning flight weeks sponsored by the Johnson Space Center's Human Adaptation and Countermeasures Office or other Reduced-Gravity Program opportunities, please contact:

Todd Schlegel, MD
Technical Monitor
Human Adaptation and Countermeasures
NASA Lyndon B. Johnson Space Center
Mail Code: SK
Houston, TX 77058
Telephone: (281) 483-9643

NASA Lyndon B. Johnson Space Center
Reduced-Gravity Office, Ellington Field
Mail Code: CC43
Houston, TX 77034
Telephone: (281) 244-9211

Explore the Zero Gravity Experiments and Aircraft Operations Web pages at:
http://zerog.jsc.nasa.gov/
http://jsc-aircraft-ops.jsc.nasa.gov